‘BRAKING’ THE CYCLE: MECHANISM OF CYTOKINESIS INHIBITION BY THE E3 UBIQUITIN LIGASE DMA1

By

Alyssa Erica Kim Johnson

Dissertation

Submitted to the Faculty of the

Graduate School of Vanderbilt University

in partial fulfillment of the requirements for

the degree of

DOCTOR OF PHILOSOPHY

in

Cell and Developmental Biology

August 2013

Nashville, Tennessee

Approved:

Professor Kathleen Gould

Professor David Miller

Professor David Cortez

Professor William Tansey

Professor Laura Lee

To my mom,

for her unfailing love and support,

and

in loving memory of my dad,

who will always be my model for strength, hard work and integrity

ACKNOWLEDGEMENTS

I am truly grateful to many people that have helped me throughout my graduate career and throughout my life, so that I could accomplish my goals. First and foremost, I thank my mentor, Kathy, who has shaped me into the best scientist I could be. She has been instrumental in guiding all of my projects, but has also given me the freedom to explore ideas on my own. I am also very grateful for the many incredible opportunities she has given me to present my work and interact with leading scientists in the field. Her success and career have been truly inspirational to me and her constant encouragement has given me the confidence to continue pursuing science as a career.

I am also grateful to many people who have collaborated with me on various projects. Scott Collier and Melanie Ohi helped with structural work to determine the oligomerization state of Dma1. We collaborated with Dan McCollum and Quan-wen Jin to characterize a molecular inhibitor of Dma1 and Dan also wrote a review of the SIN with us. Jun-Song Chen, Jianquiu Wang and Malwina Huzarska performed the mass spectrometry analyses for all of my projects, which was critical in identifying novel interacting proteins and post-translational modifications. Christine Jones has recently joined team Dma1 and is continuing many Dma1 and CHFR related projects. Also, I would like to acknowledge the Howard Hughes Medical Institute, and the Cellular, Biochemical, and Molecular Sciences training program, NIH T32 GM08554, for providing financial support to my research and contributing to my scientific development.

I would also like to thank my undergraduate advisor Maria Hledin, who let me work in her lab as freshman and inspired me to pursue graduate school. She has also given me many opportunities that have contributed to my success as a scientist. I am also

grateful to the members of my thesis committee, David Miller, Dave Cortez, Bill Tansey and Laurie Lee, for their advice and constructive criticisms over the past 5 years and to the support of Cell and Developmental Biology department.

During my time in the Gould lab, I have encountered many wonderful people that have helped me along the way and made my experience in the lab more fun. I would especially like to thank Liping Ren and Anna Feoktistova for their technical expertise, without which many of my projects would certainly not have come to fruition. Liping is a master of everything and I have learned so much from working next to her for the past 5 years. Anna has taught me almost everything I know about biochemistry, a talent that will be useful no matter what scientific questions I pursue in the future. I also really appreciate our lab assistants, Magdalena Buchowski and Donna Dunlap, for keeping the lab in order and providing an efficient working environment. Janel McLean and Nicole Rachfall have been very helpful in discussing ideas for future experiments and revising many manuscripts. When I rotated in the Gould lab, I was fortunate to be under the mentorship of Rachel Roberts-Galbraith. She has been a great friend and colleague throughout the years and I really appreciate all of the advice she has given me. Lastly, I owe a huge debt of gratitude to Adam Bohnert. Adam has been a great friend and colleague, both inside and outside of the lab, and has been a huge source of support when I was going through difficult times.

I am also very appreciative of many friends and family that have supported me throughout my life and contributed to my personal and professional development. My three best friends, Ashley Greenan, Leah Robertson and Chelsea Vanderhoff, have been a constant source of support since middle school. No matter how much time or distance

separates us, they always have my back and I have always considered them part of my family. I am also grateful to my big sister, Heather, who is always there for me and reminds me not to take life so seriously. Last, but not least, I would like to thank my parents, Toni and Jim, whose unconditional love and support has been my foundation. They have instilled in me the importance of education and hard work and I am grateful for the all of the sacrifices they have made for me. I owe all of my success to them.

TABLE OF CONTENTS

LIST OF FIGURES

CHAPTER I

INTRODUCTION

The cell is the basic unit of biological life and cell division is essential to sustain all living organisms. How cells reproduce has been studied for many years, yet there is still much that we do not understand about how cell division is controlled. Defects in the cell division cycle are linked with many developmental disorders and cancer, which manifests as uncontrolled cell proliferation. Thus, it is imperative to understand the basic principles of how cells divide in order to understand how these processes go awry to drive human diseases.

The primary concern of cell division is to duplicate the genome and divide the genetic and cytoplasmic material to produce two new cells. Faithful execution of these two tasks is critical to maintain the genomic integrity of each daughter cell. In all eukaryotic organisms, cell division requires a dynamic cellular infrastructure that directs chromosome separation, recruitment of cytokinesis proteins to the division site, assembly of a cytokinetic ring (CR) and CR constriction. Given the intricacy of these processes, it is not surprising that cell division demands a diverse cohort of proteins to orchestrate these events. These include (1) structural proteins to assemble into the mitotic spindle and CR and to provide spatial landmarks within the cell, (2) molecular motors to provide the kinetic requirements for chromosome separation and CR constriction and (3) signaling enzymes to provide temporal cues, typically by imposing activating or inhibitory messages onto their targets via post-translational modifications (Bohnert and

Gould, 2011). Coordinating these assorted molecules to ultimately divide a cell is a complicated yet vital task to guarantee that each new generation does not inherit erroneous DNA content.

Cell cycle checkpoints

The somatic cell division cycle contains four distinct phases, G1, S, G2, and M phase and eventually culminates in cytokinesis, the physical division and separation of the two new cells (Figure 1-1). To orchestrate these events faithfully, each phase must occur sequentially, such that one does not begin before the previous stage completes (Nurse, 2000). To solve the "completion" problem, several intrinsic properties of the cell ensure that cell cycle progression occurs in a unidirectional mode. For instance, at the end of mitosis, the irreversible destruction of the CDK activator, cyclin B, by the ubiquitin/proteasome system allows cells to exit mitosis and prevents cells from prematurely re-entering mitosis until the next M phase (Glotzer et al., 1991; Wickliffe et al., 2009). However, if an unexpected mistake arises, the cell utilizes a "surveillance system" called checkpoints to delay progression (Figure 1-1, (Elledge, 1996)). Checkpoints have two major responsibilities: to sense mistakes when they occur and to induce a biochemical response to delay the cell cycle. Understanding how checkpoints accomplish these tasks presents many challenges and requires a detailed analysis of their molecular mechanisms.

One key event during mitosis, the formation of a bipolar mitotic spindle, aligns chromosomes at the metaphase plate before the onset of anaphase. At this point, a checkpoint monitors mitotic spindle integrity and bipolar chromosomal attachments

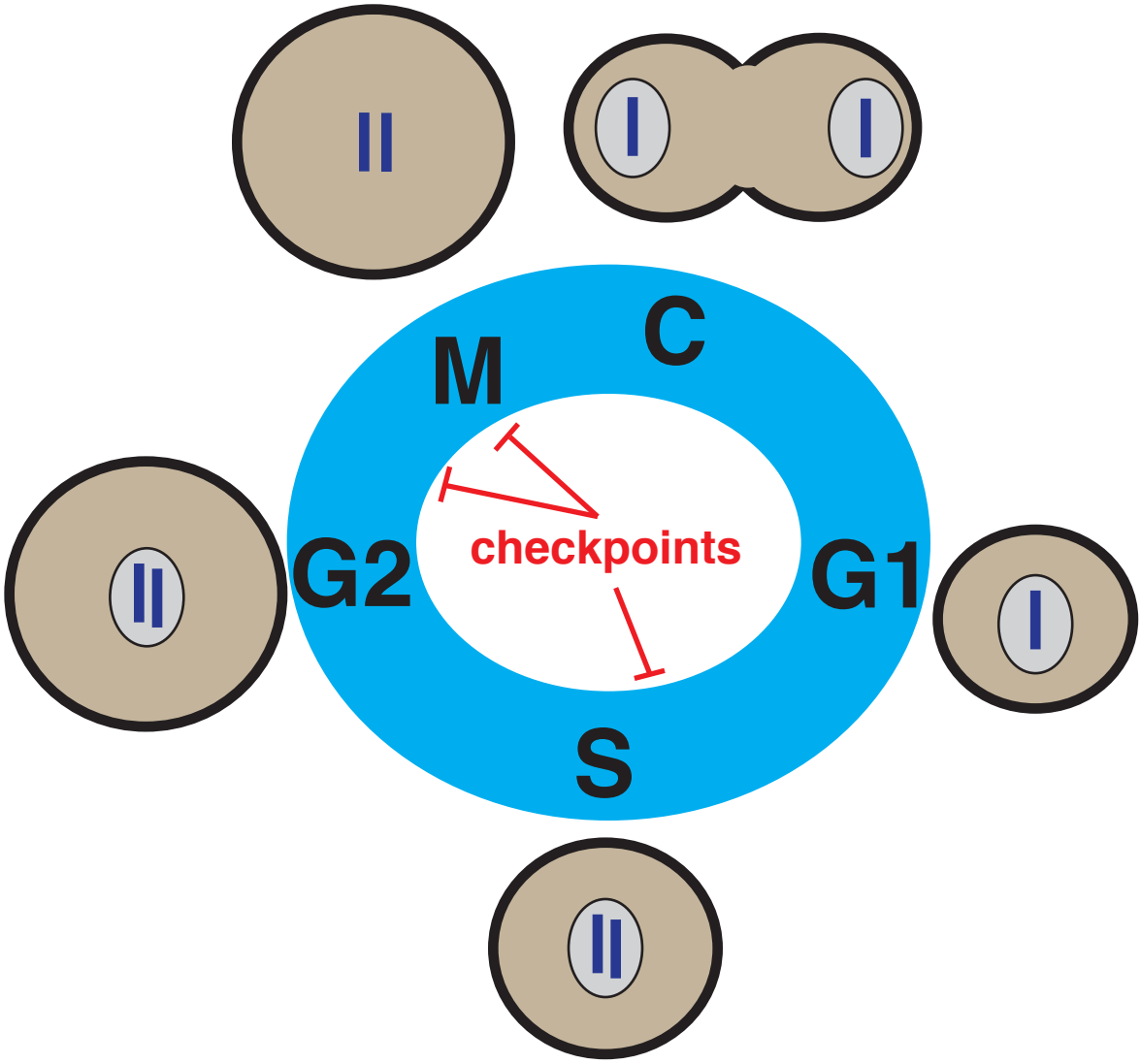

Figure 1-1

Cell cyle checkpoints. The cell division cycle consists of two growth/gap phases, G1 and G2. The genome is duplicated in S-phase and segregated to opposite sides of the cell in M-phase. Cytokinesis (C) completes the cell division process by physically dividing the two new cells. Cell cycle checkpoints stall cycle progression to prevent erroneous DNA content from being distributed to the ensuing progeny. The DNA damage response pathway stalls entry into S-phase and M-phase when DNA damage is detected and a spindle checkpoint stalls mitotic progression if chromosomes do not segregate properly.

(Amon, 1999; Musacchio and Salmon, 2007). If the cell detects a defect in the mitotic spindle, it activates a cascade of biochemical events that target the cell cycle machinery to delay anaphase onset, mitotic exit, and cytokinesis. Because distinct intrinsic networks direct each event, several mechanisms act simultaneously to sufficiently delay each process. For instance, the spindle assembly checkpoint (SAC) targets the anaphase-promoting complex (APC) to prevent securin and cyclin B destruction, which will delay anaphase onset and mitotic exit (Hwang et al., 1998; Kim et al., 1998). In addition to the SAC, studies in yeast indicate that another pathway independent of the SAC inhibits cytokinesis (Alexandru et al., 1999; Beltraminelli et al., 1999; Gardner and Burke, 2000). In the fission yeast *Schizosaccharomyces pombe,* this checkpoint pathway targets a conserved protein network called the septation initiation network (SIN) (discussed later) that is responsible to trigger cytokinesis (Guertin et al., 2002).

Schizosaccharomyces pombe **as a model system to study cell division**

Much of our current understanding of cell division derives from studying simpler model organism, such as *Schizosaccharomyces pombe*. This rod-shaped unicellular organism grows primarily at its tips, undergoes a closed mitosis (no nuclear envelope breakdown), and divides via binary fission using an actomyosin-based CR. *S. pombe* is a useful model organism to study the cell cycle because its cell size is tightly coupled to its cell cycle stage, it is amenable to genetic and biochemical study, and a comprehensive collection of deletion and temperature-sensitive mutants are readily available (Goyal et al., 2011). Because many key genes required for *S. pombe* cytokinesis are conserved in

metazoans, studies of *S. pombe* cytokinesis have pioneered many principal discoveries that have shaped our current understanding of cytokinesis in multi-cellular organisms.

To better understand cytokinesis, several genetic screens were performed in *S. pombe* that enabled the identification of genes required specifically for division site specification, CR assembly, and CR constriction/septation (Balasubramanian et al., 1998; Chang et al., 1996; Minet et al., 1979; Nurse et al., 1976). One set of mutations impacting CR assembly, constriction, and septation displayed a number of genetic interactions with each other and were thus proposed to constitute a signal transduction cascade that initiated the final steps in cytokinesis (Marks et al., 1992). Subsequent biochemical characterization and epistatic analyses led to our current understanding of their functional integration in an ordered pathway that is now termed the septation initiation network (SIN) (Figure 1-2).

The septation initiation network (SIN)

Introduction to the SIN

That mitosis (division of genetic material) precedes cytokinesis (division of cytoplasmic material) is critical to ensure the survival of each new cell and, thus, mitotic events must be intimately linked with cytokinetic events, such that they occur in an orderly fashion. Low CDK activity is a hallmark of mitotic exit and, therefore, many organisms respond to changes in CDK activity as a mechanism to couple mitosis with cytokinesis. The fission yeast *Schizosaccharomyces pombe* utilizes a conserved signaling pathway called the septation initiation network (SIN) that induces cytokinesis only when CDK activity drops in anaphase (Chang et al., 2001; Guertin et al., 2000), guaranteeing

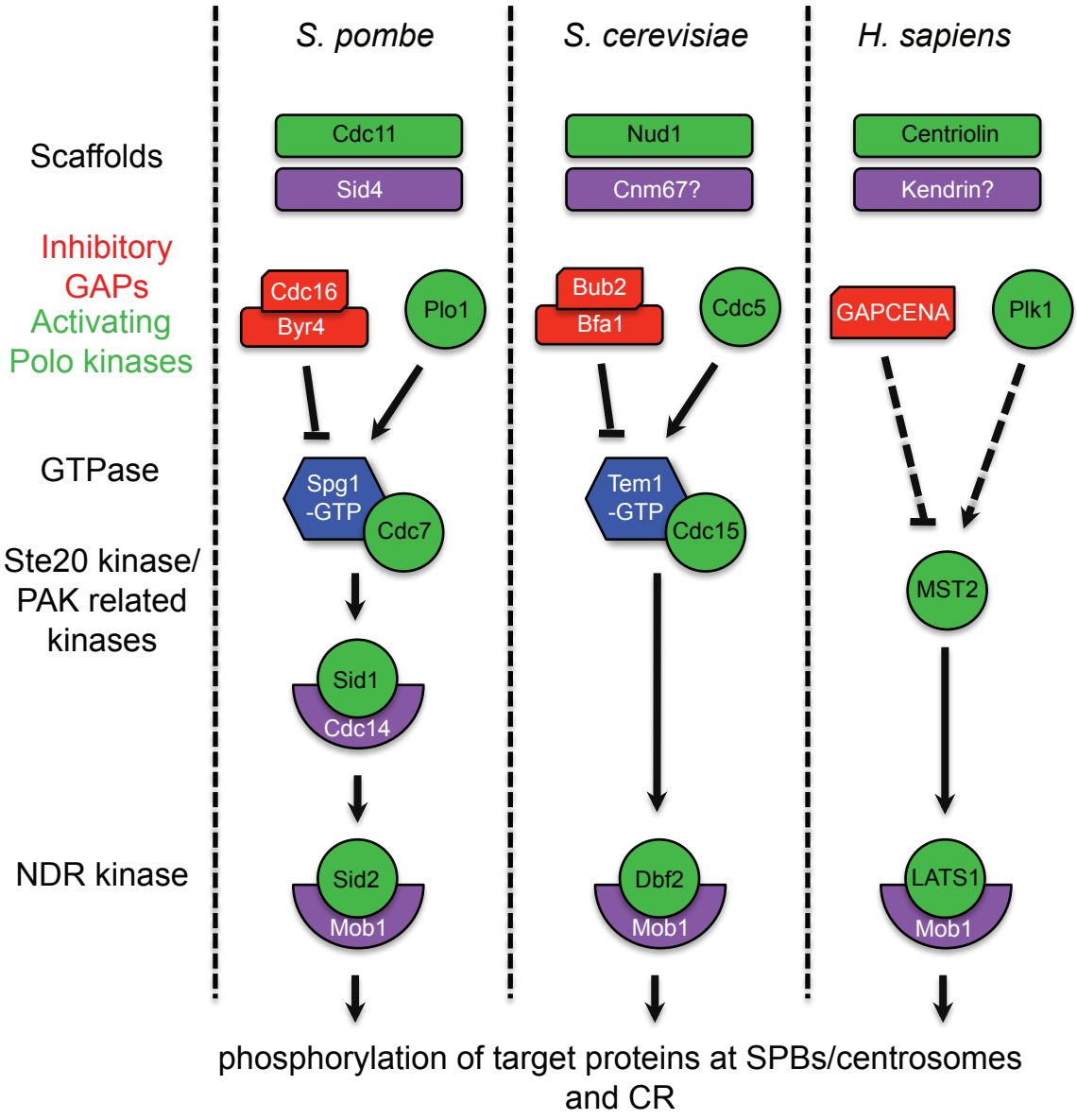

Figure 1-2

The essential signaling components of the SIN/MEN pathways in *S. pombe*, *S. cerevisiae* and *H. sapiens*.

In *S. pombe*, the SIN is anchored to SPBs via a bipartite scaffold complex, Cdc11-Sid4. During interphase, the Cdc16-Byr4 GAP complex inhibits the Spg1 GTPase to hold it in its GDP-bound form. Upon mitotic entry, Plo1 promotes Spg1 activation, perhaps through inhibition of Cdc16-Byr4 allowing Spg1 to switch to its active GTP-bound form. Spg1-GTP binds its effector kinase Cdc7 and elicits activation of the downstream SIN kinases Sid1-Cdc14 and Sid2-Mob1. Upon activation, Sid2-Mob1 translocates to the CR and presumably phopshorylates key substrates that promote CR assembly and constriction. Similar mechanisms of SIN/MEN activation also occur in *S. cerevisiae* and *H. sapiens*.

that cytokinesis occurs after chromosome segregation. A pathway homologous to the SIN, termed the mitotic exit network (MEN), exists in the budding yeast *S. cerevisiae* (Bardin and Amon, 2001; Seshan and Amon, 2004). Almost all SIN components have orthologs in the MEN and the pathways have similar organization (Figure 1-2 and 1-3A). SIN/MEN orthologs also exist in metazoans (Figure 1-2 and 1-3A), underscoring the conservation of these pathways; however, the functions of metazoan SIN/MEN pathways in cell division are less well characterized. Thus, understanding cytokinesis regulation by the yeast SIN/MEN should aid in our understanding of the metazoan pathways.

Functions of the SIN in cytokinesis

SIN mutants generate one of two phenotypes: multi-nucleate cells or multi-septated cells that fail in cell cleavage (Figures 1-3B-C). The former phenotype is caused by SIN inactivation; the latter phenotype results from SIN hyper-activity. Both scenarios uncouple cell division from nuclear division; thus, the SIN coordinates cytokinesis with other cell cycle phases.

Detailed analyses of SIN mutant phenotypes indicate that the SIN is essential for CR assembly and constriction as well as septum formation. In *S. pombe,* the anillin-related Mid1 protein and the SIN drive CR assembly in early (pre-anaphase) and late mitosis (anaphase/telophase), respectively. In early mitosis, Mid1 localizes to cortical nodes near the site of division and recruits CR components (Motegi et al., 2004; Sohrmann et al., 1996; Wu et al., 2006). These nodes then coalesce into a ring-like structure, which matures into a continuous ring (Vavylonis et al., 2008; Wu et al., 2003). A CR can assemble in both *mid1* (Sohrmann et al., 1996) and SIN mutants

A

Core SIN components			
S. pombe	***S. cerevisiae***	***H. sapiens***	**gene product**
Sid4	Cnm67p?	Kendrin?	Scaffold
Cdc11	Nud1p	Centriolin	Scaffold
Spg1	Tem1p	?	GTPase
Cdc7	Cdc15p	MST2?	Ste20 family protein kinase
Sid1	?	MST2?	PAK-related protein kinase
Cdc14	?	?	Sid1co-factor
Sid2	Dbf2p	LATS1	NDR family protein kinase
Mob1	Mob1p	MOB1A	Sid2 co-factor
Byr4	Bfa1p	?	GAP scaffold
Cdc16	Bub2p	GAPCENA	GAP
Etd1	Lte1p	?	GEF-like protein
SIN regulators			
S. pombe	***S. cerevisiae***	***H. sapiens***	**gene product**
Plo1	Cdc5p	PLK1	Polo-like protein kinase
Dma1	Dma1p/Dma2p	CHFR/RNF8	E3 ubiquitin ligase
Clp1	Cdc14p	CDC14	protein phosphatase
Cdc2	Cdc28p	CDK	protein kinase
Zfs1	Tis11p/cth1p	?	Zn finger protein
Par1	Rts1p	?	PP2A B' subunit
Csc1	Far10p	SLMAP	PP2A B''' subunit

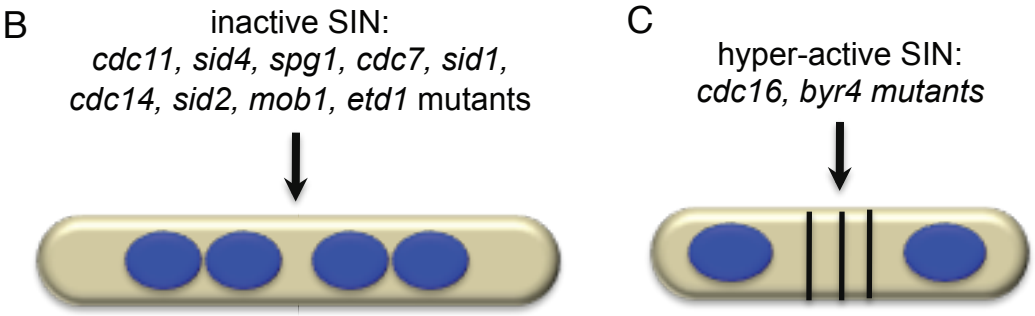

Figure 1-3
SIN homologs and SIN mutant phenotypes.
A. List of *S. pombe* SIN proteins and their homologs in *S. cerevisiae* and *H. sapiens*. B. Phenotype observed when the SIN is inactivated. Inactivating mutations in SIN activators *cdc11, sid4, spg1, cdc7, sid1, cdc14, sid2, mob1,* and *etd1* produce multinucleate cells as a result of cytokinesis failure. C. Phenotype observed when the SIN is hyper-active. Inactivating mutations in the SIN inhibitors *byr4* and *cdc16* produce multi-septated cells.

(Balasubramanian et al., 1998; Wu et al., 2003), suggesting that these two pathways are independent; however, distinct defects are observed in each case. *mid1*Δ mutants assemble ectopic rings in anaphase when the SIN becomes active, implying that the major function of Mid1 is to direct CR assembly to the correct location (Chang et al., 1996; Sohrmann et al., 1996). SIN mutants form a CR in early mitosis (presumably by the Mid1 pathway); however, it dissolves in anaphase suggesting that SIN signaling is required for CR maintenance/assembly in late mitosis (Balasubramanian et al., 1998). Disrupting both Mid1 and the SIN blocks CR assembly completely (Hachet and Simanis, 2008; Huang et al., 2008), indicating that each pathway makes important contributions to CR assembly. However, activating the SIN in interphase triggers CR assembly, demonstrating that the SIN is capable of driving CR assembly on its own (Schmidt et al., 1997). Because SIN mutants also fail to deposit septum material, the SIN might also promote the activity of enzymes involved in septum deposition, such as the glucan synthase Cps1 (Balasubramanian et al., 1998).

Although major progress has been made towards understanding Mid1-dependent CR assembly, the role of the SIN in CR assembly is less clear, particularly because the pertinent SIN substrates at the CR are unknown. The only SIN component that localizes to the CR is the terminal SIN kinase Sid2-Mob1 and, to date, the only reported Sid2 target at the CR is the Cdc14-like phosphatase Clp1 (Chen et al., 2008). During interphase, Clp1 is sequestered in the nucleolus and is released into the cytoplasm early in mitosis, such that it can localize to the CR ring and de-phosphorylate its substrates (Trautmann et al., 2001). Clp1 phosphorylation by Sid2 promotes binding of the 14-3-3 protein, Rad24, which maintains Clp1 in the cytoplasm during cytokinesis (Chen et al.,

2008; Mishra et al., 2005). Without Sid2 phosphorylation, Clp1 returns prematurely to the nucleolus and cells exhibit cytokinesis defects. One direct Clp1 target is the PCH-family protein Cdc15, which is essential for CR assembly and must be de-phosphorylated to efficiently assemble the CR (Clifford et al., 2008; Roberts-Galbraith et al., 2010). Consistent with the role of Sid2 in Clp1 regulation, Cdc15 at the CR is severely diminished when Sid2 function is compromised (Hachet and Simanis, 2008), most likely because Clp1 is not maintained in the cytoplasm to de-phosphorylate Cdc15. Thus, Sid2-dependent phosphorylation of Clp1 is important for the final steps in cytokinesis. However, other Sid2 substrates at the CR must exist, since Clp1 is non-essential, and identifying the essential Sid2 substrates will be important to completely understand how the SIN drives CR assembly and constriction.

Spindle pole bodies as a signaling hub for cytokinesis

Several studies indicate that spindle pole bodies (SPBs) provide an essential platform for SIN signaling. Specifically, ablating both mitotic SPBs results in cytokinesis failure (Magidson et al., 2006), indicating that cytokinesis requires signals emanating from SPBs. In accord with this observation, SIN components assemble at SPBs via a bipartite scaffold complex Sid4-Cdc11 (Figure 1-4A-C) (Chang and Gould, 2000; Krapp et al., 2001; Morrell et al., 2004; Tomlin et al., 2002). Sid4-Cdc11 localize to SPBs in all cell cycle phases and fluorescence recovery after photo-bleaching (FRAP) experiments indicate that association with the SPBs is stable (Feoktistova et al., 2012; Morrell et al., 2004). Another SPB protein, Ppc89, anchors the Cdc11-Sid4 scaffold to SPBs by directly binding the C-terminus of Sid4 (Rosenberg et al., 2006). Together,

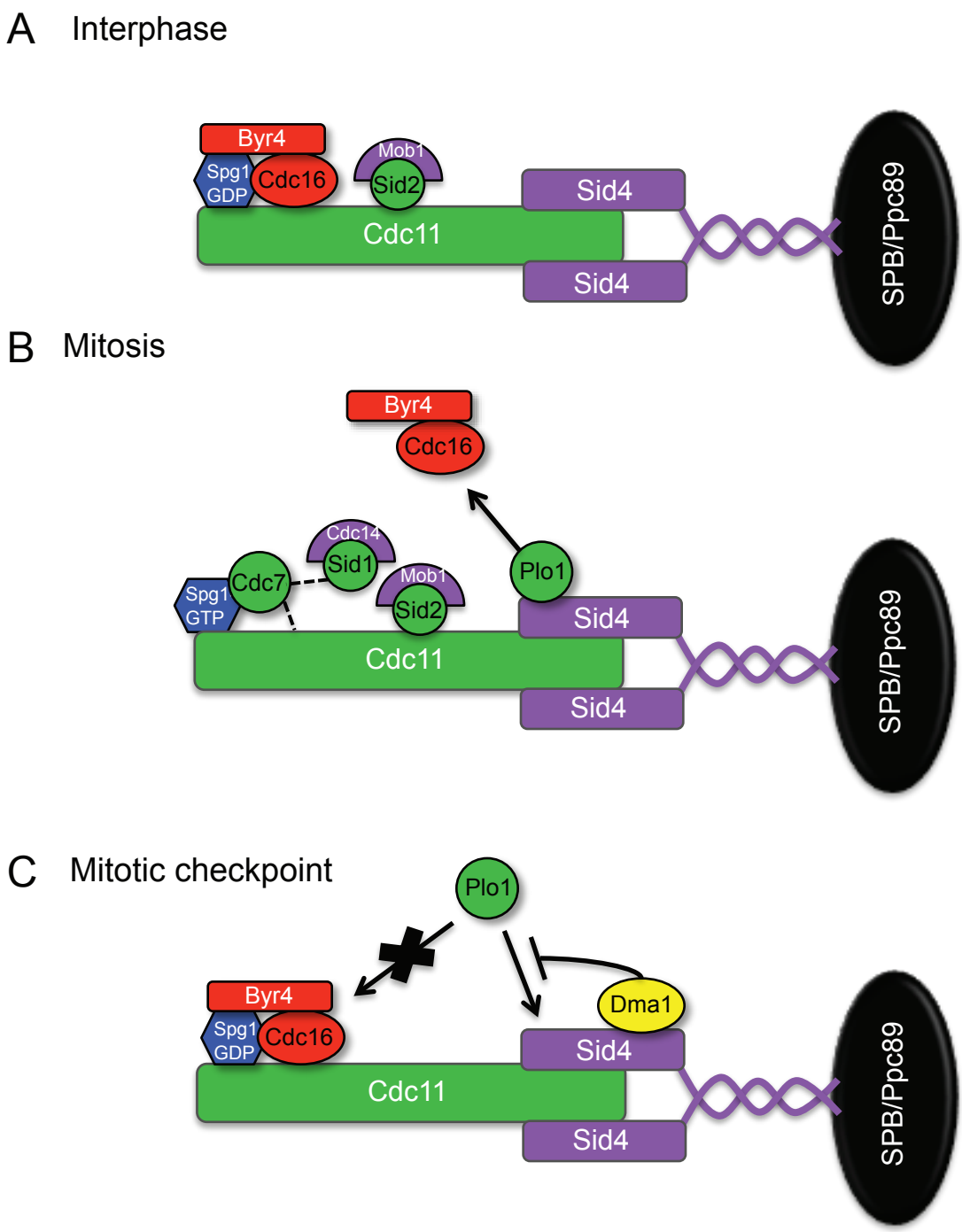

Figure 1-4

Organization of SIN components at SPBs

Localization pattern of SIN proteins during interphase (A) mitosis (B) and a mitotic checkpoint (C). Proteins in contact indicate interactions detected by two-hybrid or in vitro experiments and dashed lines indicate potential interactions based on epistatic experiments.

Sid4-Cdc11 establishes a signaling hub onto which SIN signaling components and their regulators assemble (Morrell et al., 2004).

In addition to providing a stable platform for SIN components, evidence suggests that post-translational modifications acquired by Cdc11-Sid4 modulate their scaffold functions and, thus, provide another level of SIN regulation. Prior to CR assembly and constriction Cdc11 is hyper-phosphorylated, which enhances SIN activation by promoting recruitment of downstream SIN kinases (Feoktistova et al., 2012; Krapp et al., 2003). Sid4 is ubiquitinated during a mitotic checkpoint arrest, which inhibits recruitment of an essential SIN activator (Plo1) until the checkpoint has been satisfied (Johnson and Gould, 2011). In both cases, modifying Cdc11 and Sid4 alters their binding capacity for the signaling components with which they interact and, thereby, affects SIN signaling.

Signaling through the SIN

SIN signaling progresses through sequential activation of the Ras super-family GTPase Spg1 and its downstream effectors. Spg1 localizes to SPBs constitutively by direct interaction with Cdc11 (Morrell et al., 2004) and can drive cytokinesis in any cell cycle stage when over-expressed (Schmidt et al., 1997). During interphase, Spg1 associates with a bipartite GAP, Byr4-Cdc16, which maintains Spg1 in its inactive state and is required for interphase SPB localization of Spg1 (Figure 1-4A) (Furge et al., 1999; Furge et al., 1998; Krapp et al., 2008; Song et al., 1996). Upon mitotic entry, Byr4-Cdc16 dissociates from SPBs, allowing Spg1 to switch to its GTP-bound active state (Li et al., 2000).

Spg1 activation subsequently triggers the activity of three protein kinases (Cdc7, Sid1 and Sid2) in a step-wise manner (Figure 1-2). The Ste20 family protein kinase, Cdc7, preferentially binds the GTP-bound activated form of Spg1, and the two proteins depend on each other for SPB localization when Spg1 is in its active form (Fankhauser and Simanis, 1994; Krapp et al., 2008; Sohrmann et al., 1998). Because Cdc7 preferentially binds Spg1 is in its active form, its presence at the SPB can be used to monitor Spg1 activity in vivo. Cdc7 protein levels and kinase activity do not fluctuate throughout the cell cycle; thus, Cdc7 function is mainly regulated by its SPB recruitment (Sohrmann et al., 1998). Cdc7 localizes to both SPBs early in mitosis and as the spindle elongates, Cdc7 disappears from one SPB and accumulates at the opposite SPB (Sohrmann et al., 1998). Byr4-Cdc16 returns to the SPB in which Cdc7 disappears, inactivating and preventing further SIN signaling on this pole (Li et al., 2000). Thus far, a target of the Cdc7 protein kinase has not been identified, although by analogy to the budding yeast homologs (Mah et al., 2005), Sid2 is a likely Cdc7 target.

At anaphase onset, the protein kinase Sid1 and its binding partner Cdc14 localize to the SPB with active Spg1 (Fankhauser and Simanis, 1993; Guertin et al., 2000). Sid1 requires Sid4, Cdc11, Cdc14, Spg1 and Cdc7 for its SPB recruitment placing it downstream of Cdc7 recruitment (Guertin et al., 2000). Sid1 protein levels are not cell cycle dependent; however, Sid1 kinase activity peaks in late anaphase/telophase, coincident with its SPB localization (Guertin and McCollum, 2001). Sid1-Cdc14 SPB localization also depends on decreased CDK activity (Guertin et al., 2000), which normally occurs at anaphase onset, providing one mechanism to couple exit from mitosis

with initiation of cytokinesis. Unfortunately, our knowledge of Sid1 targets is also lacking, but Sid2 and/or its binding partner Mob1 are potential substrates.

Sid2, a member of the NDR (nuclear Dbf2-related) family of kinases, and its partner Mob1 localize to SPBs constitutively and function downstream of Sid1-Cdc14 (Hou et al., 2004; Hou et al., 2000; Salimova et al., 2000; Sparks et al., 1999). Sid2 kinase activity requires Mob1 association and its activity peaks prior to septation (Hou et al., 2004; Sparks et al., 1999). Sid2-Mob1 also localize to the division site (Sparks et al., 1999), where Sid2 presumably phosphorylates its substrates to drive CR assembly and constriction. Sid2-Mob1 division site localization depends on an intact microtubule cytoskeleton (Sparks et al., 1999), but the mechanisms of Sid2-Mob1 re-localization are still unknown. Similar to other NDR family kinases, Sid2 phosphorylation is important for Mob1 association and, thus, for its catalytic activity (Hou et al., 2004). The kinase(s) that phosphorylate Sid2 are unknown, but the human Sid2 homolog, LATS1, is phosphorylated and activated by the Ste20 kinase MST2 (Chan et al., 2005), implicating Cdc7 or Sid1 as candidates. The phosphatase(s) for Sid2 are also unknown, but several studies implicate PP2A phosphatases in SIN inhibition (discussed later) and PP2A phosphatases have been reported to antagonize NDR kinases in mammalian cells (Millward et al., 1999). Because Sid2 is the terminal SIN kinase, regulating Sid2's phosphostatus is likely to be an important aspect of SIN regulation.

Asymmetry in SIN signaling

As mentioned previously, SIN signaling is asymmetric on the two SPBs during anaphase (Figure 1-5). By exploiting the slow folding nature of red fluorescent protein

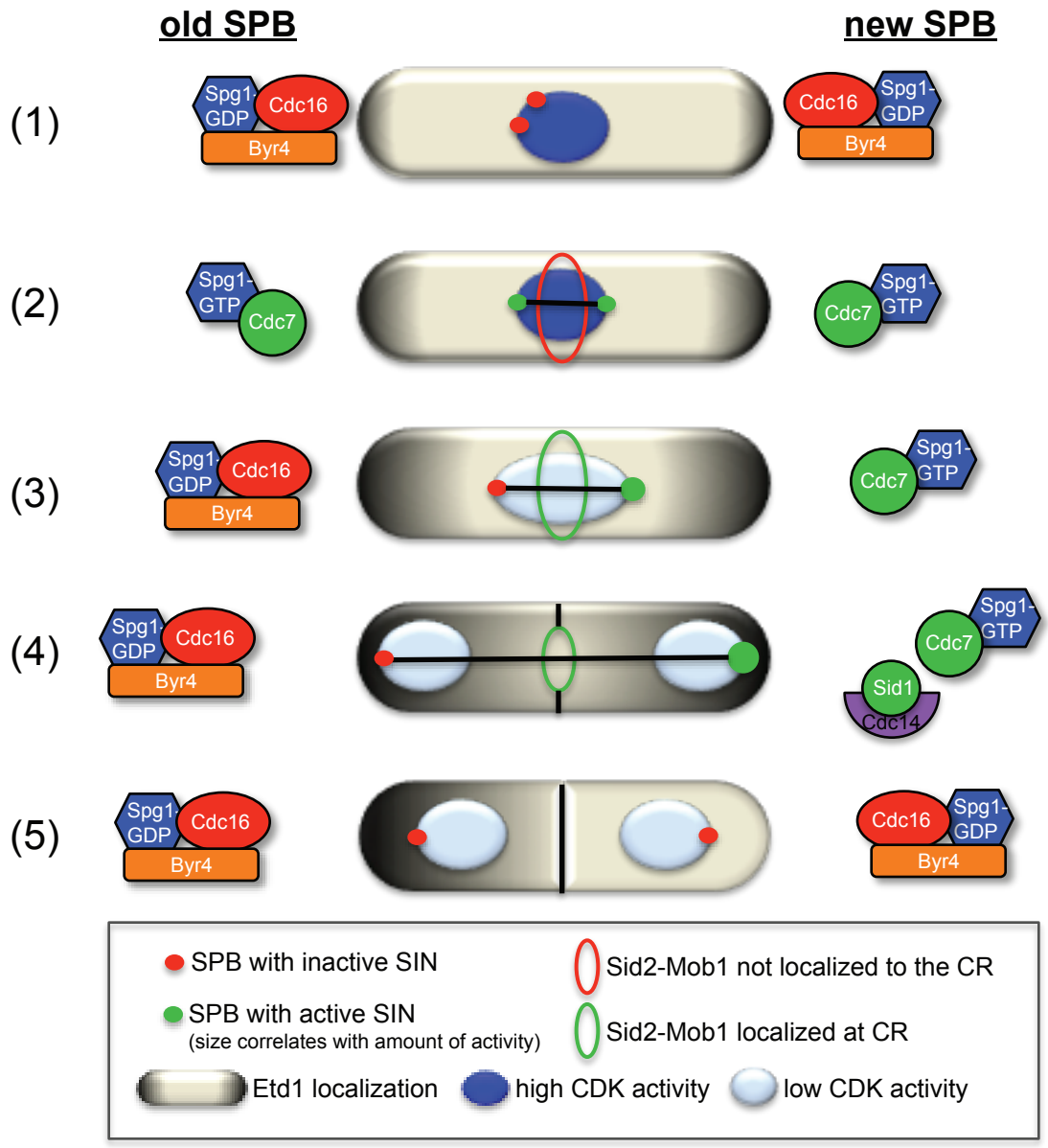

Figure 1-5

Asymmetric localization patterns of the SIN signaling proteins.
(1) In interphase and early pro-metaphase, Byr4-Cdc16 localize to both SPBs and maintains Spg1 in its GDP-bound inactive state. (2) In late pro-metaphase to metaphase, Cdc7 localizes to both SPBs via interaction with Spg1-GTP. (3) As the spindle elongates in anaphase, Cdc7 disappears from the 'old' pole and Byr4-Cdc16 returns to the 'old' pole to inactivate the SIN and establish SIN asymmetry. (4) Later in mitosis. when CDK activity is low, Sid1-Cdc14 localizes to the 'new' SPB with active SIN signaling and as the SPBs reach the cell cortex, Etd1 contacts Spg1 and further activates the SIN on the 'new' pole. Since Spg1 is bound to the inhibitory GAP complex (Byr4-Cdc16) on the 'old' pole, Etd1 is probably prevented from contacting Spg1 on the 'old' pole. Once the spindle is fully elongated, Sid2-Mob1 translocates to the division site and induces CR constriction. (5) After septation, Etd1 disappears from the cell compartment with active SIN signaling and Byr4-Cdc16 returns to this SPB to terminate SIN signaling.

(RFP) to mark the 'old' SPB, it was discovered that the SIN is hyper-activated on the 'new' SPB (Grallert et al., 2004). MEN activity is also asymmetric on the two SPBs; however, in contrast to the SIN, the MEN is active on the 'old' SPB (Pereira et al., 2001). SIN asymmetry can be monitored by examining the localization of certain SIN proteins throughout mitosis. Cdc7 localizes to both SPBs in metaphase, but becomes asymmetric once the spindle elongates (Sohrmann et al., 1998). In wild-type cells, Sid1 localizes exclusively to one of the two SPBs during anaphase (Guertin et al., 2000) and presumably the SPB that retains Cdc7, since Sid1 requires Cdc7 for SPB localization (Guertin et al., 2000). In contrast, Byr4 localizes to the interphase SPB and disappears from the 'new' pole as the SPBs separate to opposite sides of the nucleus (Cerutti and Simanis, 1999). Byr4 asymmetry precedes that of Cdc7, and Byr4 and Cdc7 SPB localizations are always reciprocal (Cerutti and Simanis, 1999). Thus, Byr4-Cdc16 and Cdc7 localization dictate SIN asymmetry in anaphase B by inactivating Spg1 on the 'old' pole and promoting SIN activity on the 'new' pole, respectively.

So why do cells possess such elaborate mechanisms to generate asymmetric SIN signaling? Results from one study demonstrated that in wild-type cells, the SIN is inactivated precisely when the CR completes constriction and asymmetric SIN signaling is important to inactivate the SIN when cytokinesis is complete (Garcia-Cortes and McCollum, 2009). Using binucleate dikaryon cells (which can have either symmetric or asymmetric SIN signaling), this study also showed that cells with symmetric SIN activity were defective in terminating SIN signaling and formed additional rings and septa (Garcia-Cortes and McCollum, 2009). Consistent with this observation, inactivating a **S**IN **i**nhibitory **P**P2A complex (SIP, discussed in the next section) results in 100% of

anaphase cells with symmetric Cdc7 localization and also produces a few cells with premature and multiple septations (Singh et al., 2011). The relatively mild defect in terminating SIN signaling displayed by SIP mutants might be explained by the observation that the SIN eventually becomes asymmetric in these mutants just before septation completes (Singh et al., 2011), indicating that other factors contribute to SIN asymmetry. Collectively, these studies suggest that SIN asymmetry contributes to silencing the SIN after cytokinesis completes. The formation of additional rings and septa could also indicate that SIN asymmetry is important to initiate cytokinesis only once and the presence of two signaling hubs creates conflicting signals, resulting in multiple rounds of septation.

The SIN in meiosis

Given its role in driving septum formation, it is not surprising that the SIN also operates during meiosis. Specifically, the SIN is activated during the second meiotic division and is required for fore-spore membrane assembly (Krapp et al., 2006). During meiosis, F-actin assembles into 4 ring structures, termed Meiotic actin rings (MeiAR). Constriction of the MeiARs is the final step in fore-spore membrane assembly and the SIN controls the rate of MeiAR constriction (Yan and Balasubramanian, 2012).

A Sid2-like kinase, Slk1, is expressed specifically during meiosis and requires the SIN for its localization to SPBs (Perez-Hidalgo et al., 2008; Yan et al., 2008). Deletion of *slk1* results in decreased sporulation efficiency and deletion of both *slk1* and *sid2* prevents sporulation completely. Thus, Slk1 and Sid2 have some redundant roles in

forespore membrane assembly, but meiotic substrates of Slk1 and Sid2 remain to be identified.

The SIN inhibitor, Dma1, is also implicated in regulating forespore membrane assembly (Krapp et al., 2010; Li et al., 2010b). Consistent with a role in meiosis, Dma1 is upregulated during meiosis I and II, and similar to its mitotic localization pattern, Dma1 requires the SIN scaffold Sid4 for its SPB localization in meiotic cells (Li et al., 2010b). How Dma1 impacts meiotic progression is not known, but genetic analyses suggest that it might influence Slk1 signaling.

SIN-like pathways in other organisms

Signaling networks homologous to the SIN exist in other organisms including the budding yeast *Saccharomyces cerevisiae* (Seshan and Amon, 2004), the filamentous fungi *Aspergillus nidulans* (Bruno et al., 2001; Kim et al., 2006; Kim et al., 2009) and basidiomycete *Ustilago mayadis* (Sandrock et al., 2006). In metazoans, many SIN homologs exist, suggesting that a similar pathway is present; however, molecular information for the human pathway is lacking (Figure 1-2 and 1-3A).

The NDR protein kinase, LATS1/WARTS, shares many functional similarities with *S. pombe* Sid2. First identified in *D. melanogaster* as members of the *hippo/salvador/warts* pathway, LATS/WARTS kinases function in signaling pathways involved in cell proliferation and apoptosis (Halder and Johnson, 2011). Similar to Sid2, LATS1 functions in mitotic exit and cytokinesis and localizes to centrosomes constitutively and to the division site in late mitosis (Bothos et al., 2005; Hirota et al., 2000; Xia et al., 2002; Yang et al., 2001; Yang et al., 2004). Like other NDR family

kinases, LATS1 associates with its co-factor/activator MOB1A, contributing to LATS1 activation (Chow et al., 2009; Hergovich et al., 2006). LATS1 and MOB1A are further activated by the Ste20 protein kinase, MST2, which shares homology with *S. pombe* Sid1 and Cdc7 (Chan et al., 2005; Hirabayashi et al., 2008). Many human Ste20 protein kinases also require association with GTPases for their activity (Dan et al., 2001); however, the GTPase(s) with which MST2 associates, if one exists, is still unknown.

The GAP protein, GAPCENA is homologous to *S. pombe* Cdc16 and localizes to centrosomes (Cuif et al., 1999). The GTPase that GAPCENA associates with at the centrosomes is not known, but identifying its centrosome-localized GTPase partner might reveal Spg1 homolog(s). Centriolin is a centrosome and mid-body localized protein that shares homology with the SIN scaffold protein Cdc11 and participates in cytokinesis (Gromley et al., 2005). Whether the signaling components for the proposed human "mitotic exit network" associate with Centriolin remains to be determined. Although it still remains to be determined, it is likely that signaling through the human network mirrors that of the yeast SIN/MEN pathways and the work in *S. pombe* could direct future studies of the human network.

Activation of the SIN by the Polo-like kinase, Plo1

Other proteins, which are not considered part of the core SIN machinery, act peripherally to modulate SIN activity. A major positive SIN regulator is the Polo-like kinase Plo1. Plo1 has myriad functions in mitosis and cytokinesis, including formation of a bipolar spindle, CR assembly, division site selection, and septum formation (Mulvihill and Hyams, 2002; Ohkura et al., 1995). Early in mitosis Plo1 concentrates at

SPBs, the mitotic spindle and the CR (Bahler et al., 1998). Plo1 directly interacts with the scaffold Sid4 and activates the SIN pathway when over-expressed (Figure 1-3B) (Morrell et al., 2004; Mulvihill et al., 1999; Ohkura et al., 1995; Tanaka et al., 2001). Thus, Plo1 has long been touted as an upstream activator of the SIN pathway; however, Plo1's target at the SIN remains unknown. Phosphorylation of the *S. cerevisiae* Byr4 homolog, Bfa1, by the Polo-like kinase Cdc5 inhibits its GAP activity and promotes its dissociation from SPBs (Geymonat et al., 2003; Hu et al., 2001). Thus, it is plausible that Byr4 is the major Plo1 target in the SIN (Figure 1-4B).

The SIN as a target of the spindle checkpoint

Several studies show that the SIN is not only required for cytokinesis, but also plays an integral role in checkpoint pathways that ensure coordination of major mitotic events. When chromosomes are not properly attached to the mitotic spindle, SIN activity is inhibited to prevent the CR from cutting through unsegregated chromosomes. One protein that inhibits the SIN under these conditions is the E3 ubiquitin ligase Dma1 (Guertin et al., 2002; Murone and Simanis, 1996). Dma1 was first identified as a SIN inhibitor in a screen aimed at identifying multi-copy suppressors of the SIN inhibitor *cdc16* (Murone and Simanis, 1996). Dma1 is a non-essential protein and loss of Dma1 causes no apparent defects to normal cell cycle progression (Murone and Simanis, 1996). However, cells lacking Dma1 fail to arrest in mitosis when the mitotic spindle is perturbed (Murone and Simanis, 1996). Furthermore, Dma1 localizes faintly at the SPBs and division site during normal cell cycle progression, but increases at the SPBs and

contractile ring during spindle damage (Guertin et al., 2002). These initial studies indicate that Dma1 delays cytokinesis in response to spindle damage (Figure 1-4C).

Structurally, Dma1 contains a Forkhead Associated (FHA) domain, which binds phospho-threonine motifs and a Ring Finger (RF) domain containing E3 ubiquitin ligase activity (Figure 1-6). Checkpoint maintenance requires the function of both domains and Dma1 localization requires the function of the FHA domain (Guertin et al., 2002). Dma1 binds the SIN scaffold, Sid4, through its FHA domain and inhibits SIN signaling when over-expressed (Guertin et al., 2002; Murone and Simanis, 1996). Although the mechanism of Dma1 function is unclear, previous work demonstrates that in *dma1Δ* cells, Plo1 localizes to the SPBs significantly earlier than in *dma1*$^{+}$ cells during a spindle checkpoint response (Guertin et al., 2002). These data suggest that Dma1 normally antagonizes Plo1 from localizing to the SPBs during the checkpoint and prevents Plo1 from activating SIN signaling and initiating cytokinesis.

FHA-RING E3 ligases in checkpoint signaling

FHA-RING E3 ubiquitin ligases represent a unique class of checkpoint proteins that bear both a phosphothreonine-binding FHA domain and a RING E3 ligase domain (Figure 1-6, (Brooks et al., 2008)). While many proteins contain either an FHA or a RING domain, metazoans encode just two proteins that contain both: CHFR (Scolnick and Halazonetis, 2000), which participates in a prophase checkpoint and RNF8 (Tuttle et al., 2007), which has a well-understood role in the DNA damage response (Yan and Jetten, 2008). Yeast homologs include *S. cerevisiae* Dma1 and Dma2 (Fraschini et al., 2004) and *S. pombe* Dma1 (Murone and Simanis, 1996).

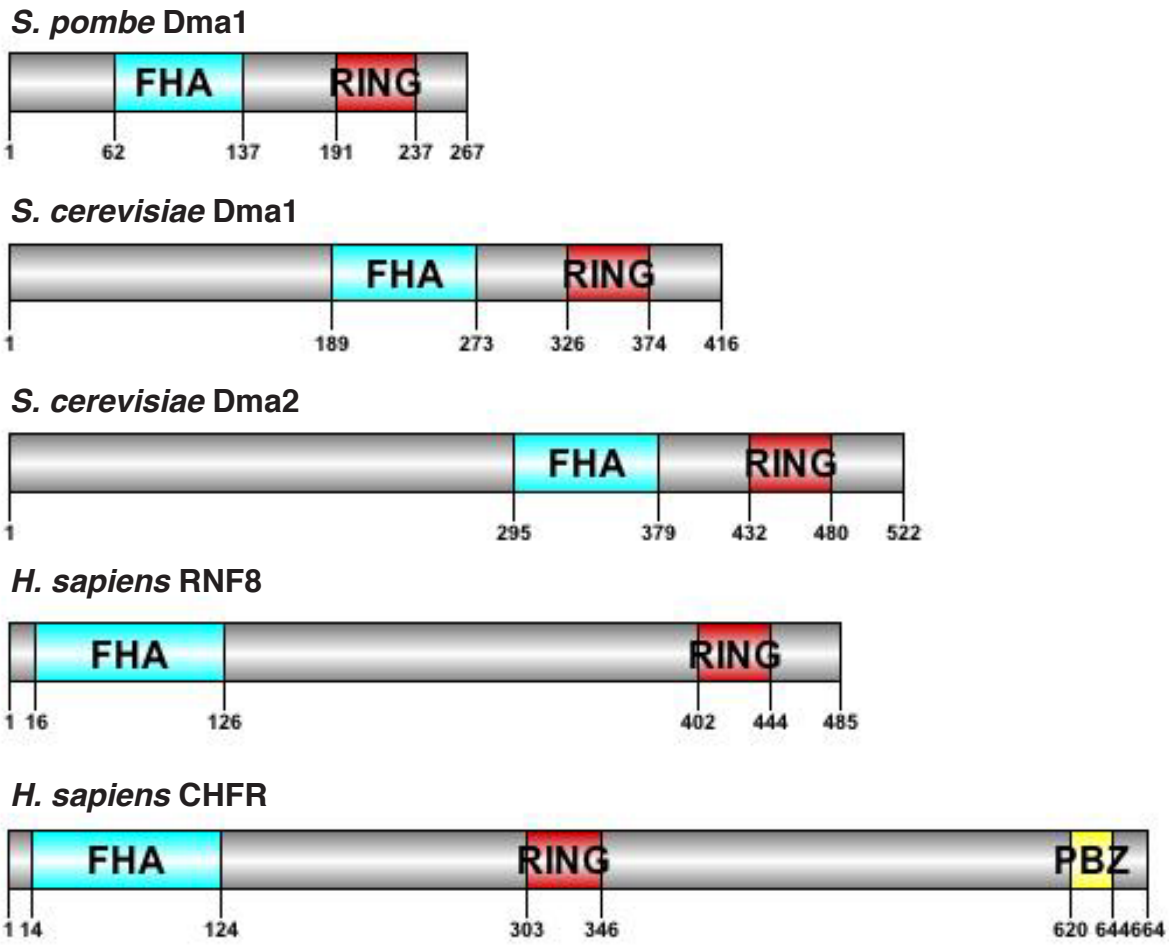

Figure 1-6

Domain architecture of Dma1 and its homologs in other organisims.

Although FHA-RING E3 ligases are dispensable for cell viability, they are critical to suppress chromosomal instabilities when cells are exposed to cytotoxic or genotoxic stresses. This is evident by the fact that deleting RNF8 predisposes mice to cancer (Li et al., 2010a). Similarly, CHFR-/- mice form tumors when exposed to low doses of carcinogens (Yu et al., 2005) and CHFR is epigenetically silenced in a variety of tumor tissues (Soutto et al., 2010; Toyota et al., 2003). Thus, FHA-RING E3 ligases likely contribute to mitotic fidelity irrespective of checkpoint stimulation, but their activities are amplified during a checkpoint arrest.

While significant differences exist between these proteins, they all have roles in antagonizing members of the Polo-like family of kinases, underscoring their functional conservation. However, whether these proteins antagonize Polo-like kinases directly or indirectly is controversial (Kang et al., 2002; Matsusaka and Pines, 2004). Resolving this conflict requires a detailed understanding of Dma1-related proteins and *S. pombe* provides many experimental advantages to dissect their mechanism of action.

Summary

Two major outstanding questions regarding Dma1 function exist: what biochemical response does Dma1 elicit to delay cytokinesis and how does Dma1 sense spindle damage? In chapter II, I will explore the mechanism of cytokinesis inhibition by Dma1. In chapter III, I will focus on understanding how signals from the kinetechore-microtubule interface are relayed to SPBs where Dma1 exerts its functions. In chapters IV and V, I will explore various mechanisms that regulate Dma1 function and discuss the major implications of these findings.

CHAPTER II

DMA1 UBIQUITINATES THE SIN SCAFFOLD SID4 TO IMPEDE THE MITOTIC LOCALIZATION OF PLO1 KINASE

Johnson A.E. and Gould K.L. (2011)

The EMBO Journal, 30:341-54

Introduction

At the end of each cell division cycle, chromosomes segregate to opposite sides of the cell and a cytokinetic ring (CR) assembles and constricts between them to physically separate the two new cells. Clearly, it is critical that chromosome segregation occurs prior to ring constriction and, thus, mitosis and cytokinesis must be coupled to ensure each new cell inherits the proper genetic complement. In the fission yeast, *Schizosaccharomyces pombe*, the septation initiation network (SIN) confers proper coordination by triggering contractile ring constriction once mitosis is complete (for review see (Krapp et al., 2004; McCollum and Gould, 2001). Thus, precise activation of the SIN is required for the fidelity of each cell division.

In the event of a mitotic error, cytokinesis must be inhibited to ensure equal partitioning of genetic material. In the fission yeast, *Schizosaccharomyces pombe*, the checkpoint protein and E3 ubiquitin ligase, Dma1, delays cytokinesis by inhibiting the septation initiation network (SIN) when chromosomes are not attached to the mitotic spindle. Dma1 binds the SIN scaffold, Sid4, and delays recruitment of Plo1 to SPBs during a checkpoint response (Guertin et al., 2002); however, the mechanism by which this occurs is unknown. In this chapter, we explore the mechanism by which Dma1

inhibits the SIN. We screened all SIN components as potential Dma1 substrates and found that the SIN scaffold protein, Sid4, is ubiquitinated *in vivo* in a Dma1-dependent manner. To investigate the role of Sid4 ubiquitination in checkpoint function, a ubiquitination deficient *sid4* allele was generated and our data indicate that Sid4 ubiquitination by Dma1 is required to prevent cytokinesis during a mitotic checkpoint arrest. Furthermore, Sid4 ubiquitination delays recruitment of the Polo-like kinase and SIN activator, Plo1, to spindle pole bodies (SPBs), while at the same time prolonging residence of the SIN inhibitor, Byr4, providing a mechanistic link between Dma1 activity and cytokinesis inhibition.

Results

The SIN scaffold, Sid4, is ubiquitinated in vivo

dma1$^+$ encodes a RF domain, which is predicted to have E3 ubiquitin ligase activity (Figure 2-1A). To determine whether Dma1 is in fact a functional E3 ubiquitin ligase, Dma1 was tagged at its endogenous C-terminus with HA_3-TAP and purified from *S. pombe* lysates. When the TAP eluate was incubated with an E1-activating enzyme and the E2-conjugating enzyme, Ubc13-Uev1a, Dma1 catalyzed formation of polyubiquitin chains *in vitro* (Figure 2-1B, left panel). To be sure that the polyubiquitin chains were formed in a Dma1-specific manner and were not a product of another E3 contaminant present in the TAP eluate, a conserved hydrophobic residue within the RF domain (I194) that is expected to disrupt interaction with its cognate E2 enzyme (Katoh et al., 2003) was mutated to alanine (Figure 2-1A). When the Dma1(I194A)-HA_3-TAP eluate was incubated with the E1 and E2 enzymes, polyubiquitin chains were not formed (Figure 2-

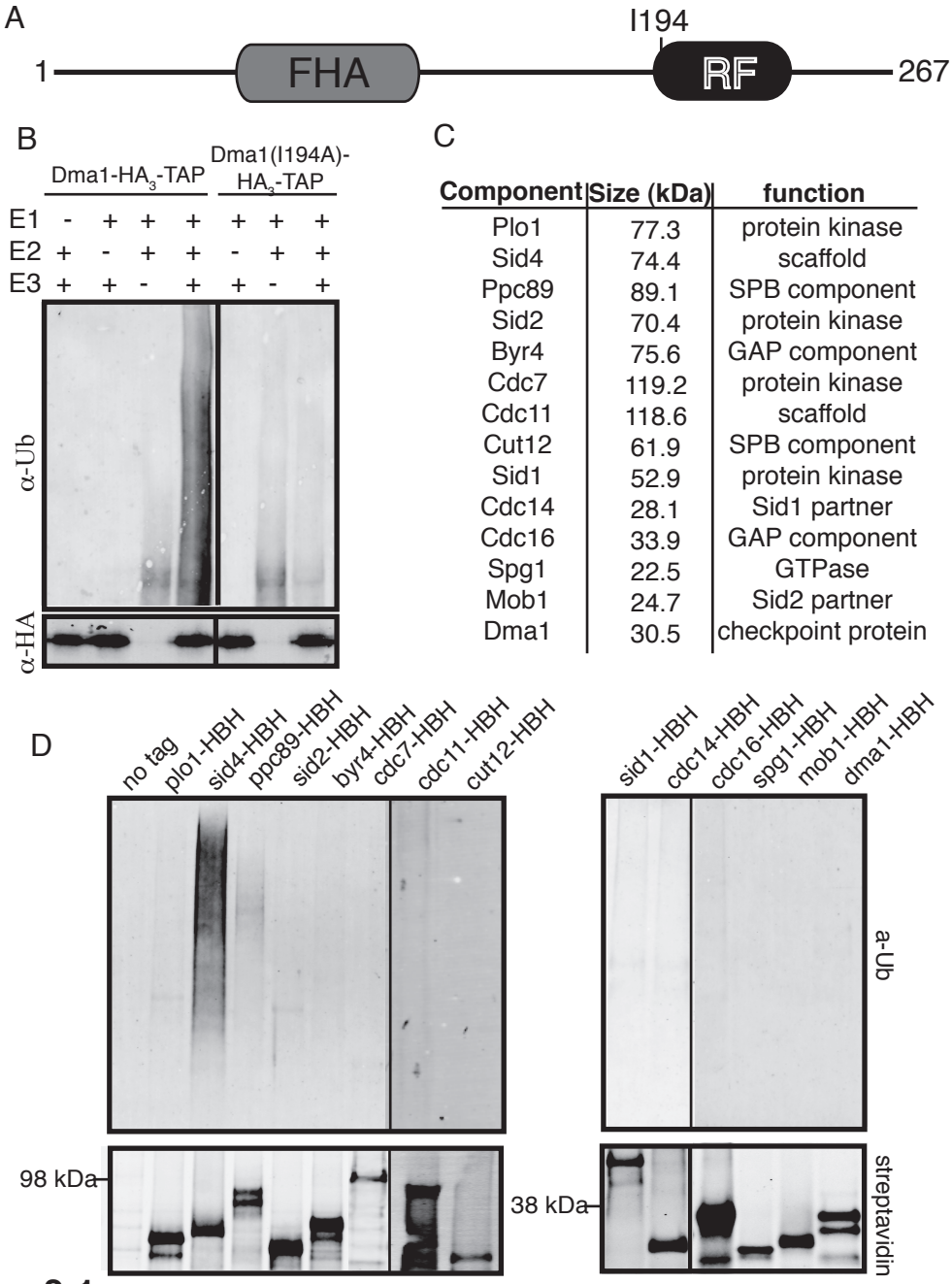

Figure 2-1

The SIN scaffold, Sid4, is ubiquitinated in vivo.

A. Schematic diagram of Dma1 protein with relative positions of Dma1 FHA and RF domains and the I194A point mutation indicated. B. In vitro ubiquitination assay using an E1-activating enzyme, the human E2-conjugating enzyme, Ubc13/Uev1a and either dma1-HA_3-TAP or dma1(I194A)-HA_3-TAP purified from *S. pombe* lysates arrested by the *nda3-KM311* mutation. C. List of SIN and SPB proteins screened for in vivo ubiquitination. D. In vivo ubiquitination assay of proteins listed in C. Each protein was purified from checkpoint-activated cells (*nda3-KM311*) and visualized by immunoblot using fluorescently labeled Streptavidin (bottom panels) and a Ubiquitin antibody (top panels).

11B, right panel). Taken together, these data indicate that the predicted RF domain of Dma1 confers ubiquitin ligase activity to the protein.

Given that the Dma1 RF domain is required to maintain a spindle checkpoint arrest and that *dma1*$^{+}$ antagonizes SIN signaling by perturbing Plo1 SPB localization (Guertin et al., 2002), we reasoned that Dma1 performed its checkpoint function by targeting Plo1 or another SIN component(s) for ubiquitination. Therefore, the *in vivo* ubiquitination status of Plo1 and every SIN component (Figure 2-1C) was examined in checkpoint-activated cells (Figure 2-1D). We also tested the ubiquitination status of the SPB component Ppc89, which is required for Sid4 association with the SPB, and Cut12, with which Plo1 also interacts at the SPB (Flory et al., 2002; MacIver et al., 2003) (Figure 2-1C). Each protein was tagged at its endogenous C-terminus with a His_6-BIO-His_6 (HBH) epitope and purified from denatured lysates using Ni^{2+}-NTA and streptavidin resin (Tagwerker et al., 2006). Proteins were purified from cells in which the spindle checkpoint had been activated using a reversible cold-sensitive mutation in the β-tubulin gene (*nda3*-KM311) (Hiraoka et al., 1984) and the ubiquitination status was determined by immunoblotting for ubiquitin. To validate that each protein was indeed purified, we also blotted with streptavidin, which recognizes the biotinylated epitope. Through this approach, we found that the SIN scaffold, Sid4, was the only protein tested to be robustly ubiquitinated *in vivo* (Figure 2-1D).

Sid4 is ubiquitinated in a Dma1-dependent manner

The finding that Sid4 is ubiquitinated *in vivo* during a checkpoint arrest suggests that it might be a Dma1 substrate. In this regard, it is noteworthy that Dma1 and Sid4

were shown previously to interact with each other by yeast two-hybrid analysis (Guertin et al, 2002). We therefore examined whether Sid4 ubiquitination required Dma1. Mutants were generated in which either the entire coding region of *dma1*$^{+}$ was deleted or single mutations within the *dma1*$^{+}$ coding region (R64 or I194) were mutated to alanine and integrated at the endogenous *dma1*$^{+}$ locus (Figure 2-2A). Mutating R64 to alanine is predicted to disrupt interaction with phosphothreonine residues (Durocher and Jackson, 2002) and impedes localization of Dma1 to SPBs and the cell division site (Figure 2-2B, compare panels I and II), while the I194A mutation eliminates Dma1 E3 ligase activity (Figure 2-1B), but does not disrupt its localization to SPBs or the division site (Figure 2-2B, compare panel I and III).

To validate that the *dma1* mutants compromise Dma1 function, each *dma1* mutant was combined with the *nda3*-KM311 mutation and tested for checkpoint function. Cells were synchronized in G2 by centrifugal elutriation, shifted to the restrictive temperature (18°C) to activate the spindle checkpoint, and septation indices were measured at 30 min intervals for 9 hrs. While the *nda3*-KM311 *dma1*$^{+}$ strain maintained a checkpoint arrest for approximately 7 hrs, the *nda3*-KM311 *dma1(R64A)* and *nda3*-KM311 *dma1(I194A)* mutant strains could not maintain an arrest and formed aberrant septa at approximately 5 hrs, which is comparable to *nda3*-KM311 *dma1Δ* cells (Figure 2-2C). Thus, the R64A and I194A mutations compromise Dma1-dependent checkpoint function.

We next examined Sid4 ubiquitination in checkpoint activated (*nda3*-KM311) *dma1Δ, dma1(R64A)* and *dma1(I194A)* mutants. Cells were shifted to 18°C for 5 hrs to activate the spindle checkpoint and Sid4 ubiquitination was examined. Strikingly, in the absence of Dma1 protein, activity or localization, Sid4 ubiquitination was abolished

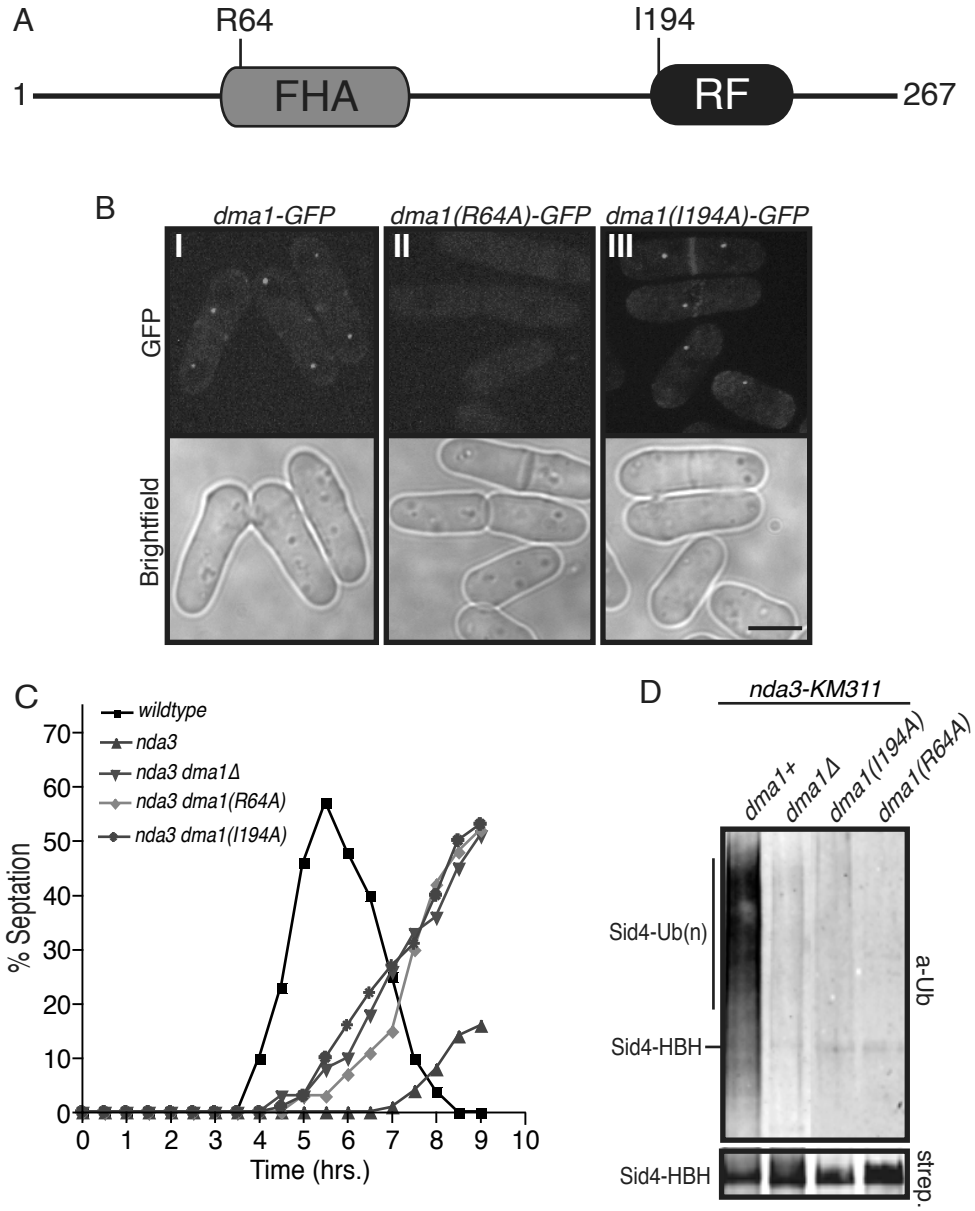

Figure 2-2

Sid4 ubiquitination requires Dma1 function.

A. Schematic diagram of Dma1 domains and positions of the R64A and I194A mutations. The R64A mutation prevents interaction with phosphothreonine motifs and I196A inactivates ubiquitin ligase activity. B. Localization of Dma1-GFP (panel I), Dma1(R64A)-GFP (panel II) and Dma1(I194A)-GFP (panel III) in cells growing in log phase. Scale bar, 5 μm. C. Spindle checkpoint assay. Cells of the indicated strains were synchronized at 32˚C in G2 by centrifugal elutriation, shifted to 18˚C, and the septation index of each strain determined every 30 minute for 9 hours. D. In vivo ubiquitination status of Sid4-HBH in *nda3-KM311 dma1*Δ or *nda3-KM311 dma1* mutants.

(Figure 2-2D). These data indicate that Sid4 is ubiquitinated in a Dma1-dependent manner.

Sid4 ubiquitination is required for Dma1-dependent checkpoint function

To determine if Sid4 ubiquitination is required for the Dma1-dependent checkpoint arrest, a ubiquitination deficient *sid4* allele was generated. Ubiquitin transfer often occurs in a sequence independent manner and can occur on multiple substrate lysines, making site identification challenging (for reviews see (Laney and Hochstrasser, 1999; Pickart, 2001). Sid4 contains 49 lysines (Figure 2-3A) and mutating all 49 sites simultaneously would likely disrupt protein function. Thus, four *sid4* mutants were made in which clusters of lysine residues were mutated that, collectively, cover every lysine within Sid4 (Figure 2-3A). Since $sid4^{+}$ is essential for viability, we first tested whether the four mutants could rescue the temperature sensitive *sid4*-SA1 mutant at the restrictive temperature (data not shown) and since they all could, each was then integrated at the endogenous $sid4^{+}$ locus to examine its *in vivo* ubiquitination status. Surprisingly, all four mutants were still ubiquitinated *in vivo* (Figure 2-3B). Therefore, in order to create a Ubiquitin-deficient *sid4* allele, we needed to generate a mutant that would eliminate more lysine residues simultaneously. However, all four mutants generated above were severely cold-sensitive (data not shown), indicating that Sid4 function was already compromised and adding more mutations would likely exacerbate these phenotypes.

Thus, as an alternative means of eliminating relevant Sid4 lysine residues without disrupting protein function, we made use of previous structure and function analyses of Sid4 and the core SPB protein, Ppc89. The N-terminal 300 amino acids of Sid4 are

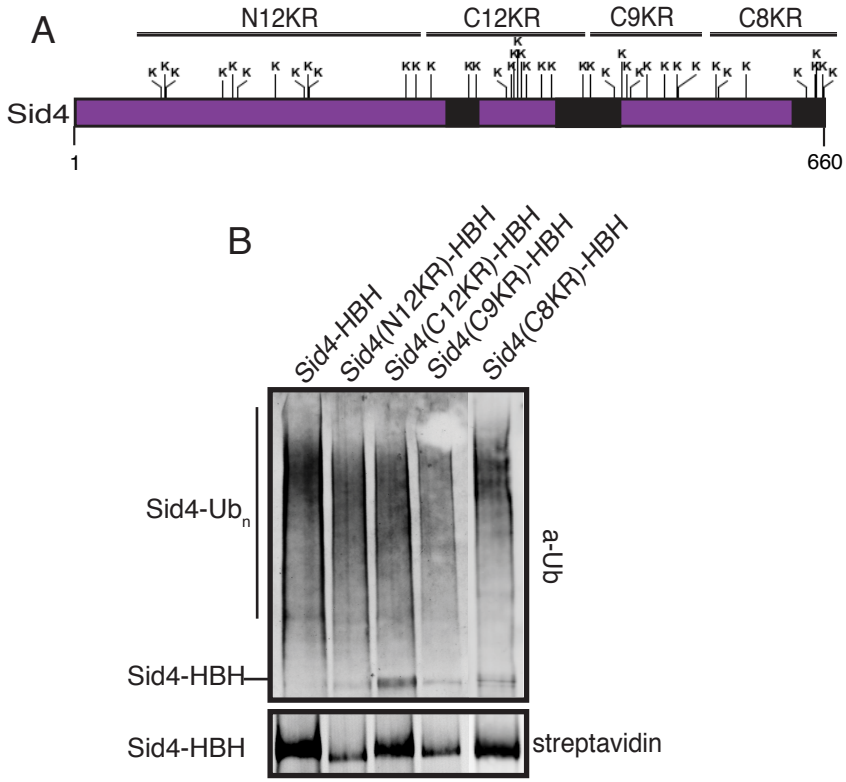

Figure 2-3

Targeted mutatagenesis of Sid4 lysines.

A. Schematic of Sid4 with lysine cluster mutants indicated. B. In vivo ubiquitination status of *sid4* mutants. Each protein was purified from checkpoint-activated cells (*nda3-KM311*) and visualized by immunoblot using fluorescently labeled Streptavidin (bottom panels) and a Ubiquitin antibody (top panels).

required for direct binding to Plo1 (Morrell et al., 2004), Cdc11 (Tomlin et al., 2002) and Dma1 (Guertin et al., 2002), indicating that this region contains the essential SIN scaffolding activity of Sid4. The C-termini of both Sid4 and Ppc89 contain several predicted coil-coil regions (Figure 2-4A, top and middle diagram respectively), which are only required for their SPB localization (Rosenberg et al., 2006). In fact, replacing the Sid4 C-terminus with the SPB targeting region of Ppc89 (Figure 2-4A, bottom diagram), rescues both the temperature sensitive *sid4*-SA1 allele at 36°C and the *sid4Δ* (Rosenberg et al., 2006). Thus, the *sid4N-ppc89C* fusion mutant, which eliminates approximately 76% of Sid4 lysines on the protein, was integrated at the endogenous $sid4^{+}$ locus and tested for *in vivo* ubiquitination. While Sid4-HBH was robustly ubiquitinated, ubiquitination of the Sid4N-Ppc89C-HBH mutant was essentially eliminated (Figure 2-4B). Importantly, *sid4N-ppc89C* mutant cells were *wildtype* for morphology and were not temperature sensitive. These data indicate that Dma1 targets the Sid4 C-terminus for ubiquitination *in vivo*.

As expected, Sid4N-Ppc89C-GFP localized to SPBs properly (Figure 2-4C panel I) and Cdc11-GFP, whose localization depends on Sid4, also localized to SPBs normally (Figure 2-4C panel II). Furthermore, Cdc11-GFP intensities at SPBs are not significantly altered in *sid4N-ppc89C* mutant cells compared to *wildtype* cells (Figure 2-5A-B). Thus, as predicted by its wildtype morphology, the Sid4N-Ppc89C mutant does not disrupt the SIN scaffold complex. To ensure that the loss of Sid4N-Ppc89C ubiquitination was not due to a failure to recruit Dma1, we examined Dma1-GFP localization and found that it was present at SPBs in *sid4N-ppc89C* mutant cells (Figure2-4C panel III), consistent with the previous observation that Dma1 interacts with the Sid4 N-terminal 300 amino acids

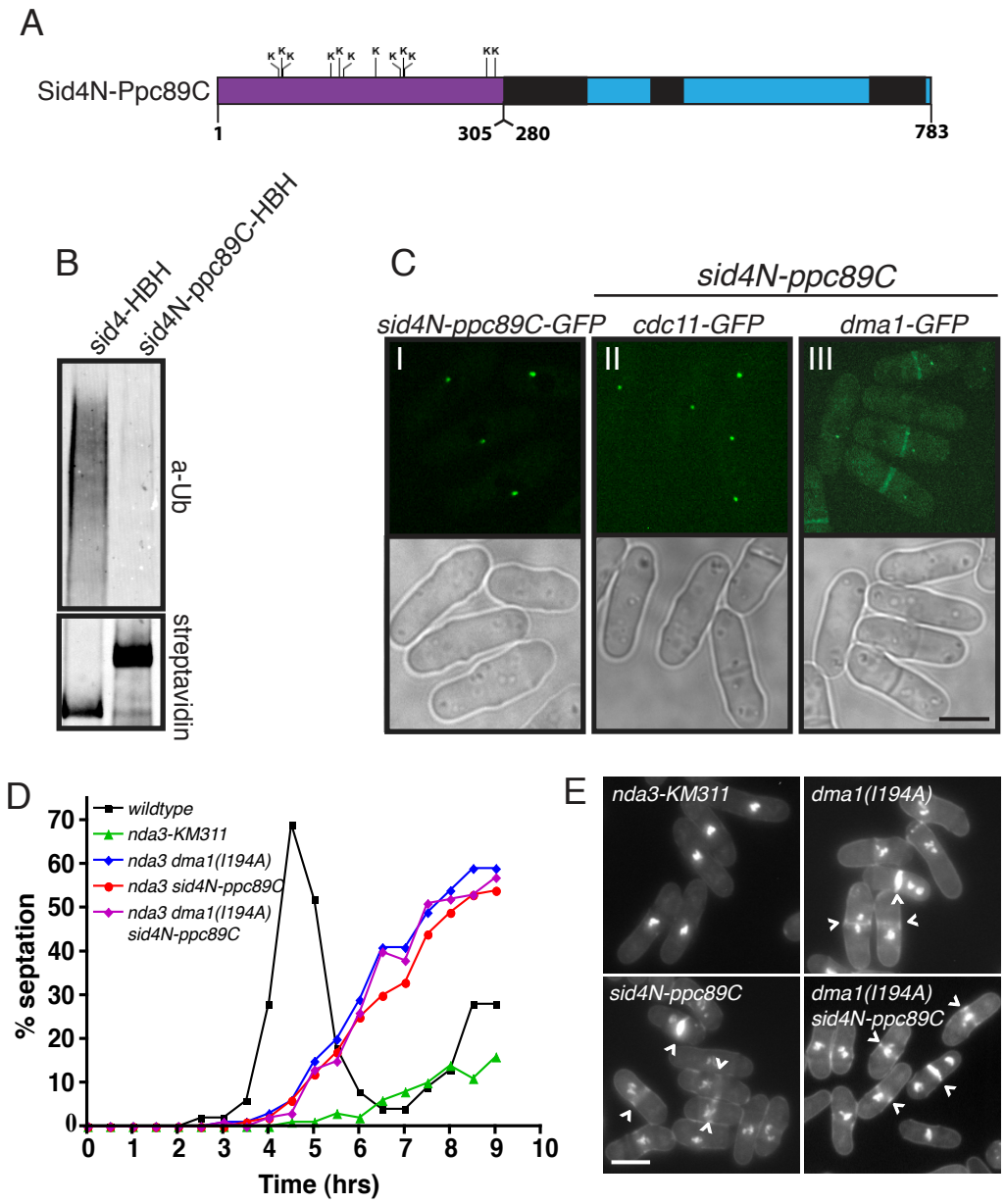

Figure 2-4

Sid4 ubiquitination is required to maintain a checkpoint arrest.

A. Schematic diagrams of Sid4 with relative positions of all 49 lysines (top), Ppc89 (middle) and the Sid4N-Ppc89C fusion mutant (bottom). Predicted coil-coil regions are shown in black. B. In vivo ubiquitination of Sid4-HBH and Sid4N-Ppc89C-HBH. C. Localization of Sid4N-Ppc89C-GFP (panel I), Cdc11-GFP (panel II), and Dma1-GFP (panel II) in sid4N-ppc89C-HBH mutant cells. Scale bar, 5 µm. D. Spindle checkpoint assay. Cells of the indicated strains were blocked at 32˚C in S phase with hydroxyurea, released into hydroxyurea-free media at 18˚C, and the septation index of each strain determined every 30 minute for 9 hours. E. Cells from each of the strains examined in D at the 7 hr time point stained with methyl blue, which stains the septa, and DAPI, which stains DNA. (^) indicate septated cells that have bypassed the checkpoint. Scale bar, 5 µm.

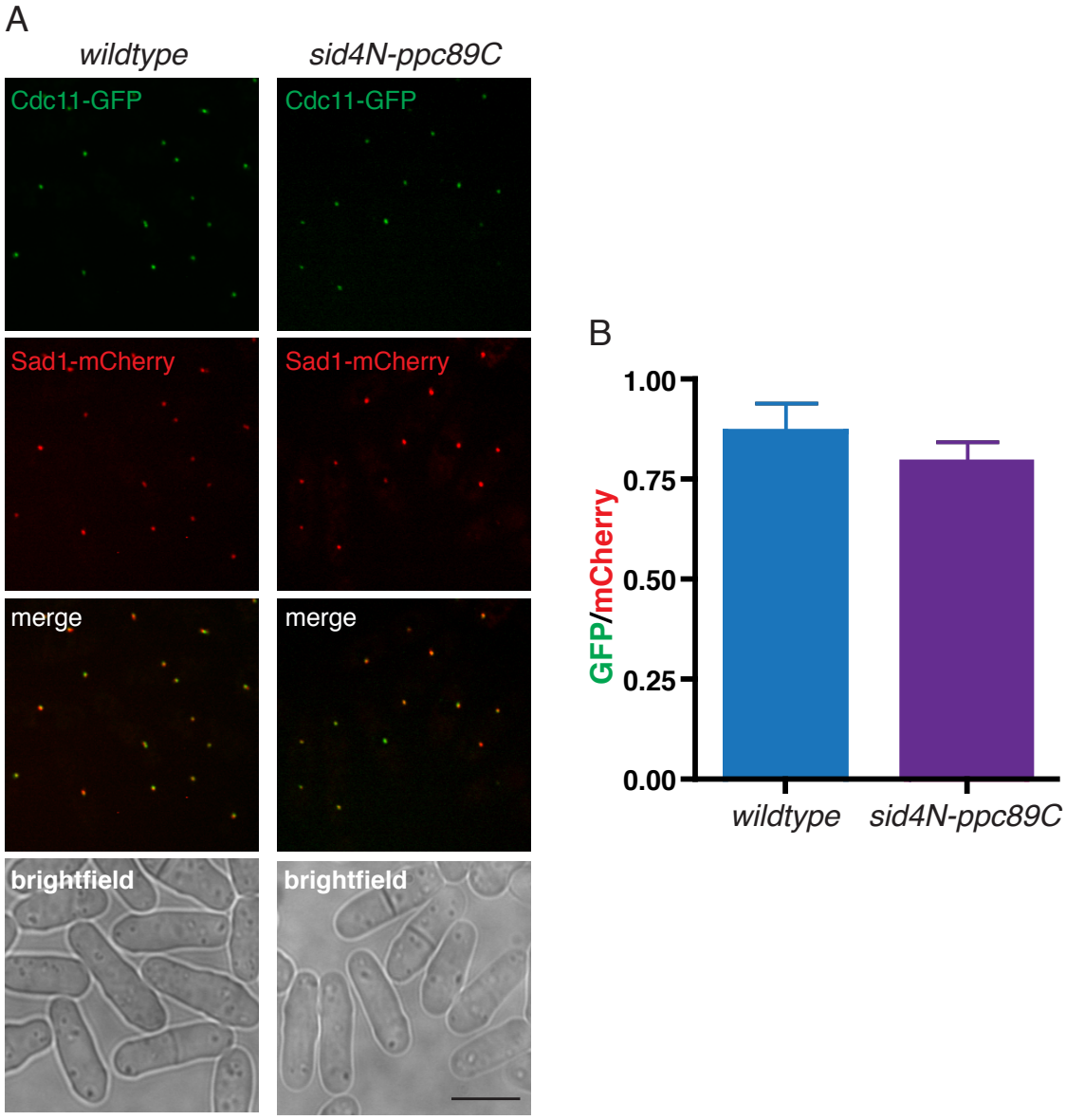

Figure 2-5

Cdc11-GFP intensity in *wildtype* and *sid4N-ppc89C* mutant cells

A. *wildtype* and *sid4N-ppc89C* cells containing *cdc11-GFP* and *sad1-mCherry* were grown to log phase and imaged. Representative images are shown. B. Cdc11-GFP and Sad1-mCherry fluorescence intensities were measured in *wildtype* and *sid4N-ppc89C* cells. GFP:mCherry intensity ratios were calculated and plotted as arbitrary units. p=0.3.

(Guertin et al., 2002). Thus, while the Sid4 N-terminus binds Dma1, its C-terminus is required for ubiquitination. Collectively, these data indicate that the *sid4N-ppc89C* mutant retains full scaffolding and essential SIN functions of *sid4*$^{+}$, but is unable to be ubiquitinated *in vivo* even in the presence of Dma1.

We then assessed the checkpoint function of the *sid4N-ppc89C* mutant. Cells were arrested in S-phase with hydroxyurea, released synchronously at 18°C to activate the spindle checkpoint, and septation indices were measured at 30 min intervals for 9 hrs. The *nda3*-KM311 strain maintained a checkpoint arrest for approximately 7 hrs (Figure 2-4D-E top left panel); however, the *nda3*-KM311 *sid4N-ppc89C* mutant formed aberrant septa (marked with (^) in Figure 2-4E bottom left panel) at approximately 5 hrs, which phenocopied the *dma1*-RF mutant (nda3-KM311 *dma1I194A*) (Figure 2-4D-E, top right panel). Importantly, a double *dma1(I194A) sid4N-ppc89C* mutant septated with similar kinetics as either mutant alone and did not display any other additive effects (Figure 2-4D-E bottom right panel), suggesting that these mutants bypass a checkpoint arrest via the same mechanism. Thus, Sid4 ubiquitination is necessary to inhibit cytokinesis during a *dma1*-dependent checkpoint arrest.

Sid4 ubiquitination antagonizes Plo1 recruitment to SPBs during a checkpoint response

When the spindle checkpoint is activated in the absence of *dma1*$^{+}$, Plo1 is recruited to SPBs earlier (Guertin et al., 2002). Because our data suggest that Dma1 ubiquitinates Sid4 when a mitotic checkpoint is activated, we tested if Sid4 ubiquitination was the biochemical signal that perturbs Plo1 recruitment to SPBs by measuring the timing of Plo1 recruitment to SPBs in checkpoint activated *sid4N-ppc89C* cells.

Endogenously expressed Plo1 fused to a single GFP is difficult to visualize *in vivo*. Thus, to improve visualization three tandem copies of GFP were fused to the C-terminus of Plo1 (Plo1-GFP_3) and used in the subsequent experiments.

nda3-KM311, *nda3*-KM311 *dma1(I194A)* and *nda3*-KM311 *sid4N-ppc89C* cells were synchronized in G2 by lactose gradient sedimentation, shifted to 18°C to activate the spindle checkpoint, and Plo1-GFP_3 was visualized at 30 min intervals for 9 hrs. In $dma1^+$ cells, Plo1-GFP_3 was not visible on SPBs until ~4-5 hrs (Figure 2-6A, D). However, in the *dma1(I194A)* mutant, Plo1-GFP_3 was detected at SPBs approximately 2 hrs earlier compared to $dma1^+$ cells and cells failed to arrest in mitosis (Figure 2-6B, D), which is similar to the premature recruitment observed previously for *dma1Δ* cells (Guertin et al., 2002). Similarly, Plo1-GFP_3 was recruited to SPBs earlier in *sid4N-ppc89C* mutant cells (Figure 2-6C, D). It should be noted that when cells are arrested in prometaphase by the *nda3*-KM311 mutation, Plo1 localizes to both SPBs; however, because the mitotic spindle does not form and SPBs do not separate in this arrest, Plo1's signal in the later time points is slightly obscured by the fact that it is localizing on two SPBs that are sometimes overlapping in the Z-axis. To be sure that we were quantitating SPB localized Plo1, Plo1-GFP_3 was co-localized with the constitutive SPB marker, Sad1-mCherry (Hagan and Yanagida, 1995)(Figure 2-6A-C, right panels). These data suggest that when the spindle checkpoint is activated, Sid4 ubiquitination antagonizes Plo1 recruitment to SPBs and thereby prevents it from reaching its substrates and activating the SIN.

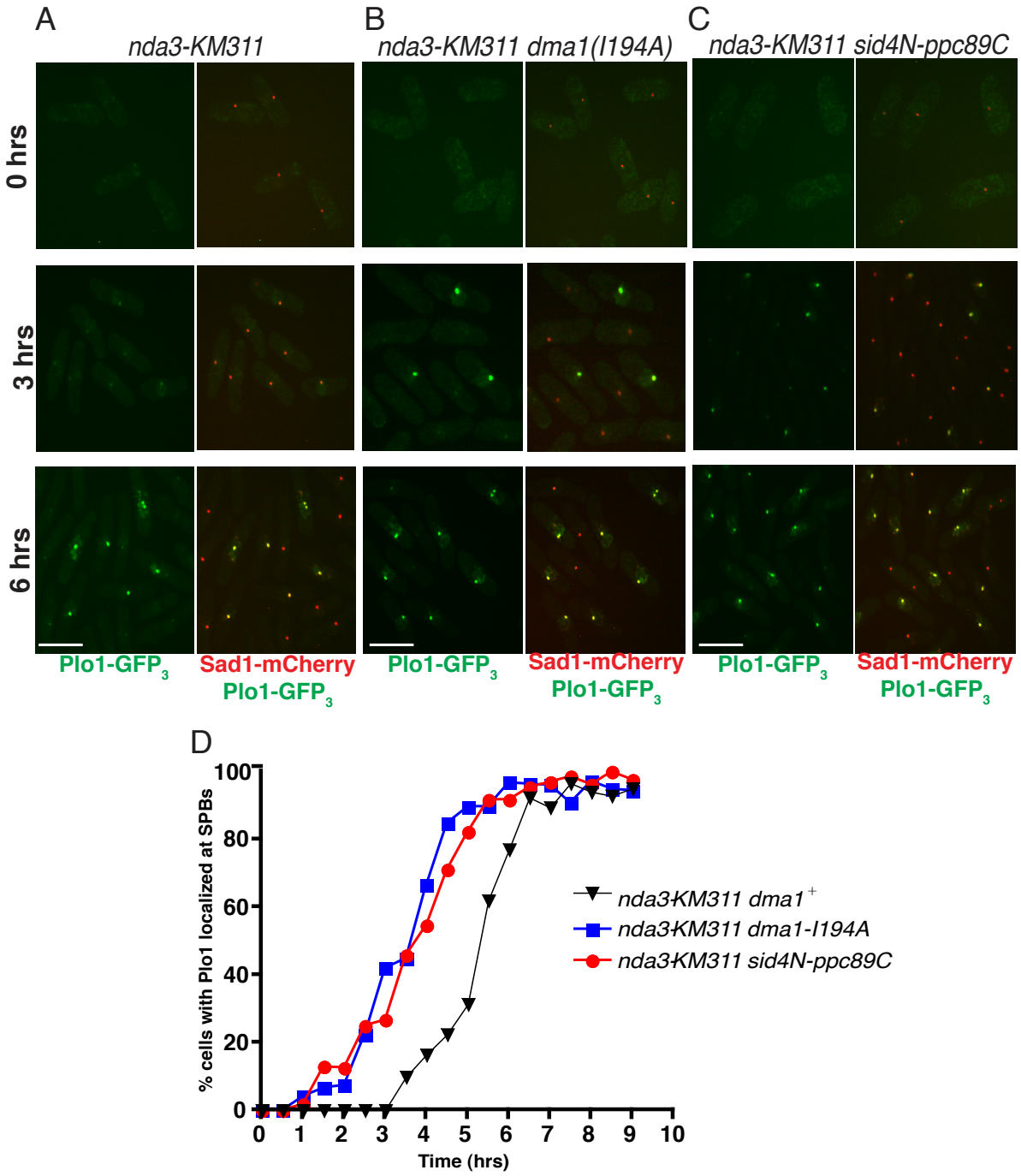

Figure 2-6

Sid4 ubiquitination delays Plo1 recruitment to the SPBs when the spindle checkpoint is activated.

A-C. *nda3-KM311* (A), *nda3-KM311 dma1(I194A)* (B) or *nda3-KM311 sid4N-ppc89C* (C) cells were synchronized at 32˚C in G2 by lactose gradient sedimentation, shifted to 18°C to activate the spindle checkpoint, and Plo1-GFP$_3$ and Sad1-mCherry localization at the SPBs were imaged periodically for 9 hrs. Scale bar, 5 μm. D. The kinetics of Plo1 recruitment to SPBs was measured for each of the strains shown by calculating the percentage of cells with Plo1-GFP$_3$ on SPBs at each time point.

Sid4 ubiquitination antagonizes Plo1 recruitment to SPBs during interphase

Since Dma1 can be detected at SPBs in the absence of checkpoint induction, we examined a potential role for Sid4 ubiquitination during normal cell cycle progression. While Sid4 was most robustly ubiquitinated during a mitotic arrest, as expected, it was also ubiquitinated in G2 cells, but significantly less ubiquitination was detected during S-phase (Figure 2-7A). Since Sid4 ubiquitination levels fluctuate throughout the cell cycle, we tested if Dma1 concentration at SPBs was also cell cycle dependent by measuring Dma1-GFP intensities at SPBs in different cell cycle stages and comparing these intensities with the constitutive SPB marker Sid4-RFP (Morrell et al., 2004). Dma1-GFP intensity was detected at low levels in prometaphase cells grown to log phase under permissible conditions (Figure 2-7B-C) and was significantly increased during a mitotic checkpoint arrest (*nda3*-KM311 arrest) (Figure 2-7B-C), suggesting that Dma1 concentrates at SPBs in response to mitotic stress. Dma1-GFP was also detected at low levels in cells arrested in G2 (*cdc25-22*) (Figure 2-7B-C), although with significantly decreased intensity compared to *nda3*-KM311 arrested cells, and it was not detected on SPBs in cells arrested in S-phase (Figure 2-7B-C). Thus, the levels of Sid4 ubiquitination correlate with the concentration of SPB-localized Dma1.

Plo1 localization to SPBs is also cell cycle regulated, accumulating at SPBs upon commitment to mitosis (Mulvihill et al., 1999). Since Sid4 ubiquitination antagonizes Plo1 localization at SPBs and Sid4 is ubiquitinated in interphase cells, we wondered if the absence of Sid4 ubiquitination would allow Plo1 to concentrate at SPBs in interphase. Thus, *dma1*$^{+}$, *dma1Δ* or *sid4N-ppc89C* cells were arrested in G2 using the temperature sensitive *cdc25*-22 mutation and Plo1-GFP_3 intensities at SPBs were measured relative to

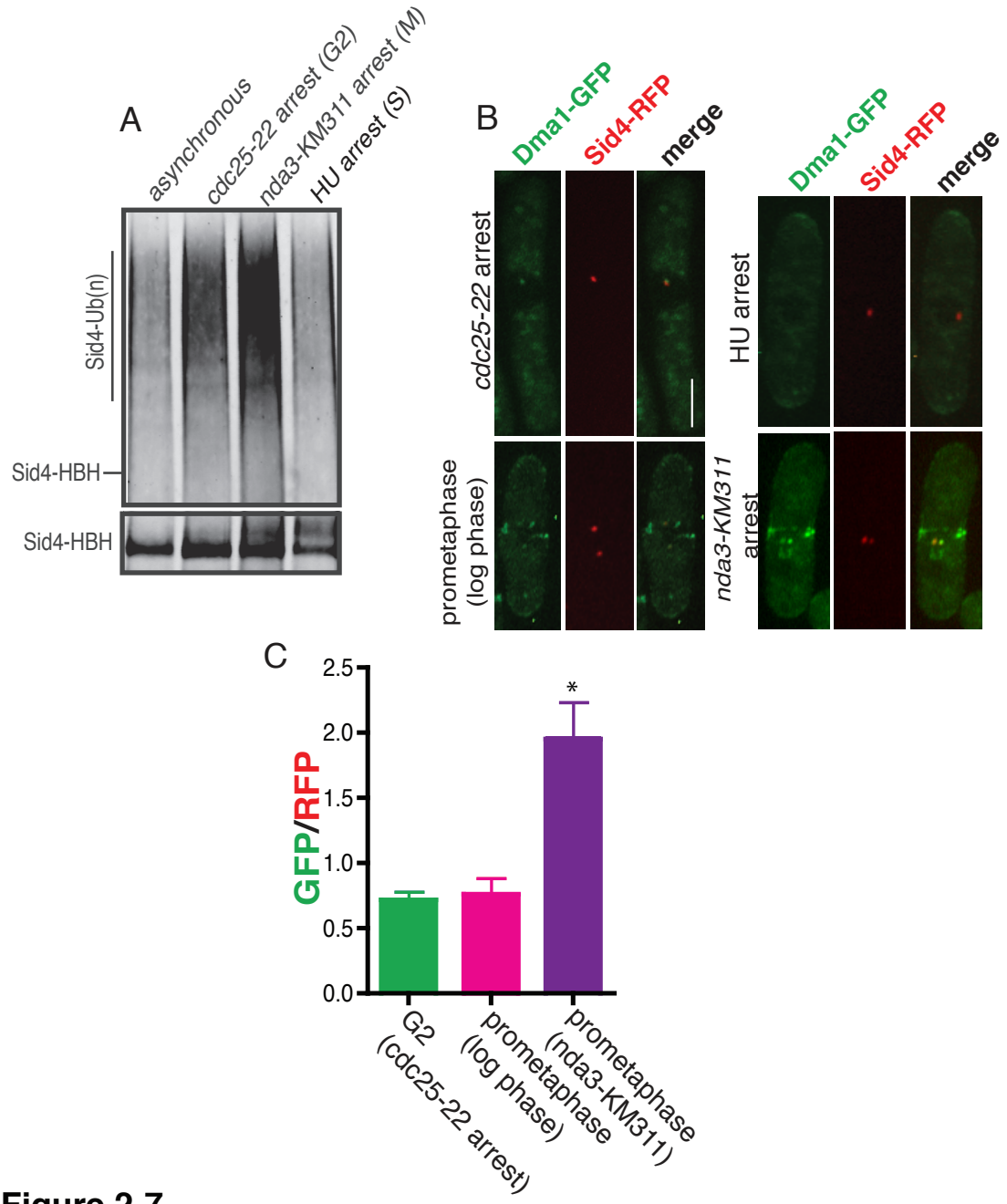

Figure 2-7

Sid4 ubiquitination correlates with Dma1 localization at SPBs.

A. In vivo ubiquitination of Sid4-HBH in asynchronous cells or cells arrested in G2 (*cdc25-22*), prometaphase (*nda3-KM311*) or S phase (Hydroxyurea; HU). B. Representative images showing Dma1-GFP and Sid4-RFP localization in a G2 arrest (*cdc25-22* arrest), an S-phase arrest (HU arrest), prometaphase cell growing in log phase, and a mitotic arrest when the checkpoint is active (*nda3-KM311* arrest). Scale bar, 5 µm. C. Quantitation of relative Dma1-GFP:Sid4-RFP intensity ratios for each of the cell cycle stages shown in B plotted as arbitrary units. For each cell cycle stage, Dma1-GFP and Sid4-RFP intensities were measured for at least 20 cells and averaged; error bars represent standard error of the mean, *p<0.05.

Sad1-mCherry. While Plo1-GFP_3 was only detected at low levels in *dma1*$^+$ cells (Figure 2-8A-B), Plo1-GFP_3 intensities at SPBs were significantly increased in *dma1Δ* cells (Figure 2-8A-B). A similar increase in Plo1-GFP_3 intensities was observed in *sid4N-ppc89C* cells, in which Sid4 ubiquitination is abolished (Figure 2-8A-B). These data suggest that Sid4 ubiquitination antagonizes Plo1 localization to SPBs during interphase as well as during a mitotic checkpoint arrest.

Byr4 is a potential Plo1 target

While the direct SIN target(s) of Plo1 has not yet been identified in *S. pombe,* the *S. cerevisiae* Plo1 homolog, Cdc5, is known to phosphorylate and inhibit the Byr4 ortholog and GAP component Bfa1, resulting in MEN activation (Geymonat et al., 2003; Hu et al., 2001). Bfa1 phosphorylation by Cdc5 inhibits its GAP activity *in vitro* and also ejects it from SPBs (Geymonat et al., 2003; Hu et al., 2001). *S. pombe* Byr4 is also a phosphoprotein (Song et al., 1996) and is hyper-phosphorylated just prior to septation (Krapp et al., 2008). Thus, the potential of Plo1 SPB recruitment influencing Byr4 phosphorylation state and SPB localization was examined.

First, Byr4 was tested as a Plo1 substrate *in vitro*. MBP and MBP-Byr4 were produced in *E. coli*, and purified on amylose resin. When purified proteins were incubated with Plo1 purified from baculovirus-infected insect cells and ^{32}P-ATP, we found that Plo1 could directly phosphorylate full length Byr4 (Figure 2-9A). Next, Byr4 phosphorylation *in vivo* was examined. As previously reported (Song et al., 1996), Byr4 was hyper-phosphorylated in a mitotic arrest (Figure 2-9B). However, in a temperature sensitive *plo1* mutant (*plo1-25*) that had been synchronized and shifted to the restrictive

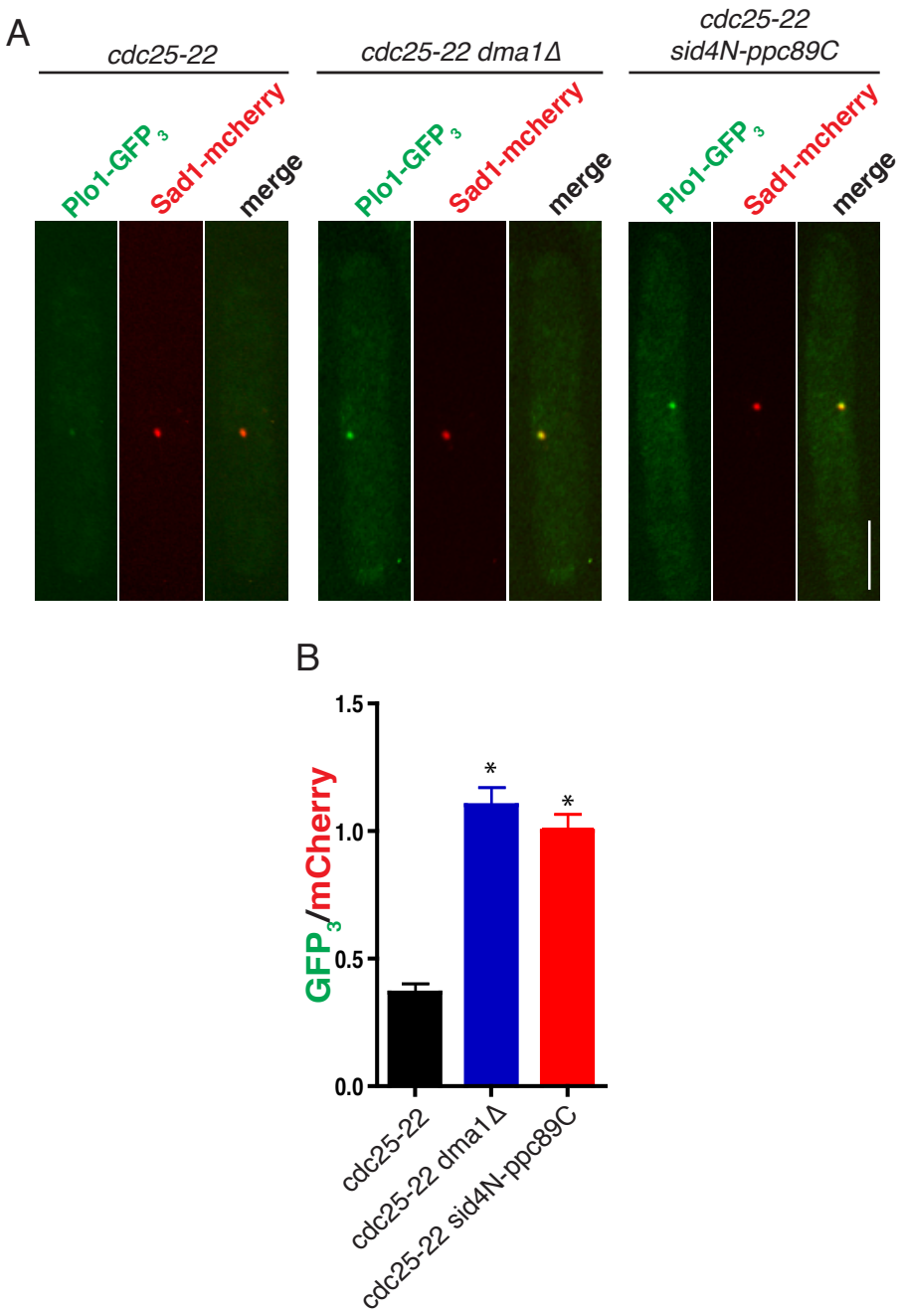

Figure 2-8

Sid4 ubiquitination prevents Plo1 recruitment to SPBs during interphase.

A. Representative images showing Plo1-GFP$_3$ and Sad1-mCherry localization at SPBs during a *cdc25-22* arrest in *wildtype* (left panels), *dma1Δ* (middle panels), and *sid4N-ppc89C* (right panels) cells. Scale bar, 5 μm. B. Quantitation of relative Plo1-GFP$_3$:Sad1-mCherry intensity ratios at SPBs for each of the strains shown in 5D plotted in arbitrary units. For each strain, Plo1-GFP$_3$ and Sad1-mCherry intensities were measured for at least 20 cells and averaged; error bars represent standard error of the mean, *$p<0.05$.

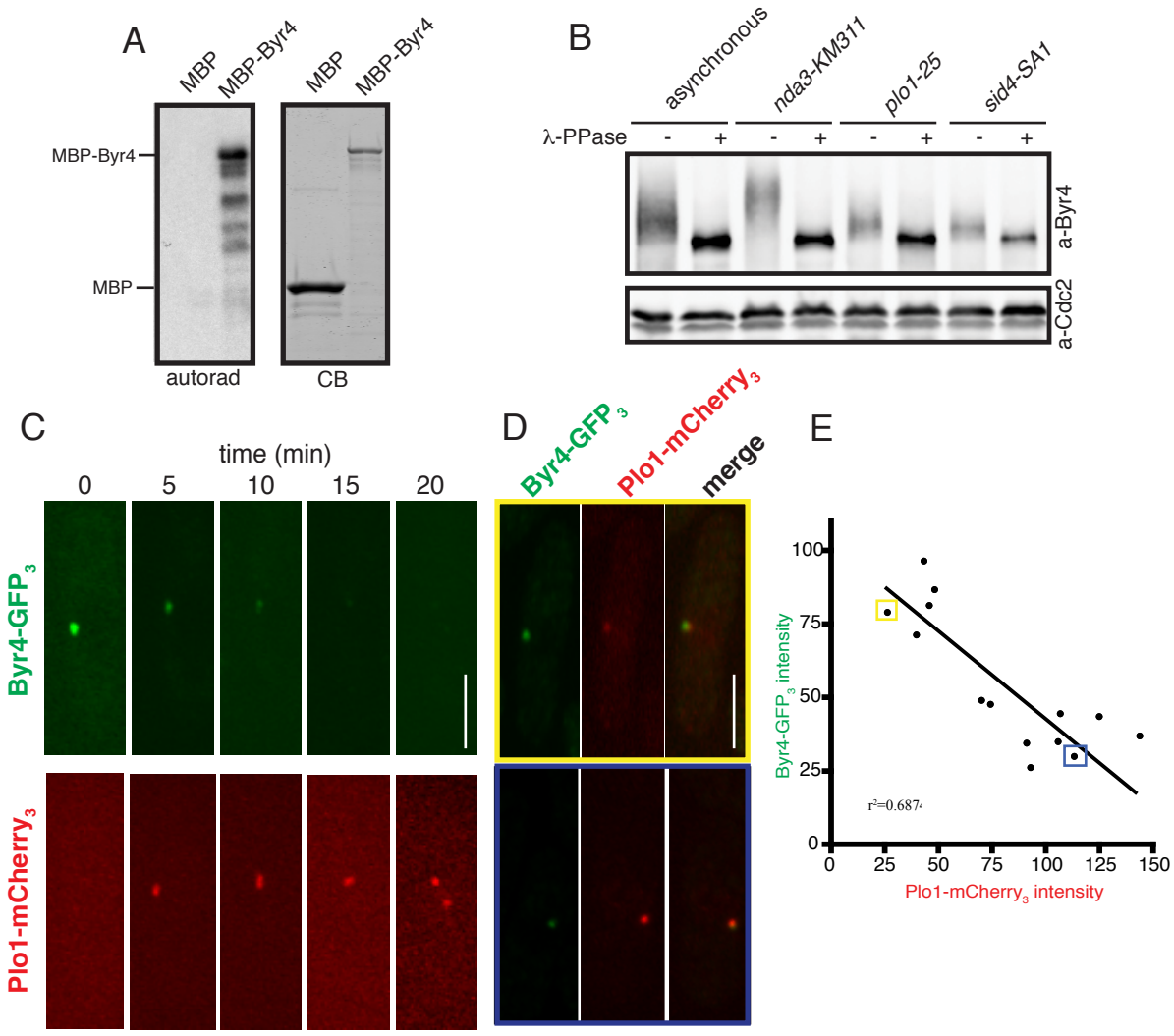

Figure 2-9

Byr4 is a potential Plo1 target.

A. Left, autoradiograph of recombinant MBP and MBP-Byr4 phosphorylated in vitro by Plo1 kinase. Right, coomassie blue (CB) gel of purified MBP and MBP-Byr4 proteins. B. Gel shifts of endogenous Byr4 immunoprecipicated from asynchronous, *nda3-KM311*, *plo1-25* or *sid4-SA1* temperature-sensitive cells, which were synchronized in S-phase by hydroxyurea and released at the restrictive temperature. Immunoprecipitates were treated with (+) or without (-) lambda phosphatase and detected by immunoblotting using an anti-Byr4 serum. C. A Byr4-GFP$_3$ Plo1-mCherry$_3$ strain was imaged via time-lapse microscopy and a representative montage is depicted. D. A Byr4-GFP$_3$ Plo1-mCherry$_3$ strain was grown to log phase and imaged. Top and bottom panels show representative images of cells in which Byr4-GFP$_3$ or Plo1-mCherry$_3$, respectively, localization to the SPB predominates. E. Byr4-GFP$_3$ and Plo1-mCherry$_3$ fluorescence intensities were measured and plotted against each other. A linear regression analysis was performed to calculate the best-fit line, r^2=0.687. The data points boxed in yellow and blue represent the intensity calculations for the top and bottom panels shown in D, respectively.

temperature, the extent of Byr4 phosphorylation was drastically reduced (Figure 2-9B). Significantly, the degree of Byr4 phosphorylation in *the plo1*-25 mutant was comparable to Byr4 phosphorylation in *sid4*-SA1 mutant cells at the restrictive temperature (Figure 2-9), indicating that Byr4 must be associated with the SPBs to become phosphorylated. Taken together, these data suggest that Plo1 contributes to the majority of Byr4 phosphorylation at the SPB.

We next examined the timing of Byr4 and Plo1 localization at SPBs relative to each other via time-lapse microscopy. To visualize Plo1 and Byr4 in the same cells, Byr4 was tagged at its C-terminus with three tandem copies of GFP (Byr4-GFP_3) and Plo1 was tagged at its C-terminus with three tandem copies of mCherry (Plo1-$mCherry_3$). *byr4-GFP_3 plo1-$mCherry_3$* cells were morphologically *wildtype*, were not temperature sensitive and did not display any observable cell cycle defects suggesting that Byr4 and Plo1 functions were not significantly compromised. In a representative movie, Byr4-GFP_3 was detected until the 10 min time point, when Plo1-$mCherry_3$ was first detected on SPBs, and continued to decrease until it was undetectable at 20 min, just prior to SPB separation (Figure 2-9C). We also quantitated the relative intensities of Byr4-GFP_3 and Plo1-$mCherry_3$ at SPBs in an asynchronous population of cells (Figure 2-9D). In the few cells in which both proteins were detected at SPBs, Byr4 and Plo1 intensities showed a strong negative correlation (Figure 2-9D-E). Collectively, these data suggest that Plo1 phosphorylation of Byr4 at SPBs promotes Byr4 dissociation from SPBs.

Sid4 ubiquitination is required to prolong Byr4 residence on SPBs during a checkpoint arrest

We next examined the kinetics of Byr4 and Plo1 localization during a checkpoint response in *nda3*-KM311 and *nda3*-KM311 *sid4N-ppc89C* mutant cells. Cells were synchronized in G2, shifted to 18°C to activate the checkpoint and Byr4-GFP_3 and Plo1-$mCherry_3$ were visualized periodically for 9 hrs. In *nda3*-KM311 *sid4*$^+$ cells, Byr4-GFP_3 was maintained on SPBs for ~3 hrs (Figure 2-10A and C). However, in the absence of Sid4 ubiquitination (*nda3*-KM311 *sid4N-ppc89C* mutant), Byr4-GFP_3 began to disappear from SPBs after just 1 hr and was absent from almost 100% of the cells by 5 hrs (Figure 2-10B-C). In both strains, the time in which SPB-localized Byr4 was absent in 50% of the cells (~5 hrs in *sid4*$^+$ cells and ~2 hrs in the *sid4N-ppc89C* mutant) corresponds to the same time in which SPB-localized Plo1 was detected in 50% of the cells (Figure 2-10C, intersections marked by dashed lines). These data suggest that when a mitotic checkpoint is activated, Sid4 ubiquitination antagonizes Plo1 SPB recruitment in order to retain Byr4 on SPBs and inhibit SIN signaling.

Discussion

Ubiquitin-mediated inhibition of cytokinesis

Mitotic exit and cytokinesis must be coupled for proper partitioning of genetic material. In *S. pombe*, this entrainment is achieved by the SIN. In this chapter, we have presented new evidence regarding how Dma1 influences SIN signaling. Our data indicate that when chromosomes are not attached properly to the mitotic spindle, Dma1

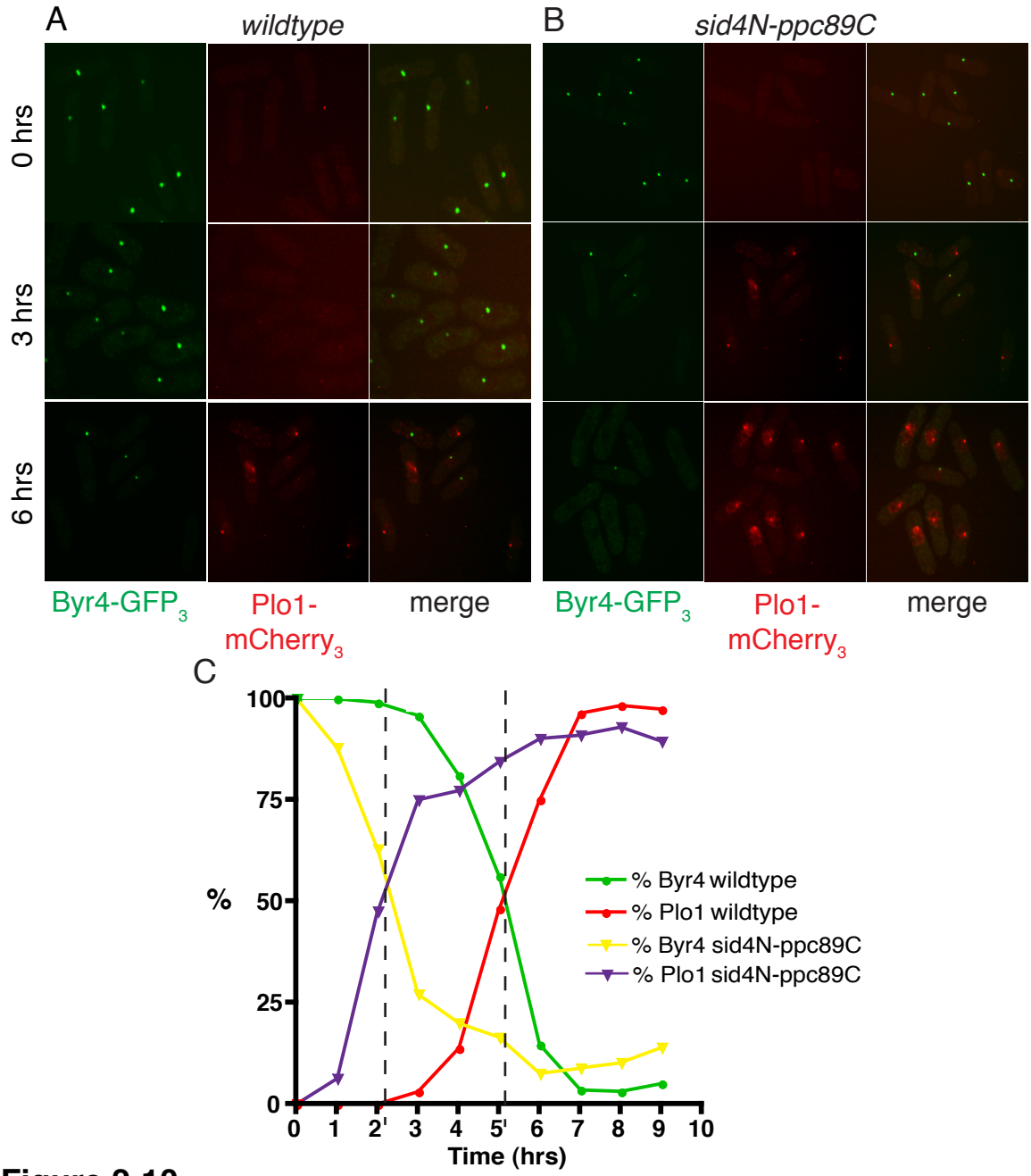

Figure 2-10

Sid4 ubiquitination is required to prolong Byr4 residence on SPBs when a mitotic checkpoint is activated.

A-B. *nda3-KM311* (A) and *nda3-KM311 sid4N-ppc89C* (B) cells were synchronized in G2 by lactose gradient sedimentation, shifted to 18°C to activate the spindle checkpoint, and Byr4-GFP$_3$ and Plo1-mCherry$_3$ localizations at the SPBs were imaged periodically for 9 hrs. Representative images of Byr4-GFP$_3$ Plo1-mCherry$_3$ and the merged images are shown for the times indicated. Scale bar, 10 μm. C. At each time point, the percentage of cells with Byr4-GFP$_3$ and Plo1-mCherry$_3$ were calculated and plotted over time. Dashed lines represent the time in which the plots for Byr4 and Plo1 intersect (~5hrs for *nda3-KM311* cells and ~2 hrs for *nda3-KM311 sid4N-ppc89C* cells).

concentrates at SPBs and ubiquitinates the SIN scaffold, Sid4 (Figure 2-11A, step 1). We propose that Sid4 ubiquitination antagonizes Plo1 localization at SPBs (Figure 2-11A, step 2) to restrict its ability to activate the SIN and cytokinesis (Figure 2-11A, steps 3 and 4).

The SIN pathway consists of several protein kinases, which assemble sequentially at the SPBs. The first kinase on the scene is Plo1, which directly binds the SIN scaffold, Sid4 (Morrell et al., 2004). Once recruited, Plo1 initiates the SIN pathway presumably by phosphorylating one or more SIN components directly; however, its direct target(s) have remained unknown to date. Here, we find that the GAP component, Byr4, is a likely Plo1 target (Figure 2-11B, step 1). Additionally, the observation that Plo1 and Byr4 localization to SPBs are negatively correlated suggests a model wherein Plo1 ejects Byr4 from SPBs (Figure 2-11B, step 2), highlighting yet another conserved mechanism between the *S. pombe* SIN and the *S. cerevisiae* MEN. Subsequently, expulsion of the GAP complex from SPBs relieves the inhibition of the GTPase, Spg1, which subsequently facilitates recruitment of the SIN kinases, Cdc7 and Sid1-Cdc14 (Figure 2-11B, steps 3 and 4, respectively), and finally allows Sid2-Mob1 to accumulate at the division site to trigger cytokinesis (Figure 2-11B, step 5). During a checkpoint response, the delayed Plo1-mediated phosphorylation of Byr4 would detain Byr4 on SPBs and thereby prevent cytokinesis from occurring prior to chromosome segregation (Figure 2-11B, steps 3 and 4).

We have also uncovered a potential role for Dma1 during normal cell cycle progression. Here, we find that Dmal's SPB concentration varies according to cell cycle stage and, consistent with our model, its concentration correlates with the degree of Sid4

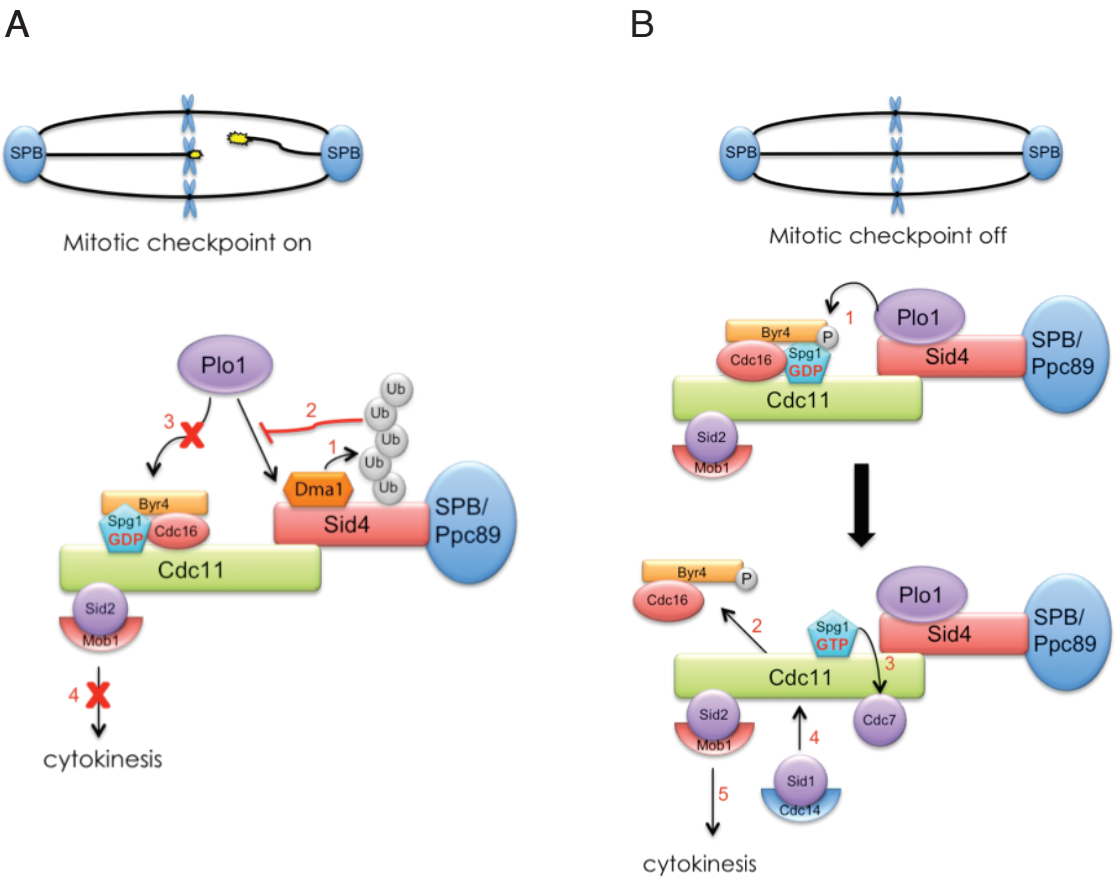

Figure 2-11

Model of Dma1 inhibition of the SIN during a mitotic checkpoint.

A. Proposed mechanism of Dma1 inhibition of the SIN when the mitotic checkpoint is active. B. Mechanism of SIN activation when chromosomes are properly attached to the mitotic spindle and the checkpoint is satisfied.

ubiquitination. It is possible that in addition to its role as a mitotic checkpoint protein, Dma1 cooperates with other SIN inhibitors to minimize SIN activity during interphase. However, these basal levels of Dma1 and Sid4 ubiquitination are likely not sufficient when SIN activity must be kept low for longer periods, such as during a checkpoint arrest. Thus, Dma1 might be "activated" during a checkpoint response, at least in part, through additional SPB recruitment. This is supported by the fact that Dma1 intensities increase significantly at SPBs and Sid4 ubiquitination is observed more robustly when a mitotic checkpoint is activated. In order to understand how Dma1 responds to a mitotic checkpoint, it will be pertinent to identify upstream factors that regulate the extent of Dma1 recruitment to SPBs during normal cell cycle progression and in response to a mitotic checkpoint.

Distinct roles of SPB-localized Plo1 kinase in mitosis and cytokinesis

Plo1 accumulates at the mitotic, but not the interphase SPB, through association with Sid4 (Morrell et al., 2004) and at least two other SPB components, Cut12 (Mulvihill et al., 1999) and Pcp1 (Fong et al., 2010). Its recruitment upon commitment to mitosis is dependent on cyclin-dependent kinase (CDK) activity; however, a hypermorphic Cut12 mutant (*stf1*-1) can bypass a *cdc25*-22 arrest by increasing Plo1 recruitment to SPBs and increasing its kinase activity suggesting that the Plo1-Cut12 interaction promotes mitotic entry (Mulvihill et al., 1999). Similarly, Plo1's association with Pcp1 also seems to have a role in promoting mitotic entry since the mitotic defects observed in a temperature sensitive *pcp1* mutant that exhibits reduced Plo1 localization at SPBs can be rescued by a *wee1* mutant that causes premature mitotic entry (Fong et al., 2010). Here, we find that

the absence of Sid4 ubiquitination also allows Plo1 to accumulate at SPBs in interphase; however, this on its own did not affect normal cell cycle progression and cells did not bypass a *cdc25*-22 arrest. Given that Cut12 (Bridge et al., 1998) and Pcp1(Flory et al., 2002) associate with the nuclear side of the SPB, while Sid4 resides on the cytoplasmic face (our unpublished data), suggests that the role of Plo1 in promoting mitotic entry is spatially restricted to the nuclear SPB surface, while its association with Sid4 on the cyctoplasmic surface may have a distinct role in regulating cytokinesis.

How does Sid4 ubiquitination antagonize Plo1?

The fact that Sid4 is ubiquitinated might suggest that Sid4 polyubiquitination signals it for degradation by the proteasome, thereby preventing access of Plo1 to core SIN components. However, mimicking a checkpoint response by over-expressing *dma1*$^{+}$ does not alter Sid4 protein levels or disrupt its localization at SPBs (Guertin et al., 2002) and fluorescence recovery after photobleaching experiments indicate that Sid4 is stably bound to the SPB (Morrell et al., 2004). Furthermore, the other major SIN scaffold protein, Cdc11, whose localization to the SPBs depends on Sid4, remains localized to SPBs during *dma1*$^{+}$ overexpression (Guertin et al., 2002) and its intensity at SPBs is not affected in the *sid4N-ppc89C* mutant, indicating that Dma1 does not disrupt the Cdc11-Sid4 scaffold complex. An alternative possibility is that ubiquitination physically masks the Plo1 binding site. However, both Plo1 (Morrell et al, 2004) and Dma1 (Guertin et al, 2002) physically interact with the N-terminus of Sid4, while Sid4 ubiquitination appears to occur on the C-terminus. We do not rule out this possibility, however, due to the lack of information about Sid4's three-dimensional conformation. Sid4 is predicted to contain

several intrinsically unstructured regions and it has been proposed that some scaffold proteins are intrinsically unstructured to increase their flexibility and versatility for the proteins that they bind (reviewed in (Cortese et al., 2008). Potentially, ubiquitination might induce a structural change within Sid4 that alters the Plo1 binding site, reducing Sid4 affinity for Plo1. To address these outstanding questions, structural studies of Sid4 will be required.

From our studies, it is clear that Sid4 is ubiquitinated *in vivo*. However, the type of ubiquitin modification formed on Sid4 remains to be characterized. Because Sid4 is not targeted for degradation, it is unlikely that it is poly-ubiquitinated with K48-linked chains. Our *in vitro* studies indicate that Dma1 forms poly-ubiquitin chains with the E2 enzyme complex, Ubc13-Uev1a, which specifically forms K63-linked chains (Hofmann and Pickart, 1999). Also, the Dma1-related proteins, CHFR (Bothos et al., 2003), RNF8 (Plans et al., 2006) and *S. cerevisiae* Dma1 and Dma2 (Loring et al., 2008), have all been shown to function with Ubc13 *in vitro* and/or *in vivo*. K63-linked poly-ubiquitin chains are not typically associated with proteasome-mediated degradation, but regulate proteins by other mechanisms (for reviews see (Ikeda and Dikic, 2008; Pickart and Fushman, 2004). Recent studies indicate that the linear architecture of K63-linked chains can provide a scaffold to recruit proteins with ubiquitin-binding domains in a spatially and temporally regulated manner (Kim et al., 2007; Komander et al., 2009; Sims and Cohen, 2009). Potentially, K63-linked chains could recruit an unidentified factor to Sid4 that antagonizes either Plo1 binding or its kinase activity.

Yet another possibility is that Sid4 is not poly-ubiquitinated, but multi-ubiquitinated. Our observation that mutating all endogenous lysines within Sid4 in large

clusters has no impact on the extent of Sid4 ubiquitination supports this idea and indicates that Dma1 has loose specificity toward its target lysine(s). We have attempted to examine Sid4 ubiquitination *in vitro* to address this issue and to validate Sid4 as a direct Dma1 substrate. However, given that Dma1 binds Sid4 through its FHA domain, it is likely that Sid4 must first be phosphorylated on a threonine residue in order to interact with Dma1 and establishing the proper *in vitro* conditions will require phospho-characterization of Sid4. Thus, characterizing the type of ubiquitin modification on Sid4 will be a challenging, yet important future endeavor necessary to understand the detailed mechanism by which it antagonizes Plo1 SPB recruitment.

Conservation of mechanism

Although previously assumed based on its domain architecture, we have shown here for the first time that Dma1 is in fact a *bonafide* ubiquitin ligase. Four other proteins with similar architecture and activity, the human tumor suppressor protein, CHFR (Scolnick and Halazonetis 2000), human RNF8 (Tuttle et al., 2007), and *Saccharomyces cerevisiae* proteins, Dma1 and Dma2 (Fraschini et al., 2004) have also been implicated in mitotic checkpoints for which the pertinent substrates are unknown. It has been reported that CHFR can directly ubiquitinate the human Polo-like kinase, Plk1, in *Xenopus laevis* extracts (Kang et al., 2002) and down-regulates Plk1 protein levels in human cells (Shtivelman, 2003). These studies suggest that CHFR might directly ubiquitinate Polo-like kinases, targeting them for degradation. However, other reports indicate that a CHFR-dependent checkpoint arrest does not require the function of the proteasome at all, since cells can arrest when treated with proteasomal inhibitors (Matsusaka and Pines,

2004). Here, we find that in *S. pombe*, Plo1 localization to SPBs is at least in part regulated by ubiquitination of its scaffold rather than ubiquitination of itself. Indeed, we obtained no evidence that Plo1 or Dma1 was ubiquitinated during a mitotic checkpoint response. Whether similar mechanisms operate in other organisms to control Polo-like kinase activity during mitotic checkpoints will be important future studies.

CHAPTER III

CK1 IS REQUIRED FOR A MITOTIC CHECKPOINT THAT DELAYS CYTOKINESIS

Introduction

Failure to accurately partition genetic material during cell division causes aneuploidy and drives tumorigenesis (Kops et al., 2005). Cell cycle checkpoints safeguard cells from such catastrophes by impeding cell cycle progression when mistakes arise. To accomplish this complicated yet vital task, checkpoints employ a diverse cohort of signaling proteins. Many checkpoint proteins harbor a phospho-dependent protein-protein interaction domain coupled to a catalytic domain, affording them the ability to modify substrates in a stimulus-dependent manner (Jin et al., 2006). One such class of proteins is the FHA-RING E3 ligases that execute their cell cycle checkpoint functions by signaling to the core cell cycle machinery. However, they act downstream of primary checkpoint signals and their domain architecture indicates that they respond to signals generated by protein kinases. Indeed, *S. pombe* Dma1 requires its FHA domain for proper localization to SPBs and the cell division site (Guertin et al., 2002), CHFR requires its FHA domain for its anti-proliferative effects (Fukuda et al., 2008) and during the DNA damage response ATM phospho-primes the repair factor MDC1 for RNF8 recruitment (Kolas et al., 2007).

While the DNA damage response kinases are well defined, none of the kinases involved in mitotic phospho-priming of FHA-RING E3 ligases are known. In chapter II,

we showed that Dma1 ubiquitinates Sid4 to obstruct Plo1's SPB localization and thus Plo1's ability to trigger the SIN and cytokinesis (Johnson and Gould, 2011). In this chapter, we report that fission yeast CK1 is an essential component of the Dma1-dependent mitotic checkpoint pathway. *S. pombe* CK1 paralogs, *hhp1* and *hhp2,* concentrate at SPBs during a mitotic checkpoint arrest and phosphorylate the scaffold protein Sid4. CK1-mediated phosphorylation of Sid4 generates a binding motif for Dma1's FHA domain that is required for Sid4 ubiquitination and checkpoint function. Collectively, these data establish a novel function for CK1 in executing a mitotic checkpoint.

Results

Sid4 phosphorylation on T275 and S278 recruits Dma1 via its FHA domain

Because *S. pombe* Dma1 requires its phospho-threonine binding FHA domain to localize to SPBs and the cell division site (Guertin et al., 2002), we surmised that Dma1-Sid4 interaction depends on Sid4's phospho-status. Thus, we examined the SDS-PAGE mobility of Sid4 in checkpoint-activated cells using the cold-sensitive β-tubulin mutant *nda3*-KM311 (Toda et al., 1983). In *dma1*$^{+}$ cells, many slower migrating Sid4 isoforms were detected, which collapsed into a discrete ladder upon phosphatase treatment (Figure 3-1A, lanes 1 and 2). These bands are ubiquitinated isoforms because they collapse into a single band in the absence of *dma1*$^{+}$ (Figure 3-1A, lane 4) and Dma1 is required for Sid4 ubiquitination (Johnson and Gould, 2011). In *dma1Δ* cells, a single slower migrating form of Sid4 was detected, which was collapsed by phosphatase treatment, indicating that Sid4 is phosphorylated in vivo (Figure 3-1A, lanes 3 and 4). In vivo

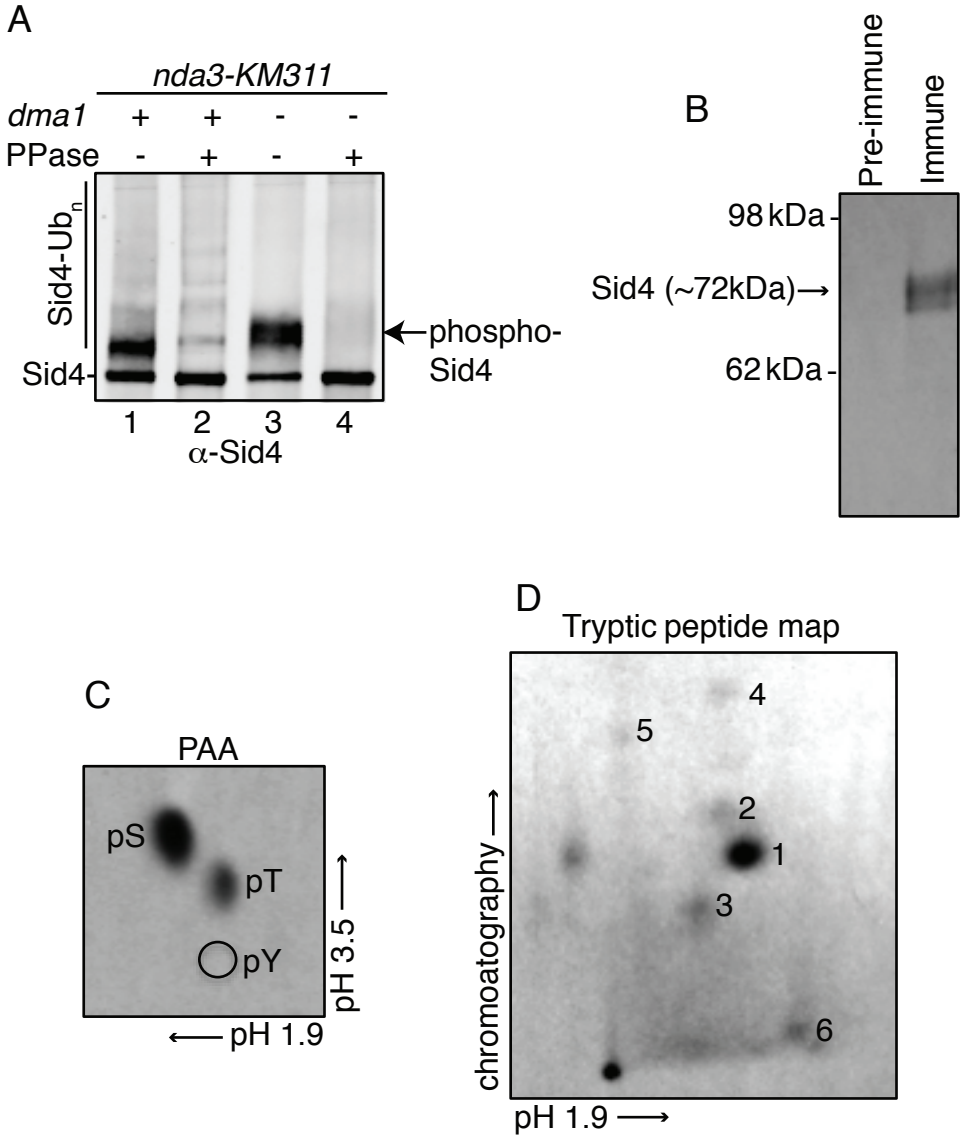

Figure 3-1

Sid4 is a phospho-protein in vivo.

A. Sid4 isoforms detected by immunoblotting in the presence and absence of *dma1* and lambda phosphatase treatment. B. Pre-immune and anti-Sid4 immunoprecipitates from *mts3-1 rad3Δ dma1Δ* cells that were labeled in vivo with ^{32}P-orthophosphate. Phosphorylated proteins were detected by SDS-PAGE and autoradiography. C. Phosphoamino acid analysis of wildtype Sid4. The position of standards is indicated and the phosphoamino acids were detected by autoradiography. D. Tryptic phosphopeptide mapping of wildtype Sid4. Phosphopeptides were detected by autoradiograph.

radiolabeling experiments validated Sid4 as a phospho-protein and revealed that Sid4 is phosphorylated on serines and threonines (Figure 3-1B-D). The constitutive presence of an unmodified Sid4 isoform indicates that only a subpopulation of Sid4 is modified (Figure 3-1A). Collectively, these data indicate that Sid4 is ubiquitinated and phosphorylated in vivo.

Sid4 was hyper-phosphorylated in cells arrested in mitosis with an active spindle checkpoint (*nda3-KM311*) compared to all other cell cycle arrests (Figure 3-2). Notably, Sid4 was not hyper-phosphorylated to the same extent in *mts3-1* mutants (Seeger et al., 1996), which arrest in metaphase do to a proteasome defect (Figure 3-2), suggesting that some Sid4 phosphorylation is specific to spindle checkpoint activity. To identify Sid4 phospho-site(s) required for Dma1 interaction, we employed a targeted mutagenesis approach. Because Dma1 interacts with the N-terminus of Sid4 (aa1-300) (Guertin et al., 2002) and Dma1's FHA domain is predicted to bind phosphorylated threonines, we performed alanine scanning of the 15 threonines in Sid4's N-terminus, substituting *sid4* mutant alleles for the endogenous gene at its native locus (Figure 3-3A-B). T275, a site that is conserved in other *Schizosaccharomyces* species (Figure 3-3C), was the only threonine required for Sid4 ubiquitination (Figure 3-3B-D).

FHA domain binding studies indicate that residues in the pT+3 position contribute to FHA binding specificity (Durocher et al., 2000). Although mutating S278 to alanine abolished Sid4 ubiquitination (Figure 3-3D), mutating S278 to a glutamate did not affect Sid4 ubiquitination (Figure 3-3D). This indicates that a negative charge in the pT+3 position is required to stabilize Dma1 interaction with T275-phosphorylated Sid4 and thus S278 must also be phosphorylated. Mutating residues immediately adjacent to T275

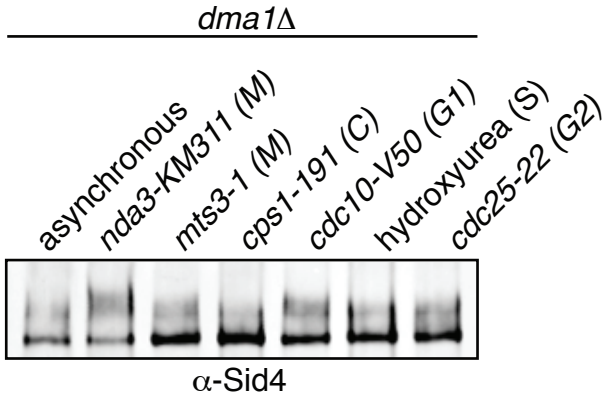

Figure 3-2

Sid4 is hyper phosphorylated during a mitotic checkpoint arrest.
Sid4 was immunoprecipitated from the indicated strains and detected by immunoblot.

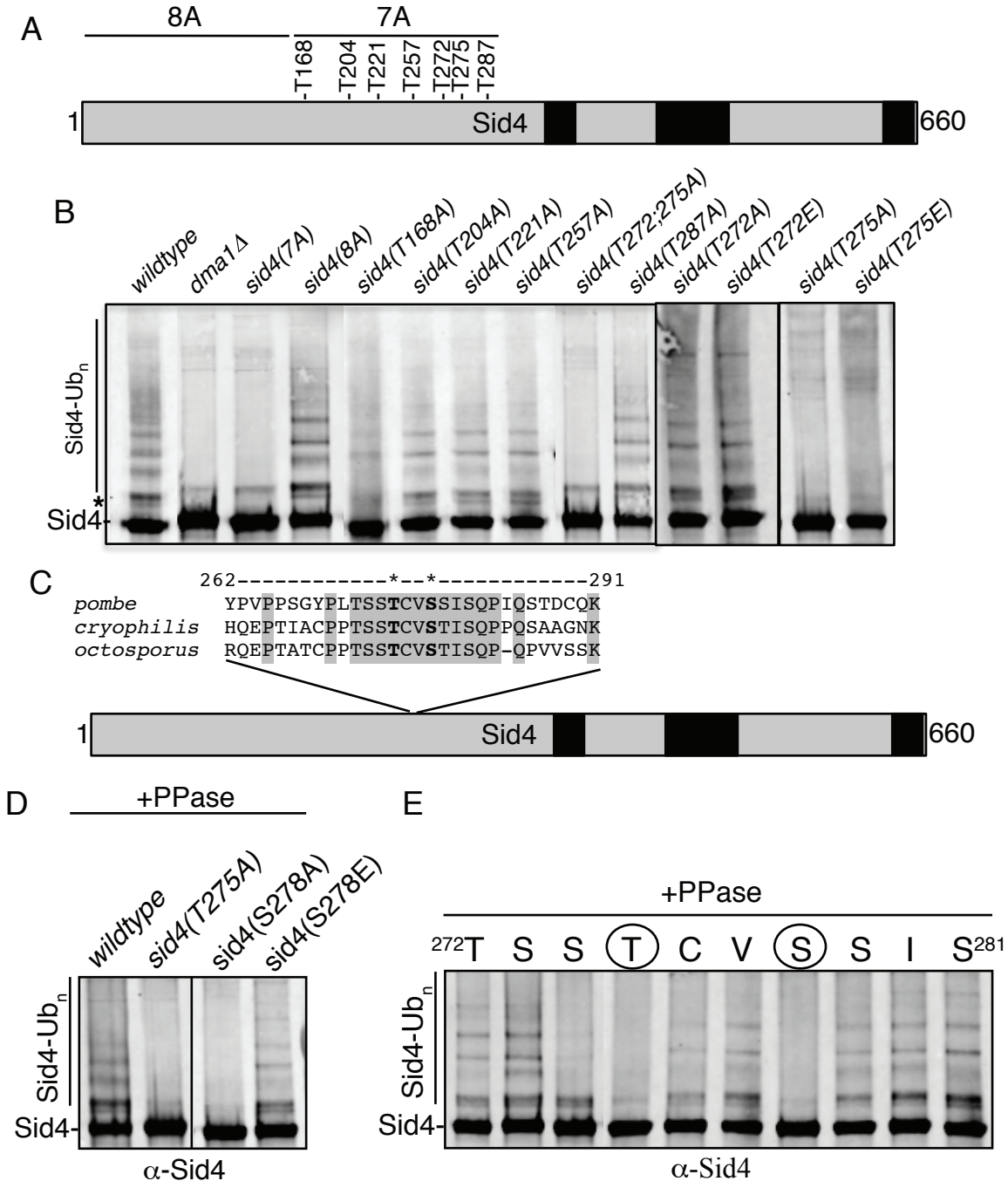

Figure 3-3

T275 and S278 are required for Sid4 ubiquitination.

A. Schematic diagram of Sid4 showing the position of threonines in Sid4's N-terminus. B. In vivo ubiquitination status of Sid4 threonine mutants. C. Schematic diagram of Sid4 with the relative position of the Dma1 binding site. ClustalW alignment of the Dma1 binding sequence from *S. pombe, S. cryophilis* and *S. octosporus*. D-E. Sid4 from the indicated strains was immunoprecipitated from denatured cell lysates, treated with phosphatase and visualized by immunoblotting.

and S278 did not affect Sid4 ubiquitination, implying that T275 and S278 are the only residues critical for this event (Figure 3-3E). Although Dma1-GFP still localized to SPBs in *sid4(T275A)* mutant cells (Figure 3-4A), combining *sid4(T275A)* with a mutation in the second SIN scaffold, *cdc11-123,* eliminated Dma1-GFP SPB localization, though each individual mutant did not affect its localization (Figure 3-4B). These data indicate that Dma1 has at least two binding partners at SPBs and that mutation of T275 on Sid4 specifically abrogates Dma1-Sid4 interaction.

Because T275 and S278 are necessary for Sid4 ubiquitination, we examined whether phosphorylation of these two sites was sufficient to foster binding to Dma1's FHA domain. Sid4 phospho-peptides spanning the putative Dma1-binding region (aa271-282) were incubated with a recombinant Dma1 fragment containing the FHA domain (aa 1-143; His-FHA) and tested for their ability to interact. While the unphosphorylated peptide, or peptides phosphorylated on either T275 or S278 alone, did not support His-FHA binding, a peptide with both T275 and S278 phosphorylated (pT275,pS278) bound the His-FHA fragment (Figure 3-5A). This interaction requires a functional FHA domain because a mutation in the FHA domain (R64A) predicted to disrupt interaction with the phosphorylated target site abolished the association (Figure 3-5A). A phospho-mimetic peptide (T275E,S278E) did not bind the FHA domain, indicating that negatively charged amino acids do not effectively mimic phosphorylation in this context (Figure 3-5B). This is consistent with our finding that Sid4(T275E) mutants are not ubiquitinated in vivo (Figure 3-3B). Thus, phosphorylation on both T275 and S278 is necessary and sufficient to support binding of the Dma1 FHA domain to Sid4 and Sid4 ubiquitination.

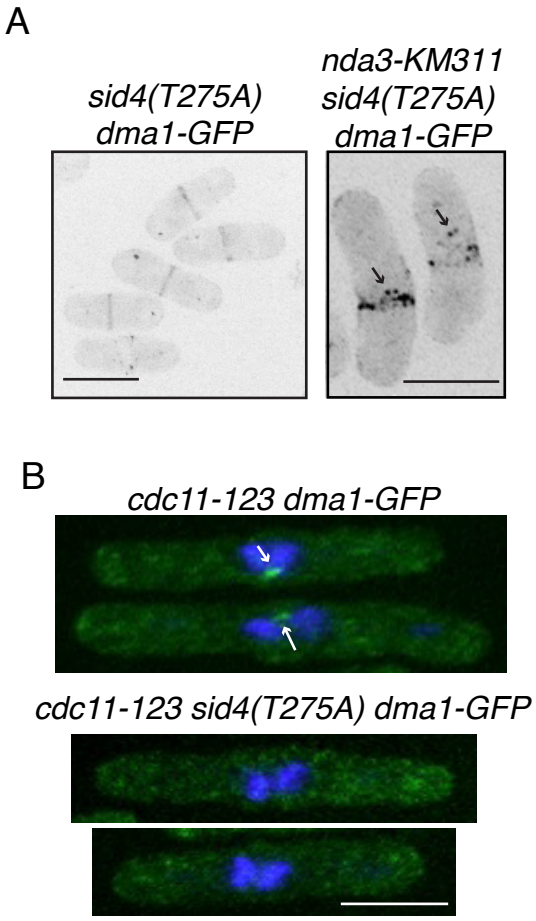

Figure 3-4

Dma1 localization in *sid4(T275A)* mutants.

A. dma1-GFP localization in asynchronous (left) or *nda3-KM311* (right) arrested *sid4(T275A)* cells. B. Dma1-GFP localization in *cdc11-123* or *cdc11-123 sid4(T275A)* cells that were grown at 25°C to mid-log phase and shifted to 36°C for 3.5 hrs.

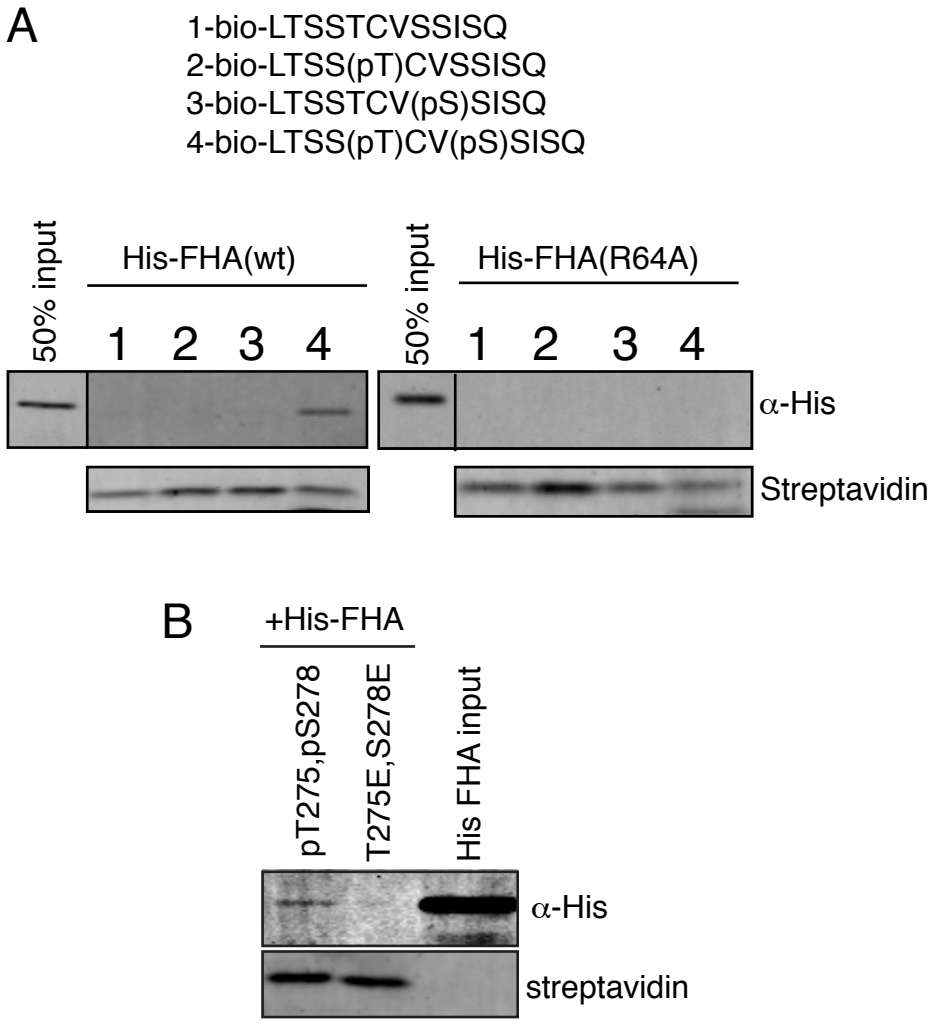

Figure 3-5

Dma1's FHA domain binds a pTXXpS motif on Sid4.

A-B. Synthetic Sid4 peptides (aa271-282) conjugated to streptavidin beads were incubated with recombinant His-FHA (aa1-143) and bound proteins were detected by immuno-blotting.

Sid4 phosphorylation on T275 and S278 is required for the Dma1-dependent checkpoint

Given that phosphorylation of T275 and S278 recruits Dma1 to Sid4 for subsequent Sid4 ubiquitination, we examined whether phosphorylation of these sites was stimulated in response to spindle checkpoint activation. To detect phosphorylation of T275 and S278 in vivo, we generated a phospho-specific antibody to these two phospho-sites (pT275,S278) (Figure 3-6A). Indeed, phosphorylation of these sites was detected at increased levels in checkpoint-stimulated cells (*nda3-KM311*) compared to cells growing asynchronously or cells arrested in mitosis in the absence of a spindle checkpoint (*mts3-1*) (Figure 3-6B). Thus, Sid4 phosphorylation on T275 and S278 is stimulated in response to a mitotic checkpoint.

To examine whether the checkpoint was negatively affected in *sid4(T275A)* mutants as we would predict, *nda3-KM311* cells were synchronized in S-phase with hydroxyurea treatment, released to 19°C to activate the mitotic checkpoint and monitored for their ability to maintain the arrest. *nda3-KM311* cells held a checkpoint arrest for 6-7 hrs, whereas *nda3-KM311 sid4(T275A)* cells bypassed the arrest after 5 hrs (Figure 3-6C). This is comparable to *nda3-KM311 dma1Δ* cells, which also evaded the arrest after 5 hrs. Importantly, *nda3-KM311 sid4(T275A) dma1Δ* cells did not exhibit additive defects, indicating that both mutations function in the same pathway (Figure 3-6C). These data indicate that mutating T275 eliminates Dma1-dependent checkpoint signaling.

In corroboration of these findings, *sid4(T275A)* mutants were refractory to *dma1* over-expression lethality (Figure 3-6D). Furthermore, *sid4(T275A)* mutants were synthetically sick with mutation of another SIN inhibitor *cdc16-116* and suppressed the

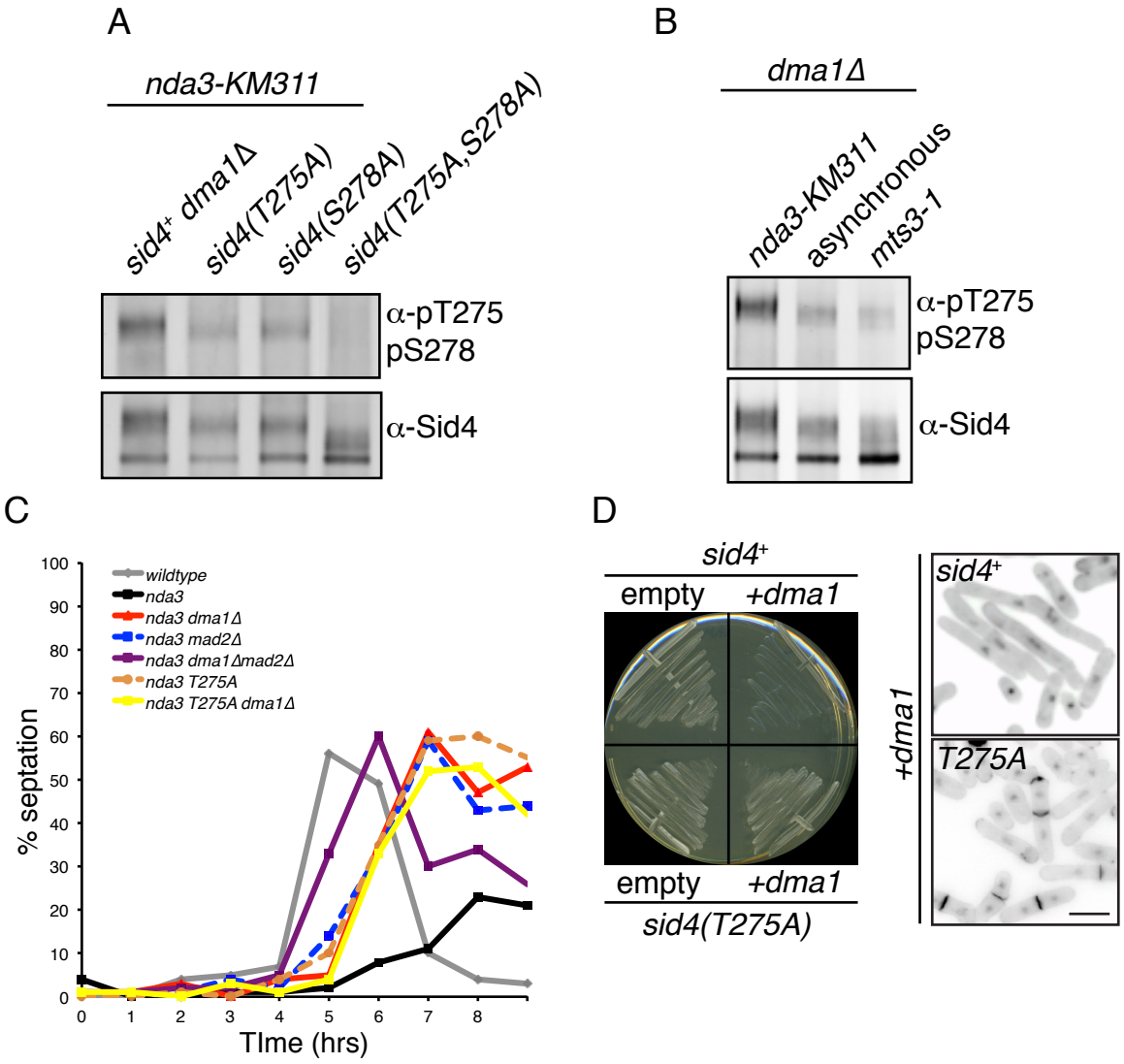

Figure 3-6

***sid4(T275A)* mutants compromise checkpoint function and suppress *dma1*⁺ over-expression lethality.**

A-B. Sid4 was immunoprecipitated from the strains indicated using a Sid4 antibody and detected by immunoblot using Sid4 and pT275,pS278 antibodies. C. Spindle checkpoint assay. n=3, *p<0.001 compared to wildtype, NS=not significant when compared to each other. D. Over-expression of dma1 in sid4+ or sid4(T275A) mutant cells. Growth of the transformants was observed on agar plates (left) after de-repression of the nmt41 promoter and their phenotypes were analyzed by DAPI (DNA) and methyl blue (septa) staining (right). Inverted grayscale images are shown, scale bar, 5 μm.

temperature-sensitive lethality of positive SIN regulator mutants *spg1-106, sid2-250, cdc11-136, plo1-1* and *plo1-24c* (Figure 3-7A-C). These genetic data imply that eliminating T275 phosphorylation produces a hypermorphic *sid4* allele due to loss of cytokinesis inhibition by Dma1-mediated ubiquitination.

Dma1 functions upstream of the SIN inhibitor Cdc16, whose *S. cerevisiae* homolog, Bub2, functions independently of the kinetochore-localized SAC components (Alexandru et al., 1999; Fraschini et al., 1999; Li, 1999). Over-expression of the kinetochore-based SAC activator, *mph1,* does not drive Dma1 to SPBs (data not shown), implying that Dma1 similarly functions in a kinetochore-independent SAC pathway. To test this, we compared the checkpoint defects of *sid4(T275A)* and *dma1*Δ mutants to *mad2*Δ mutants. *mad2*Δ cells bypassed the checkpoint arrest with similar kinetics as both *dma1*Δ and *sid4(T275A)* and a double *dma1*Δ *mad2*Δ mutant displayed an additive checkpoint defect phenotype (Figure 3-6C). Thus, similar to *S. cerevisiae*, a kinetochore-independent SAC exists in *S. pombe*, which is dependent on *dma1*.

CK1 is required for Sid4 ubiquitination and associates with the SIN pathway during a mitotic checkpoint

To identify the protein kinase(s) directing Dma1-Sid4 interaction, we screened a comprehensive non-essential protein kinase deletion collection (Bimbo et al., 2005) for loss of Sid4 ubiquitination and found that deleting any single kinase did not abolish Sid4 ubiquitination (data not shown). Similarly, we screened all available essential temperature-sensitive or analog-sensitive kinase mutants and did not identify any that eliminated Sid4 ubiquitination (data not shown). Finally, we screened several multi-

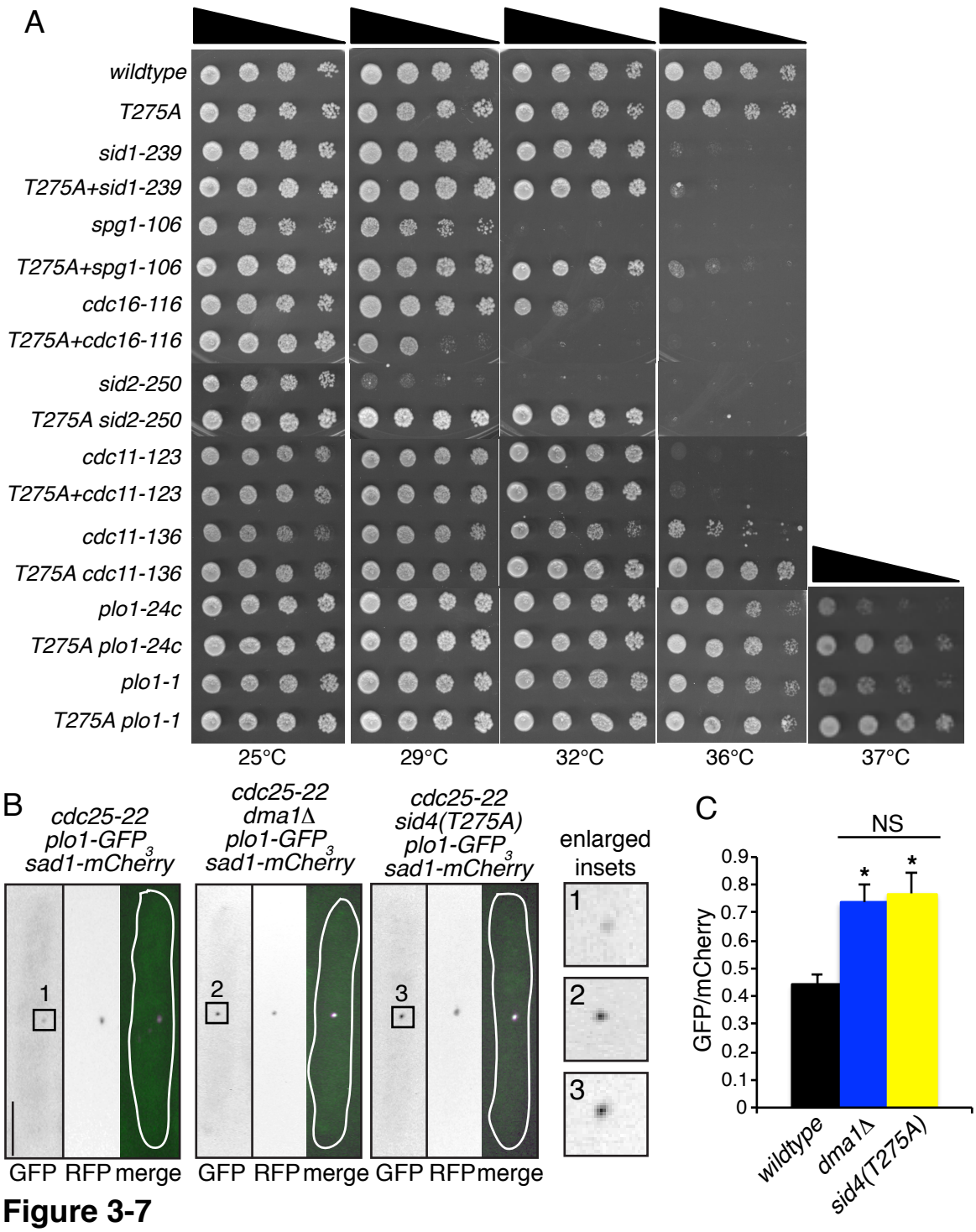

Figure 3-7

***sid4(T275A)* mutant produces a hypermorphic *sid4* allele.**

A. The indicated strains were grown at 25°C, and spotted in 5X serial dilutions and incubated at the indicated temperatures. B. Plo1-GFP$_3$ co-imaged with the SPB marker Sad1-mCherry in cells arrested in G2 by the cdc25-22 mutation. GFP and mCherry images were converted to inverted grayscale images, scale bar, 5 µm. C. Quantitation of Plo1-GFP$_3$ at SPBs . Values are represented as GFP/mCherry ratios. n=20, *p<0.001 compared to wildtype cells, NS=not significant when compared to each other.

kinase deletions based on sequence homology within their kinase domains (Bimbo et al., 2005), as these should have similar phosphorylation consensus sites (data not shown). The results of this screen indicated that only *S. pombe* CK1 homologs, *hhp1* and *hhp2,* are required for Sid4 ubiquitination (Figure 3-8A).

CK1 is a conserved kinase important for many cellular processes including cell proliferation and chromosome segregation (Knippschild et al., 2005). Human CK1δ/ε, which are most related to Hhp1/2, localize to centrosomes and inhibition of these two isoforms results in aberrant mitoses (Behrend et al., 2000). In cells growing asynchronously, both Hhp1-GFP and Hhp2-GFP localized to the nucleus, SPBs, and the cell division site, although Hhp2-GFP was more prominent at the division site compared to Hhp1-GFP (Figure 3-8B). When the checkpoint was activated, Hhp1-GFP and Hhp2-GFP localized predominantly to SPBs (Figure 3-8C), a pattern that mirrors Dma1 localization (Johnson and Gould, 2011).

Consistent with the localization analyses, Hhp1-HA_3-TAP and Hhp2-HA_3-TAP co-purified several SPB proteins from checkpoint-activated cells, including many SIN proteins (Figure 3-9A). When purified from *nda3-KM311 hhp1Δ* cells, Hhp2-HA_3-TAP co-purified more SPB proteins compared to *nda3-KM311 hhp1*$^+$ cells (Figure 3-9A), suggesting that Hhp1 is the dominant kinase at SPBs, but Hhp2 may compensate if Hhp1 is absent. Hhp1-GFP localization at SPBs is Sid4 independent (Figure 3-9B), but requires Ppc89, a protein that tethers Sid4 at SPBs (Figure 3-9C). Interestingly, human CK1δ/ε is tethered to centrosomes by the scaffold protein CG-NAP (Sillibourne et al., 2002), which forms a complex with another centrosomal scaffold protein Kendrin

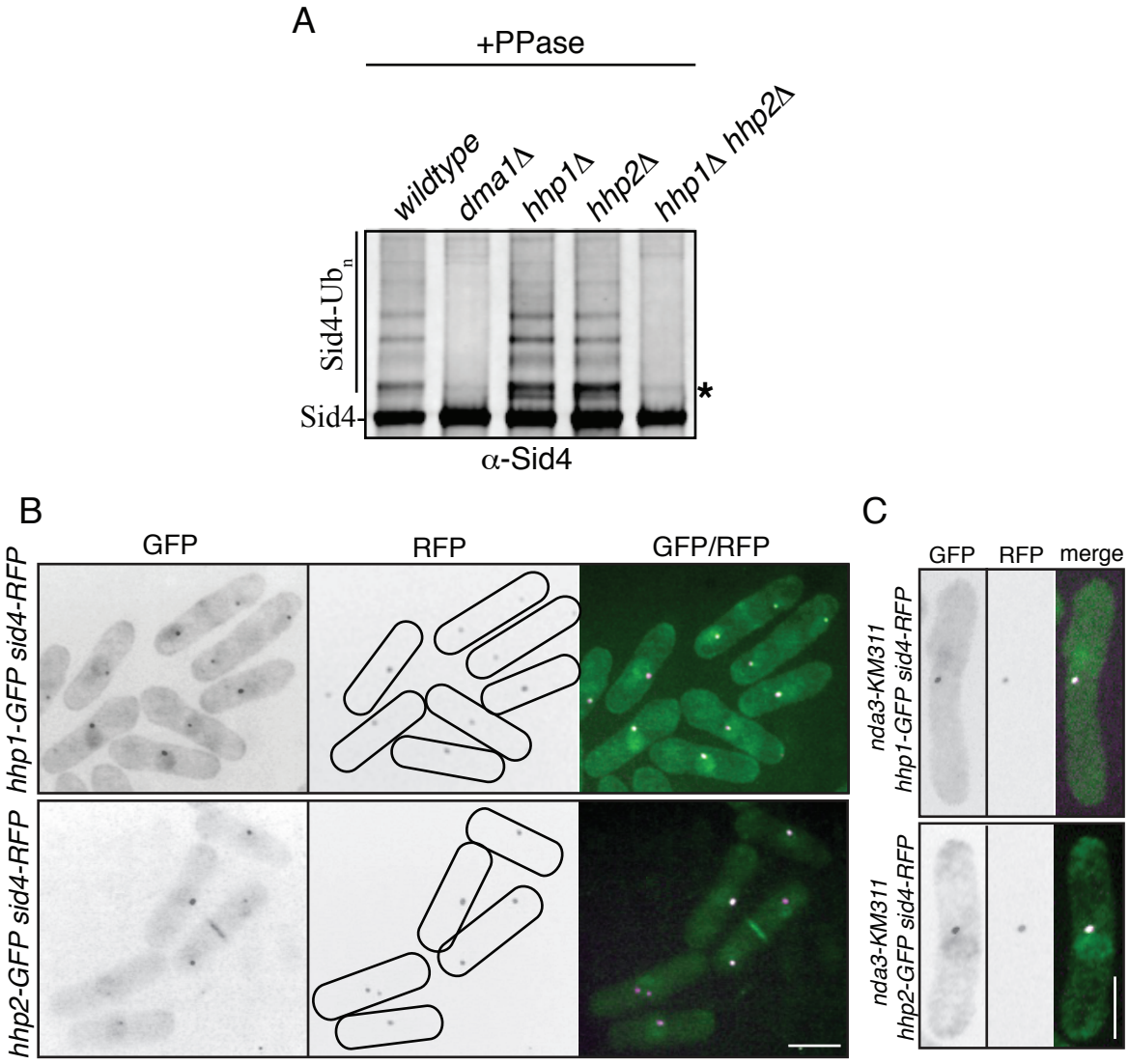

Figure 3-8

CK1 is required for Sid4 ubiquitination and localizes to SPBs during a mitotic checkpoint.

A. Sid4 was immunoprecipitated from the indicated strains and treated with lambda phosphatase before visualizing by immunoblotting. *background band. B and C. Hhp1-GFP and Hhp2-GFP co-imaged with the SPB marker Sid4-RFP in live cells growing asynchronously (B) or in cells arrested in mitosis with an active spindle checkpoint (C). Inverted grayscale images are shown for GFP and RFP, scale bar, 5 μm.

A

			nda3-KM311 hhp1-HA$_3$-TAP		*nda3-KM311 hhp2-HA$_3$-TAP*		*nda3-KM311 hhp1Δ hhp2-HA$_3$-TAP*	
Accession #	**Protein**	**description**	**TSC**	**%**	**TSC**	**%**	**TSC**	**%**
SPBC3H7.15	Hhp1	CK1	7290	77%	8	30%	0	0%
SPAC23C4.12	Hhp2	CK1	13	34%	3191	79%	2695	78%
SPCC1739.11c	Cdc11	Centriolin	166	43%	0	0%	147	48%
SPAC6G9.06c	Pcp1	Pericentrin	137	51%	22	17%	291	69%
SPAC4H3.11c	Ppc89	SIN scaffold	119	43%	19	21%	212	60%
SPBC244.01c	Sid4	SIN scaffold	74	44%	0	0%	113	64%
SPAC24B11.11c	Sid2	SIN kinase	41	36%	7	14%	50	45%
SPAC222.10c	Byr4	SIN GAP	35	27%	0	0%	27	32%
SPBC32F12.04	Gtb1	γ-tubulin	34	51%	23	31%	15	35%
SPBC21.06c	Cdc7	SIN kinase	17	17%	0	0%	12	14%
SPCC417.07c	Mto1	MT organizer	20	17%	23	20%	202	59%
SPBC649.05	Cut12	SPB protein	15	21%	0	0%	77	68%
SPCC1682.04	Cdc31	Centrin	7	28%	0	0%	13	47%

B

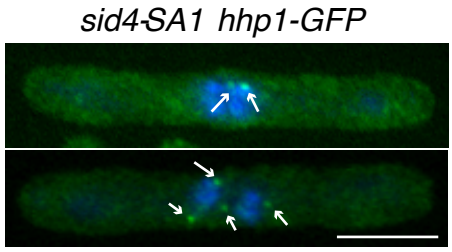

C

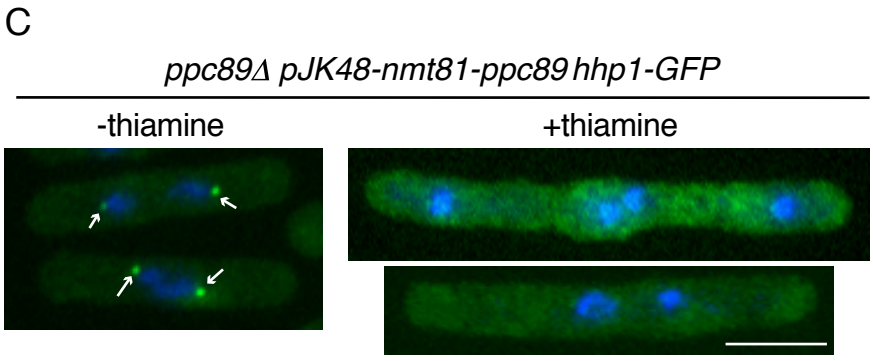

Figure 3-9

Hhp1 and Hhp2 physically associate with the SIN pathway.

A. Localization of Hhp1-GFP (green) in *sid4-SA1* mutant cells. B. Localization of Hhp1-GFP (green) in a *ppc89* shut-off strain (-thiamine, *ppc89* expression on; +thiamine, *ppc89* expression off). DAPI staining of the DNA is also shown (blue). C. Hhp1-HA$_3$-TAP or Hhp2-HA$_3$-TAP was purified from checkpoint-activated cells and interacting proteins were identified by 2D-LC/MS. TSC=total spectral counts, %=percent sequence coverage.

(Takahashi et al., 2002), a putative Sid4 homolog. Thus, CK1's centrosomal tethering mechanism may be conserved.

Since CK1 localizes in the nucleus and SPBs, it is in a prime position to transmit signals from the nucleus to SPBs. Accordingly, Hhp1-GFP became less pronounced at SPBs and re-accumulated in the nucleus as *nda3-KM311* cells released from a checkpoint block (Figure 3-10A). This prompted us to examine whether Hhp1's strong mitotic SPB localization depended on spindle checkpoint activation. Indeed, compared to mitotic cells with no checkpoint activation, Hhp1-GFP intensity at SPBs was significantly higher when a mitotic checkpoint was activated (Figure 3-10B-C). These data indicate that Hhp1/2 display dynamic localization patterns and accumulate at SPBs in response to spindle checkpoint activation.

CK1 phospho-primes Sid4 for Dma1-mediated ubiquitination

The canonical CK1 consensus sequence is $p(S/T)X_{1-2}(S/T)$ and a negatively charged amino acid can sometimes substitute for the N-terminal phospho-amino acid (Knippschild et al., 2005). However, CK1 does not always require N-terminally phosphorylated or acidic amino acids (Cegielska et al., 1998; Cegielska et al., 1994; Swiatek et al., 2006). Because CK1 is required for Sid4 phosphorylation on T275 and S278 in vivo (Figure 3-11A), we examined whether CK1 directly phosphorylates these sites in vitro. Full length Sid4-myc_6 was produced through an in vitro transcription/translation system and phosphorylated by recombinant CK1δ, which we found to have the same specificity toward Sid4 as Hhp1/2 (data not shown). CK1 phosphorylation of Sid4-myc_6 was detected with the phospho-T275,S278 antibody,

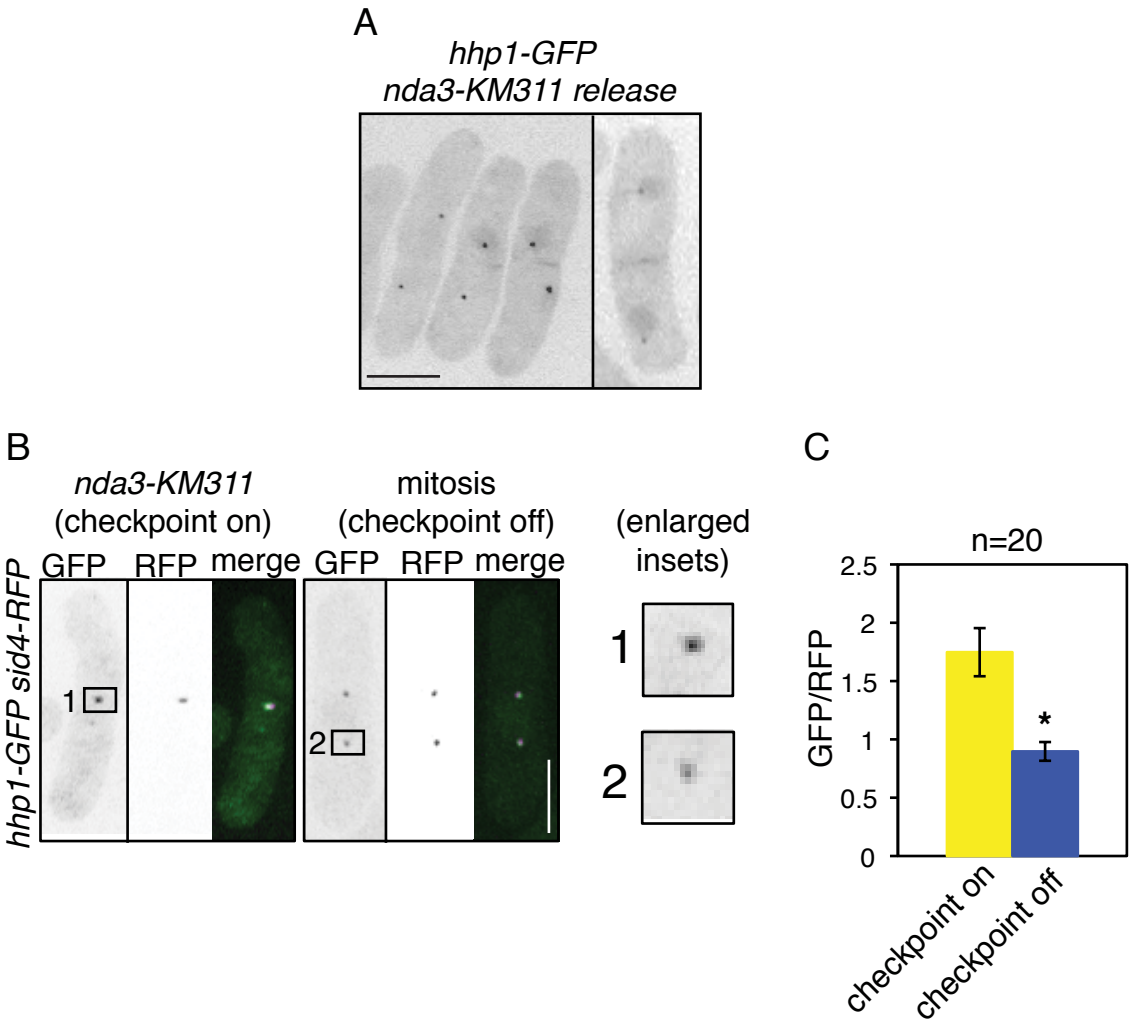

Figure 3-10

CK1 concentrates at SPBs during a mitotic checkpoint arrest.

A. Hhp1-GFP imaged in cells released from a pro-metaphase arrest. Inverted grayscale images are shown, scale bar, 5 μm. B. Hhp1-GFP imaged in checkpoint-activated and asynchronously growing mitotic cells. Inverted grayscale images are shown for GFP and RFP, scale bar, 5 μm. C. Quantitation of Hhp1-GFP at SPBs in the strains used in B. Values are represented as GFP/RFP ratios. n=20 cells, *p<0.001 compared to "checkpoint off" cells.

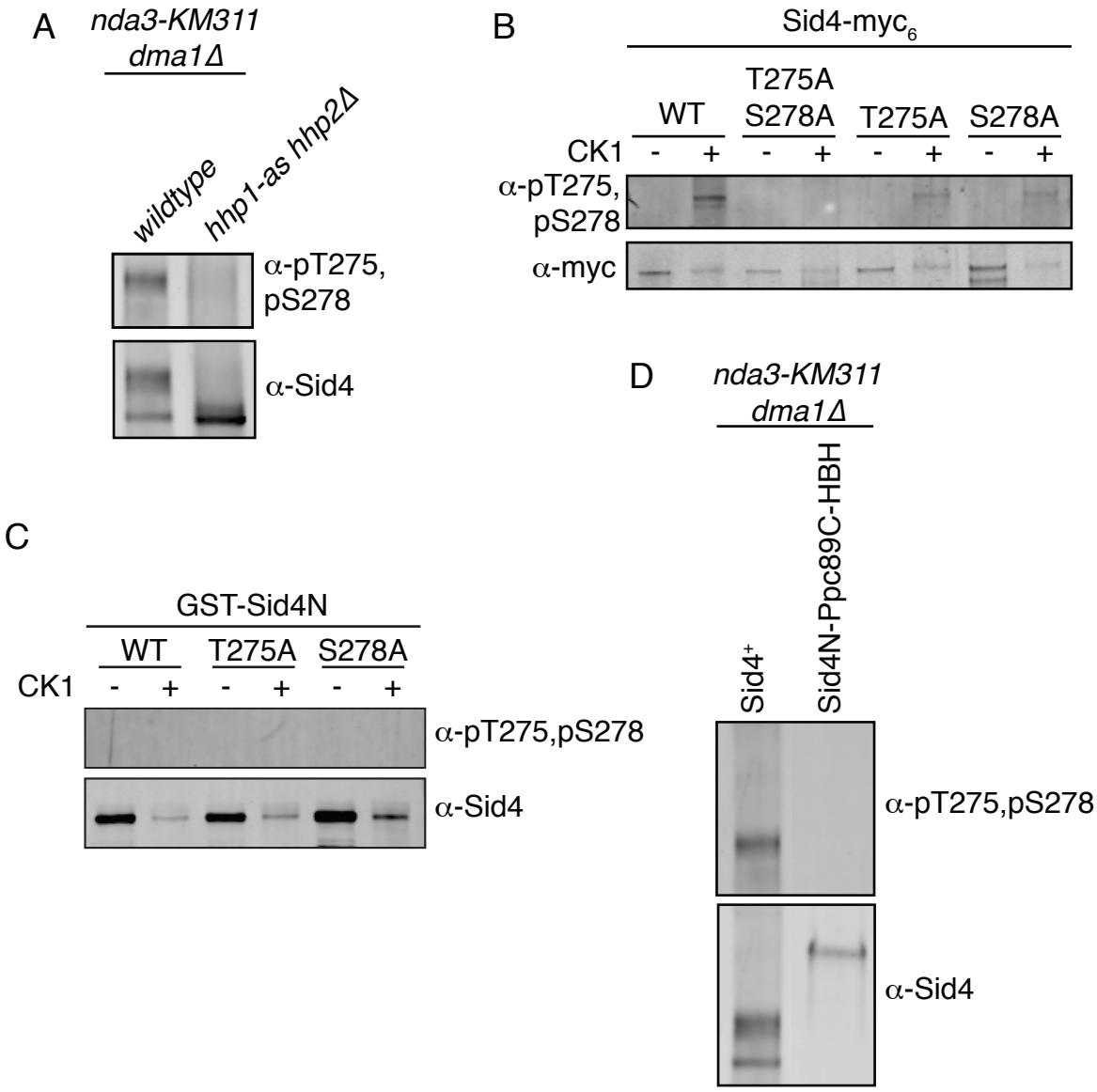

Figure 3-11

CK1 phosphorylates full-length Sid4 on T275 and S278.

A. Sid4 protein was immunoprecipitated from the indicated strains and detected by immunoblotting. B. Full-length Sid4-myc or Sid4-myc mutants were produced via an in vitro transcription/translation reaction, phosphorylated by CK1 and detected by immunoblot. C. GST-Sid4N (aa1-300) proteins were purified from bacteria, phosphorylated by CK1 and detected by immunoblot. D. Sid4 or Sid4N-Ppc89C-HBH were purified from checkpoint activated cells (*nda3-KM311 dma1*Δ) and detected by immunoblot.

indicating that CK1δ directly phosphorylates one or both sites (Figure 3-11B). As expected, Sid4(T275A,S278A)-myc$_6$ incubated with CK1δ was not detected by the phospho-T275,S278 antibody (Figure 3-11B). Sid4(T275A)-myc$_6$ and Sid4(S278A)-myc$_6$ single mutants incubated with CK1δ were detected by the phospho-antibody, albeit to a lesser extent, indicating that CK1 phosphorylates both sites in vitro (Figure 3-11B).

Surprisingly, we found that whereas CK1 phosphorylated Sid4 on T275 and S278 in the context of the full-length protein, it did not phosphorylate these sites when the C-terminus was removed (Figure 3-11C). Accordingly, a Sid4N-Ppc89C fusion that lacks Sid4's endogenous C-terminus and was not ubiquitinated in vivo (Johnson and Gould, 2011) is also not phosphorylated on T275 or S278 (Figure 3-11D). Thus, the Sid4 C-terminus is required for N-terminal CK1-mediated phosphorylation. Although atypical, a tertiary structural requirement for CK1-mediated phosphorylation was previously described (Cegielska et al., 1998; Cegielska et al., 1994). Specifically, CK1ε phosphorylates full-length SV40 large T-antigen on two sites in the N-terminus of T-antigen, but does not phosphorylate a C-terminally truncated mutant even though it retains these sites (Cegielska et al., 1998; Cegielska et al., 1994). Thus, similar to CK1ε phosphorylation of T-antigen, CK1 recognizes its target sites on Sid4 through an unconventional mechanism requiring non-linear elements of the protein's structure.

Because CK1 phosphorylates Sid4 on T275 and S278 directly, we next examined whether CK1 was required for the Dma1-dependent checkpoint. Because *hhp1-as hhp2*Δ mutants exhibit a significant delay in G2 due to unrelated cell cycle defects, we were precluded from examining their mitotic checkpoint competency directly. However, *hhp1-as hhp2*Δ cells were refractory to *dma1* over-expression (Figure 3-12A), suggesting

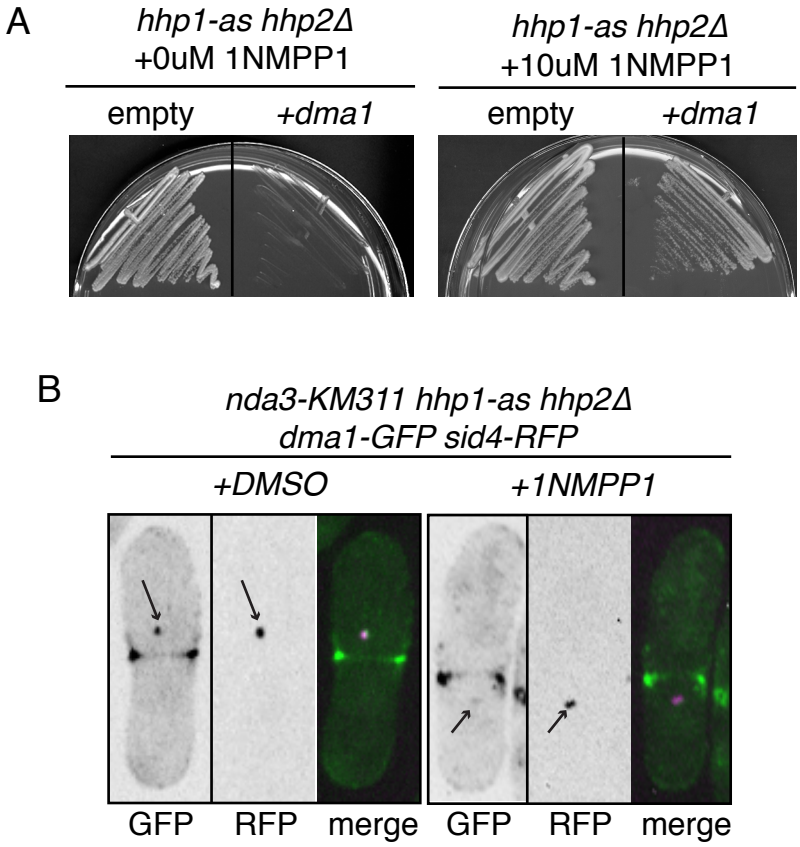

Figure 3-12

CK1 is required for Dma1-dependent signaling.

A. Over-expression of *dma1* in *hhp1-as hhp2*Δ cells. Growth of transformants was observed on agar plates in the presence or absence of 1NMPP1 ATP analog after de-repression of the *nmt41* promoter. B. Dma1-GFP was co-imaged with Sid4-RFP in *nda3-KM311 hhp1-as hhp2*Δ cells. Cells were arrested in mitosis at 18°C for 5.5 hrs and either DMSO or 1NMPP1 was added to the media for 1 hr before imaging.

that CK1 is required for Dma1-dependent signaling. Furthermore, Dma1-GFP localization at SPBs in checkpoint-activated cells is dependent on *hhp1/2* (Figure 3-12B). Collectively, these data establish CK1 as the major proximal upstream signaling component that recruits Dma1 to Sid4 during a mitotic checkpoint.

Discussion

We have discovered a novel function of the highly conserved protein kinase CK1 in the Dma1 signaling pathway that delays cytokinesis when cells encounter mitotic stress. Our data support a model (Figure 3-13) wherein *S. pombe* CK1-mediated phosphorylation of Sid4 generates a binding motif (pTXXpS) that recruits Dma1 via its phospho-threonine binding FHA domain. Subsequently, Dma1 ubiquitinates Sid4 to antagonize Plo1 recruitment and consequently prevents Plo1 from activating the SIN and cytokinesis (Guertin et al., 2002; Johnson and Gould, 2011).

In the DNA damage response pathway, ATM and ATR are the major sensors for DNA damage and phosphorylation of their targets recruit downstream checkpoint proteins and repair factors that amplify the checkpoint response (Ciccia and Elledge, 2010). Similarly, several protein kinases including Mps1, Bub1 and Aurora B have been implicated in sensing microtubule-kinetochore attachments and recruiting spindle checkpoint proteins to kinetochores to inhibit the anaphase promoting complex/cyclosome (APC/C) (Musacchio and Salmon, 2007). Our identification of CK1 as an upstream activator of the Dma1-dependent checkpoint pathway is the first insight into a mitotic molecular sensor for the FHA-RING E3 ligase family. It was recently discovered that CK1δ phospho-primes a viral E3 ligase, which binds and hijacks RNF8

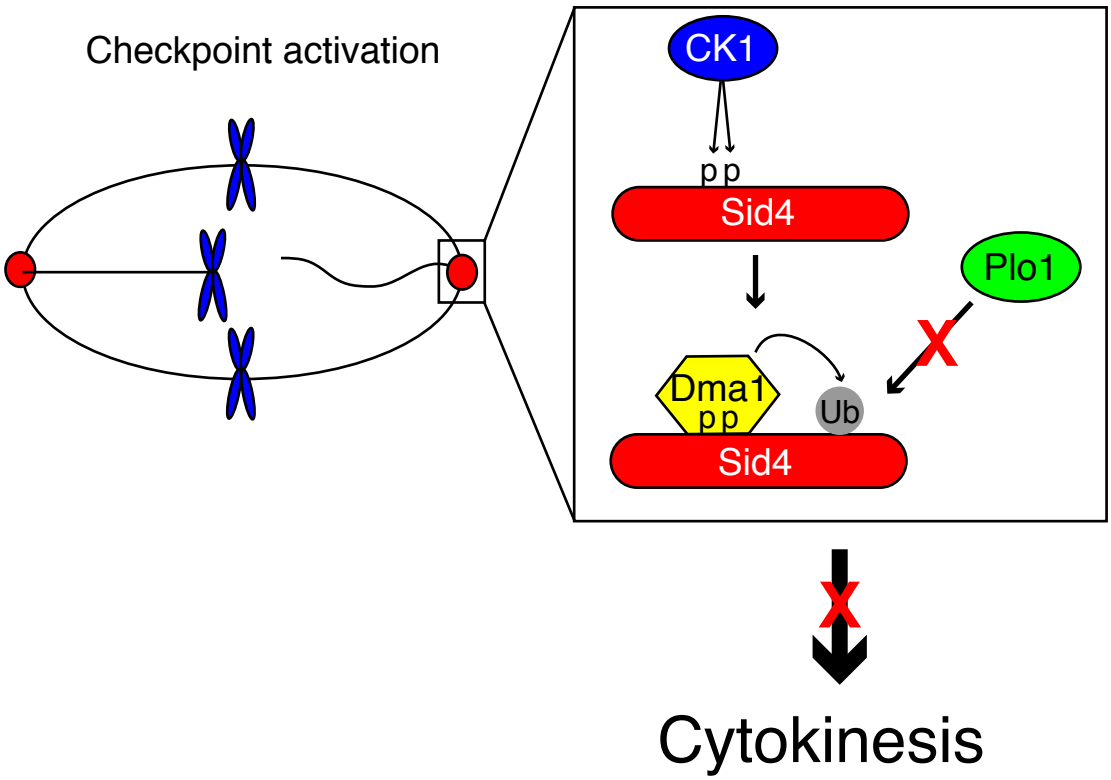

Figure 3-13

Model for CK1 activation of the Dma1-dependent checkpoint pathway.
Upon checkpoint activation, CK1 concentrates at SPBs and phosphorylates the SIN scaffold Sid4 on T275 and S278. CK1 mediated phosphorylation of Sid4 recruits Dma1 via its FHA domain, which subsequently ubiquitinates Sid4. Sid4 ubiquitination impedes Plo1 localization to SPBs, restricting Plo1's ability to promote cytokinesis.

away from its cellular target MDC1 (Chaurushiya et al., 2012). Taken together, these studies might represent a paradigm for CK1 phosphoregulation of FHA-RING E3 ligase targeting.

We have also established CK1 and Dma1 as components of a kinetochore-independent SAC pathway. In contrast to the kinetochore-based SAC pathway that monitors successful MT-chromosome attachments, it has been proposed that the Bub2/Cdc16-dependent branch of the SAC, which is based at SPBs, monitors chromosome segregation by sensing MT-SPB tension or kinetochore-SPB interactions (Li, 1999). CK1 is ideally situated in the nucleus and at SPBs to detect MT-SPB attachments/tension and transmit signals to SPBs, where Dma1 executes its checkpoint function. Because human CK1δ/ε also localizes in the nucleus and at centrosomes (Milne et al., 2001), our identification of CK1 as a prospective sensor of the Bub2/Cdc16-dependent checkpoint pathway could help to reveal the mechanical and/or biochemical signals that trigger a centrosome-based SAC pathway in multiple organisms.

CHAPTER IV

FISSION YEAST DMA1 REQUIRES RING DOMAIN DIMERIZATION FOR ITS UBIQUITIN LIGASE ACTIVITY AND MITOTIC CHECKPOINT FUNCTION

Johnson A.E., Collier S.E., Ohi M.D., and Gould K.L. (2012)

The Journal of Biological Chemistry, 287:25741-8

Introduction

E3 ubiquitin ligases facilitate the final step in protein ubiquitination by promoting transfer of Ubiquitin from the E2 enzyme to a target lysine residue on the substrate (Pickart, 2004). Two distinct classes of E3 ligases exist, which are classified by the presences of either a RING or HECT domain. RING domain E3 ligases have been thought to mainly act as scaffolds to bring the E2~Ub complex in proximity to the substrate (Deshaies and Joazeiro, 2009); however, recent evidence suggests that RING domains might also allosterically activate their cognate E2 (Ozkan et al., 2005). In contrast, HECT domain E3s first ligate ubiquitin to an active cysteine residue on themselves before actively catalyzing ubiquitination of the substrate (Rotin and Kumar, 2009). In addition to either a HECT or RING domain, many E3s also contain a substrate recognition motif that provides substrate specificity.

Many RING domain E3 ligases can multimerize and this has proven to be important for their function; however, the nature of these oligomeric complexes varies widely. Some RING E3s, such as RNF4 (Liew et al., 2010), cIAP (Mace et al., 2008), and Siah (Polekhina et al., 2002) self-interact to form homodimers, while others interact with distinct RING E3 ligases to form heterodimers, such as Mdm2-MdmX (Linares et

al., 2003), Ring1b-Bmi1 (Wang et al., 2004) and Brca1-Bard1 (Hashizume et al., 2001). In addition to these smaller complexes, some RING E3s can also form higher order oligomers either with themselves or with other RING E3s (Poyurovsky et al., 2007). While it is not completely clear why many RING E3s need to multimerize for their function, recent studies suggests that two RING domains might be required to spatially accommodate the E2~Ub conjugate (Plechanovova et al., 2011).

In this chapter, we show that Dma1 forms a homodimer via its RING domain and dimerization is required for its E3 ligase activity. Accordingly, mutant cells expressing a constitutively monomeric form of Dma1 are defective in their mitotic checkpoint response and Sid4 ubiquitination is abolished, demonstrating that Dma1 requires dimerization in vivo. Furthermore, in the absence of dimerization, Dma1 has reduced localization at SPBs and the cell division site, suggesting that dimerization is required for proper Dma1 localization. Thus, Dma1 forms an obligate dimer via its RING domain, which is essential for efficient transfer of ubiquitin to its substrate(s). These studies further support the mechanistic paradigm that many RING E3 ligases function as RING dimers.

Results

Dma1 self-associates in vivo via its RING domain

Since many RING E3 ubiquitin ligases self-associate to form homodimers or associate with other RING E3s to form heterodimers, we asked whether Dma1 self-associated in vivo. Diploid cells were generated in which one allele of *dma1* was tagged with sequences encoding a $V5_3$ epitope and the other *dma1* allele was tagged with

sequences encoding a $flag_3$ epitope. By immunoprecipitation, we found that Dma1-$flag_3$ and Dma1-$V5_3$ could interact in vivo (Figure 4-1A). Furthermore, full-length Dma1 could interact with itself in a yeast 2-hybrid experiment, suggesting that this interaction might be direct (Figure 4-1B).

We then tested a variety of Dma1 fragments in a yeast 2-hybrid assay to map the region of self-interaction. Deletion of the N-terminal FHA domain and mid region (aa1-186) did not affect Dma1 self-interaction; however, deletion of the RING domain and the C-terminal residues flanking the RING domain (aa192-end) abolished interaction indicating that this region is necessary for self-interaction (Figure 4-1B). The RING domain with the C-terminal tail (aa187-end) interacted with both full-length Dma1 and itself, and truncating the C-terminal tail on this fragment to aa246 did not abolish the interaction (Figure 4-1B). However, truncating the entire C-terminal tail abolished the interaction and the C-terminal tail alone (aa240-252) was not sufficient for interaction, indicating that the RING domain and at least 10 residues flanking the RING domain are required for interaction (Figure 4-1B). Thus, Dma1's self-interaction region is contained in aa187-246, which includes the RING domain.

Dma1's RING domain forms a dimer

We next determined the oligomeric state of Dma1's RING domain. Recombinant His_6- Dma1(aa187-end) was affinity purified on His-bind resin followed by gel filtration and its approximate molecular weight was determined by sedimentation velocity analytical ultracentrifugation (SVAU) (Figure 4-2A). SVAU traces of His_6-Dma1(aa187-end) in 150 mM NaCl indicate that the majority (66%) of the protein exists in an ~23 kDa

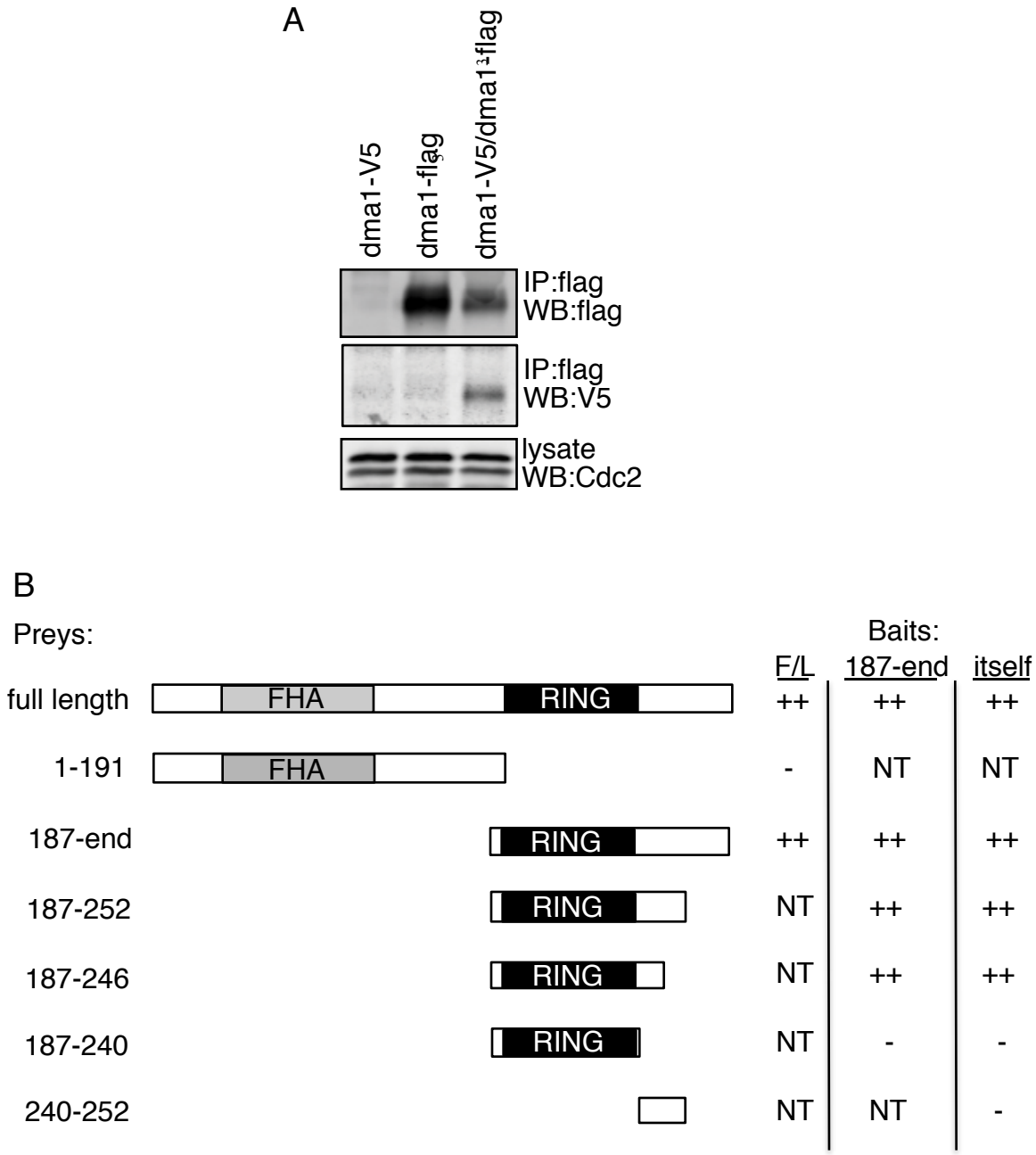

Figure 4-1

Dma1 self-associates in vivo.

A. Co-immunoprecipitation of Dma1-V5$_3$ and Dma1-flag$_3$ from diploid cells. B. Schematics of Dma1 fragments that were tested for yeast 2-hybrid interaction and summary of their interactions (++ interaction comparable to wildtype, - no interaction detected, NT-not tested).

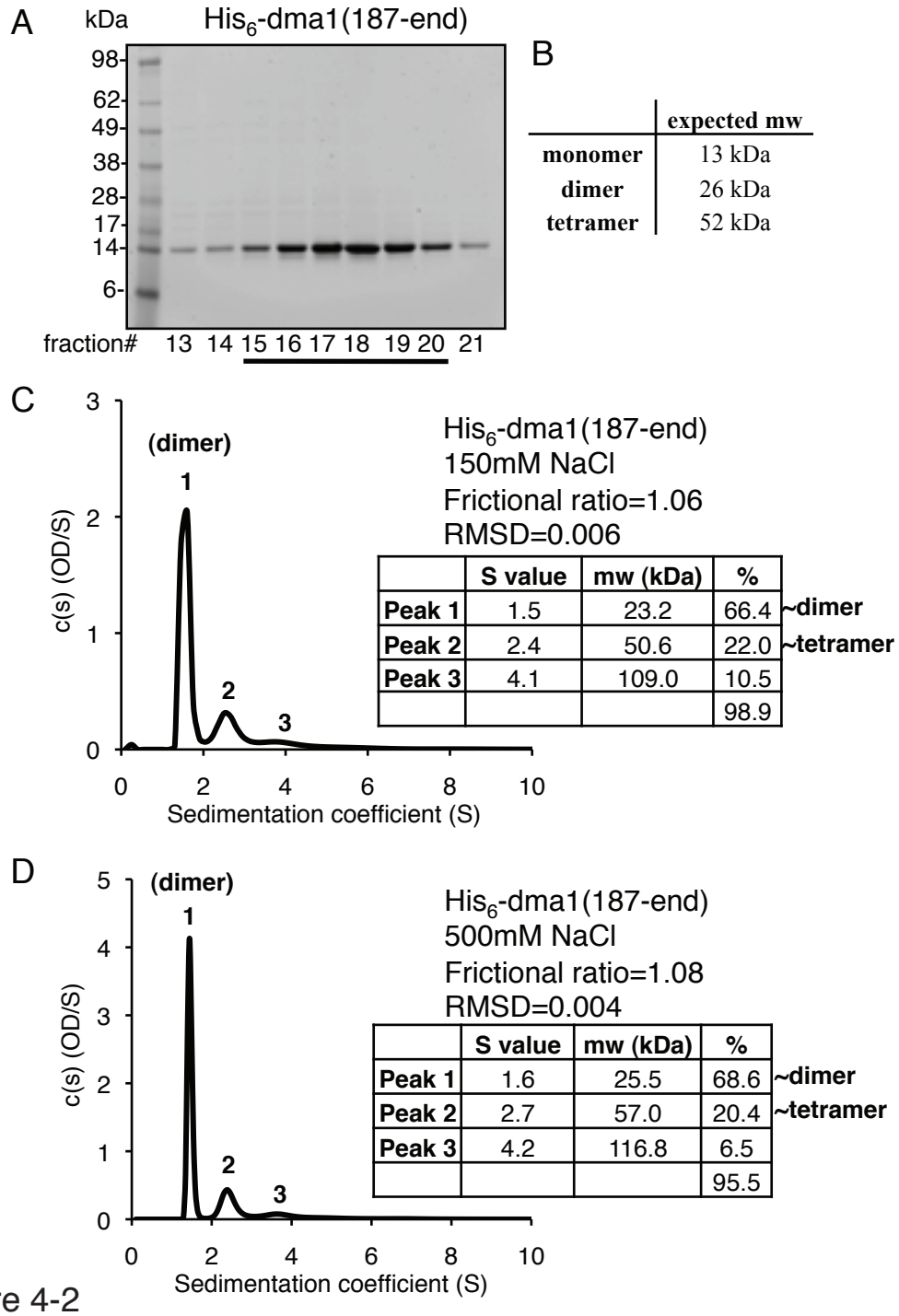

	expected mw
monomer	13 kDa
dimer	26 kDa
tetramer	52 kDa

	S value	mw (kDa)	%	
Peak 1	1.5	23.2	66.4	~dimer
Peak 2	2.4	50.6	22.0	~tetramer
Peak 3	4.1	109.0	10.5	
			98.9	

	S value	mw (kDa)	%	
Peak 1	1.6	25.5	68.6	~dimer
Peak 2	2.7	57.0	20.4	~tetramer
Peak 3	4.2	116.8	6.5	
			95.5	

Figure 4-2

The Dma1 RING domain preferentially forms a dimer in vitro.

A. His6-Dma1(aa187-end) was affinity purified on His-bind resin followed by gel filtration. Fractions 15-20 were combined and concentrated for sedimentation velocity analytical ultracentrifugation (SVAU). B. Expected sizes of Dma1 oligomers. C. SVAU analysis of His6-Dma1(aa187-end) in 150 mM NaCl. S-values, determined molecular weights and % abundance are given for each indicated peak. D. SVAU analysis of His6-dma1(aa187-end) in 500 mM NaCl. S-values, determined molecular weights and % abundance are given for each indicated peak.

complex (S=1.5), consistent with the molecular weight of a dimer (Figure 4-2B-C). Two larger ~50 kDa and ~109 kDa species were also detected; however, these species made up only 22% and 11% of the total population, respectively (Figure 4-2C). Significantly, there was no detectable peak at ~13 kDa, the expected size of a monomer (Figure 4-2B). Increasing the salt concentration to 500 mM did not disrupt the amount of the dimer complex that was present (69%, S=1.6) and did not generate any detectable monomers, suggesting that this complex is stable (Figure 4-2D). These data indicate that Dma1's RING domain preferentially forms a stable dimer complex in vitro.

Residues in the C-terminal tail are critical for Dma1 dimerization

To identify specific residues that are required for Dma1 dimerization, we generated a homology-based model of Dma1's RING domain from the known structure of the homodimeric RNF4 ring domain (Liew et al., 2010). From this model, several residues were identified that appeared in the dimer interface and that were also conserved in other *Schizosaccharomyces* Dma1 proteins and in the *S. cerevisiae* Dma1 and Dma2 proteins (Figure 4-3A). Selected residues were then mutated in the Dma1(aa187-end) fragment and tested for interaction in a yeast 2-hybrid assay. Mutation of F206 to alanine or L241 and V245 together to alanine disrupted self-interaction (Figure 4-3B).

To validate that Dma1(L241,V245A) and Dma1(F206A) mutants were monomeric in vivo, we constructed *dma1(L241,V245A)-V5$_3$/dma1(L241,V245A) flag$_3$* and *dma1(F206A)-V5$_3$/dma1(F206A) flag$_3$* diploids and performed a reciprocal coimmunoprecipitation experiment. While Dma1-flag$_3$ was able to interact with Dma1-V5$_3$, Dma1(L241,V245A)-flag$_3$ did not pull down a detectable amount of

A

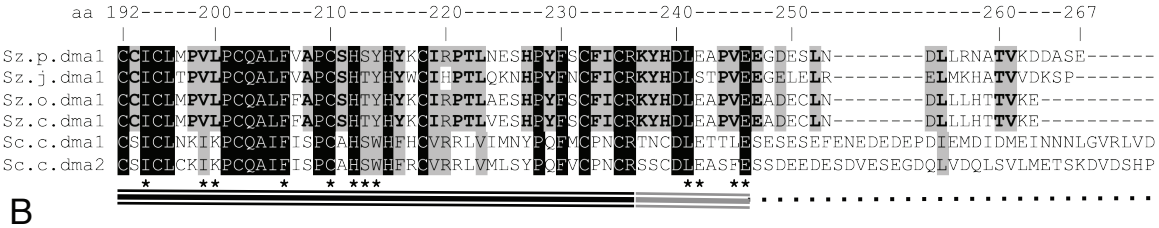

B

Mutation	Region	2-hybrid interaction
I194A	RF domain	++
C210;H212A	RF domain	+
V199;L200A	RF domain	++
F206A	RF domain	-
S213A	RF domain	++
S213E	RF domain	++
Y214A	RF domain	++
Y214F	RF domain	++
L241;V245A	C-terminal tail	-
E242;E246A	C-terminal tail	++

C

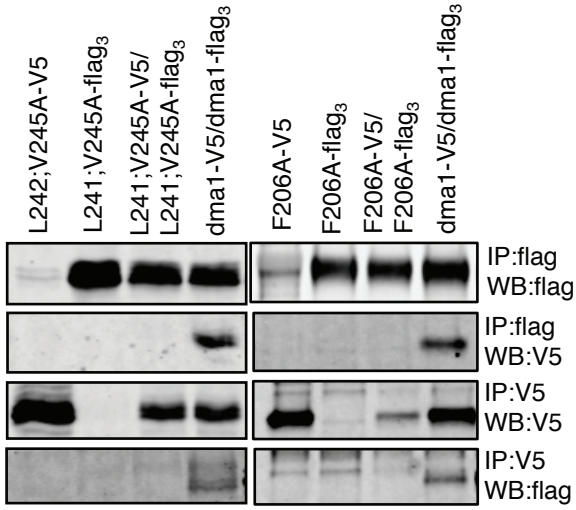

Figure 4-3

F206, L241 and V245 are critical for Dma1 dimerization.

A. ClustalW alignment of the RING domain and C-terminal flanking residues from *S. cerevisiae* Dma1 (YNL116W) and Dma2 (YHR115C) and *Schizosaccharomyces* Dma1 homologs: *S. pombe* (SPAC17G8.10c), *S. japonicus* (SJAG02169.4), *S. octosporus* (SOCG04269.5), and *S.cryophilus* (SPOG00270.3). Amino acid numbers correspond to *S. pombe* Dma1 amino acid positions. Conserved residues are highlighted and asterisks indicate amino acids that were tested for involvement in self-interaction. The dotted line indicates the region of Dma1 that was dispensable for self-interaction in yeast 2-hybrid experiments, the gray bar underlines the C-terminal flanking residues that were required for self-interaction in 2-hybrid experiments and the black bar underlines the core RING residues. B. Summary of point mutations that were tested for 2- hybrid interaction. (++ interaction comparable to wildtype, + interaction weaker than wildtype, - no interaction detected). C. Co-immunoprecipitation experiments from *dma1-V5$_3$/dma1-flag$_3$*, d*ma1(L241,V245A)- V5$_3$/dma1(L241,V245A)-flag$_3$* and *dma1(F206A)-V5$_3$/dma1(F206A)-flag$_3$* diploid cells.

Dma1(L241,V245A)-$V5_3$ or vice versa, suggesting that Dma1(L241,V245A) primarily exists as a monomer in vivo (Figure 4-3C). Similarily, Dma1(F206A)-$V5_3$ did not co-precipitated with Dma1(F206A)-$flag_3$ (Figure 4-3C). Collectively, these data confirm that residues in the core RING domain as well as residues in the C-terminal tail flanking the RING are important for Dma1 dimerization.

Dma1 dimerization is required for proper localization

To determine how dimerization affects Dma1 function in vivo, we first wanted to examine if disrupting Dma1 dimerization affected its stability or localization. Dma1-GFP, Dma1(L241,V245A)-GFP and Dma1(F206A)-GFP protein levels were compared and no changes to total protein levels were detected (Figure 4-4A). There were also no detectable differences in the amount of protein that could be immuno-precipitated, indicating that the amount of soluble protein is also not affected (Figure 4-4A). Thus, it is unlikely that disrupting Dma1's oligomerization state affects its protein stability.

We next examined where constitutively monomeric Dma1 localized. Dma1 normally localizes to both SPBs during mitosis and also to the cell division site and localization to these sites is dependent on its FHA domain (Guertin et al., 2002). Surprisingly, we found that both Dma1(L241,V245A)-GFP and Dma1(F206A)-GFP mutants localized strongly to just one of the two SPBs during mitosis and had significantly reduced localization at the cell division site (Figure 4-4B). As expected, monomeric Dma1 still required its FHA domain to localize to the one SPB, since inactivating the FHA domain (R64A) abolished Dma1(L241;V245A)-GFP localization to all structures (Figure 4-4C).

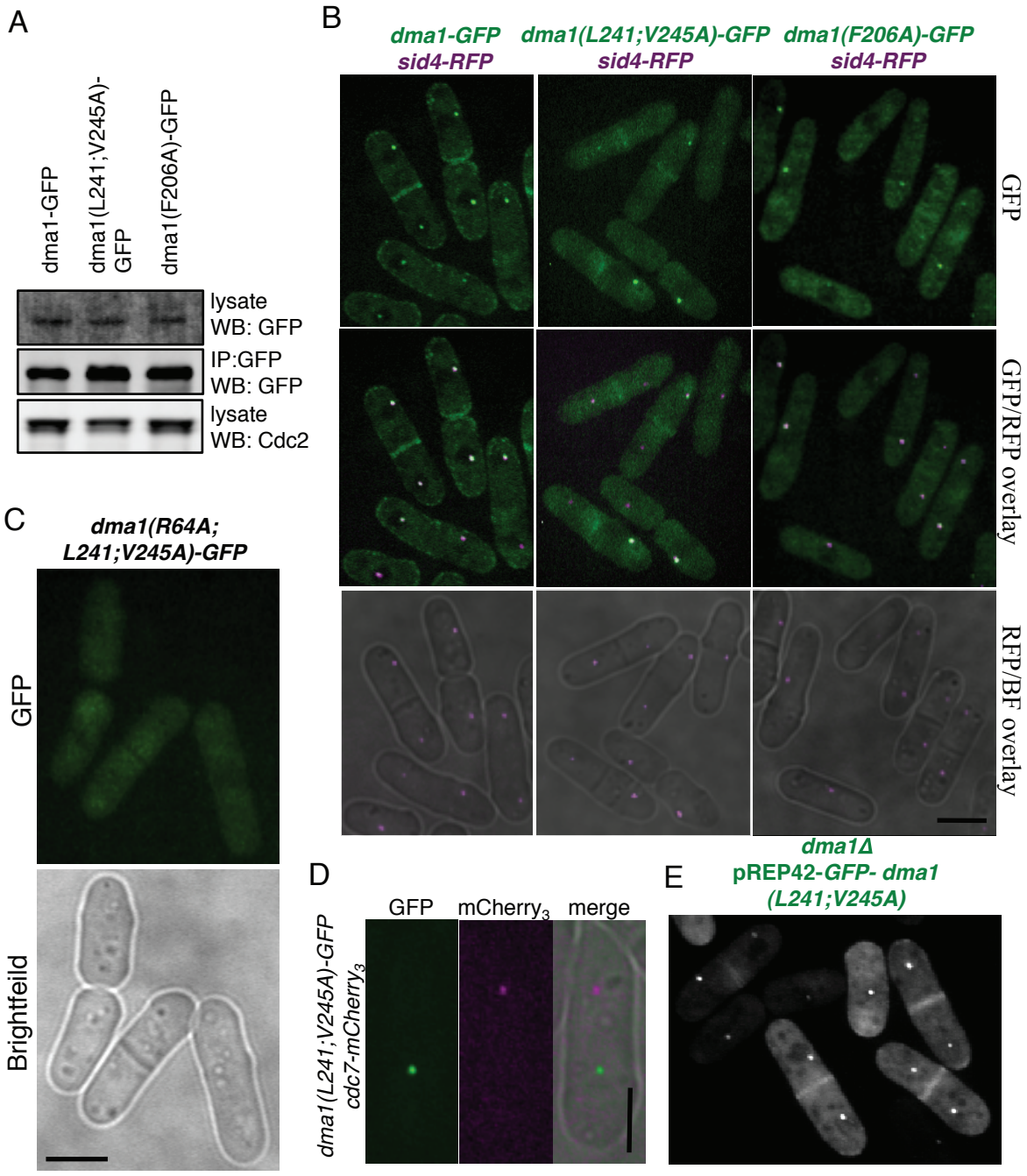

Figure 4-4

Monomeric Dma1 exhibits defective intracellular localization.

A. Protein levels of Dma1-GFP, Dma1(L241;V245A)-GFP and Dma1(F206A)-GFP. Cdc2 blot is shown as a protein loading control. B. Dma1-GFP, Dma1(L241;V245A)-GFP or Dma1(F206A)-GFP were imaged with Sid4-RFP (magenta) in live cells. Scale bar, 5 um. C. Dma1(R64,L241,V245A)-GFP localization. Scale bar, 5 um. D. Representative live cell image of Dma1(L241,V245A)-GFP with Cdc7-mCherry3 (scale bar, 5 um, n=5 cells). E. pREP42-GFPdma1(L241,V245A) was overproduced in dma1Δ cells and the cells were imaged live. Scale bar, 5 um.

During early mitosis, the SIN is first activated on both SPBs and then during anaphase it becomes inactivated on one SPB and hyperactivated on the other SPB (Johnson et al., 2012). Asymmetric activation of the SIN is governed by asymmetric distribution of specific SIN proteins and is important for precise timing of cytokinesis (Garcia-Cortes and McCollum, 2009). Since Dma1 is a SIN inhibitor, we were interested in knowing to which SPB monomeric Dma1 was predominantly localizing. Thus, we imaged Dma1(L241,V245A)-GFP with the SIN kinase Cdc7, which only localizes to the SPB with active SIN signaling during anaphase (Sohrmann et al., 1998). Co-imaging of Dma1(L241,V245A)-GFP with Cdc7-mCherry$_3$ showed that Dma1(L241,V245A)-GFP always localized to the opposite SPB as Cdc7, indicating that monomeric Dma1 predominantly localizes to the SPB in which the SIN is inactive (Figure 4-4D).
Given that a small amount of monomeric Dma1 was detected at the cell division site, we reasoned that Dma1 might have reduced localization everywhere and was only strongly detectable at one SPB. Consistent with this idea, over-expression of GFP-dma1(L241,V245A) restored localization to both SPBs and the cell division site (Figure 4-4E). Collectively, these data indicate that dimerization is required for proper Dma1 localization at SPBs and the cell division site.

Dimerization of Dma1 is essential for its E3 ligase activity and checkpoint function

During a mitotic checkpoint, Dma1 is required to inhibit cytokinesis to prevent chromosome mis-segregation (Guertin et al., 2002; Murone and Simanis, 1996). To test whether Dma1's oligomeric status affects its function, we assessed whether *dma1(L241,V245A)* or *dma1(F206A)* cells could maintain a mitotic checkpoint arrest.

Cells were synchronized in S-phase with hydroxyurea (HU) and released to 18°C to activate the spindle checkpoint (using the cold-sensitive β- tubulin mutant, *nda3-KM311*). Septation indices were measured at 0 hrs and 7 hrs. At 7 hrs, only 6.5% of *nda3-KM311 dma1*$^{+}$ cells had slipped from the arrest, whereas 41.8% of *nda3-KM311 dma1Δ*, 36.7% of *nda3-KM311 dma1(L241,V245A)* and 36% of *nda3-KM311 dma1(F206A)* cells had slipped from the arrest (Figure 4-5A-B). These data indicate that dimerization is required for checkpoint function.

Dma1 can auto-ubiquitinate in vitro (Johnson and Gould, 2011) and we decided to test whether the defect in checkpoint function observed in the mutants was due to mislocalization alone or if it was also due to compromised E3 ligase activity. Dma1-GFP, Dma1(L241,V245A)-GFP and Dma1(F206A)-GFP were immunoprecipitated and incubated with an E1 enzyme and the E2 enzyme complex Ubc13/Uev1 for 90 min. Auto-ubiquitinated proteins were detected by immunoblotting with α-GFP antibody. In contrast to Dma1-GFP, neither monomeric mutant could form poly-ubiquitin chains in vitro, indicating that they are not active E3 enzymes (Figure 4-5C). We further tested the activity of the monomeric mutants in vivo by examining Sid4 ubiquitination, a known target of Dma1. Consistent with the in vitro analysis, Sid4 ubiquitination was abolished in cells expressing either *dma1(L241;V245A)* or *dma1(F206A)* (Figure 4-5D). Collectively, these data indicate that loss of checkpoint function in *dma1(L241,V245A)* and *dma1(F206A)* cells is due to its mislocalization and loss of E3 ligase activity.

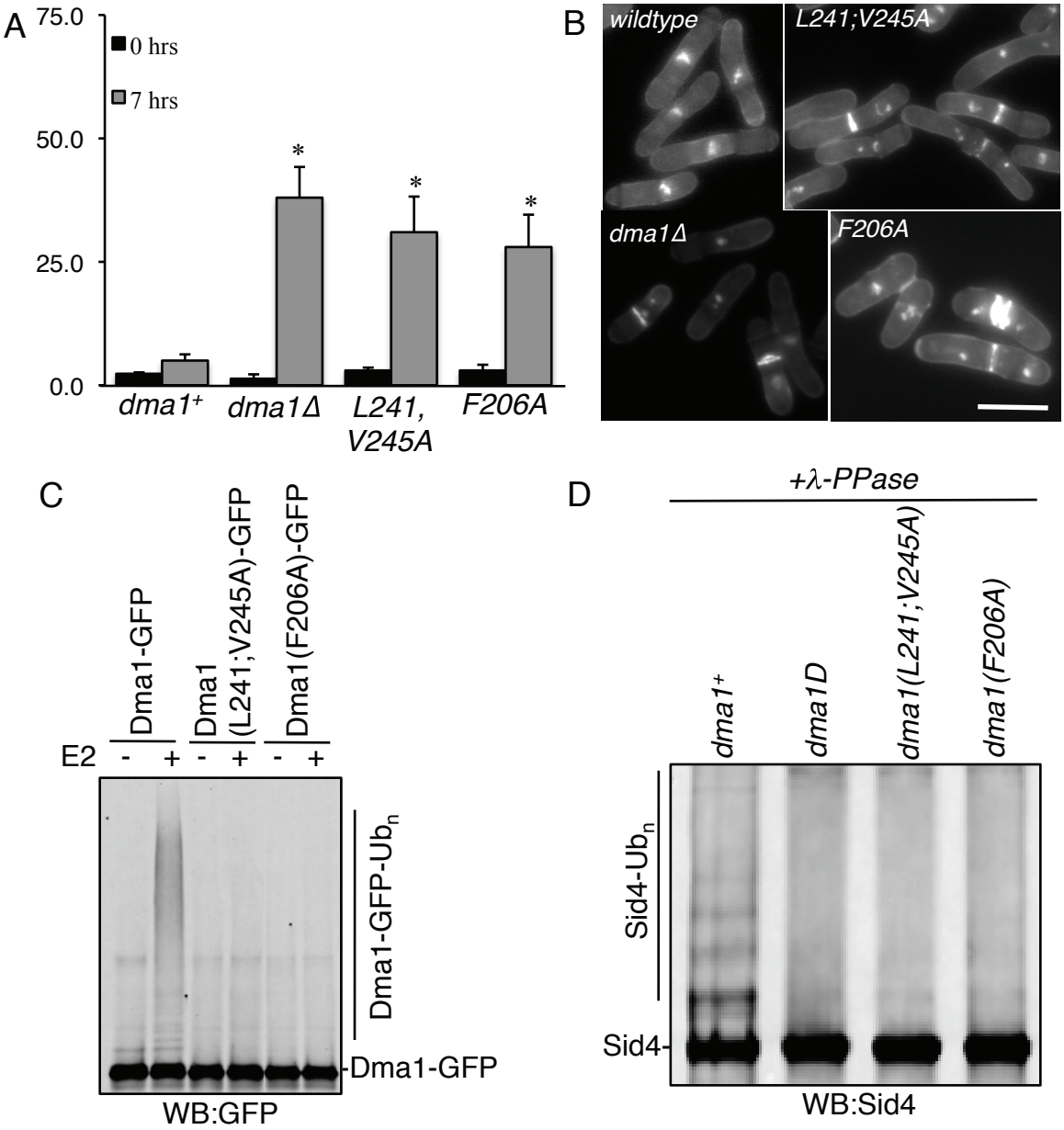

Figure 4-5

Dma1 dimerization is essential for its checkpoint function and E3 ligase activity. A. Checkpoint assay with *nda3-KM311 dma1*$^{+}$, *nda3-KM311 dma1*Δ, *nda3-KM311 dma1(L241,V245A)* and *nda3-KM311 dma1(F206A)* cells. (n=3, *p<0.05 compared to *nda3-KM311 dma1*$^{+}$) B. Representative images of cells from the 7 hr time point for each strain indicated stained with DAPI and methyl blue. Arrows indicate aberrant septa. Scale bar, 10 um. C. In vitro ubiquitination assay. Dma1-GFP, Dma1(L241,V245A)-GFP and Dma1(F206A)-GFP were immunoprecipitated and incubated with an E1 activating enzyme, ATP, ubiquitin and either with (+) or without (-) the E2 conjugating enzyme complex, Ubc13-Uev1. Ubiquitinated proteins were detected by immunoblotting with a α-GFP antibody. D. Sid4 ubiquitination in vivo. Sid4 was immunoprecipitated with anti-Sid4, treated with lambda protein phosphatase and resolved via SDS-PAGE. Ubiquitinated proteins were detected by immunoblotting with anti-Sid4 serum.

Discussion

Several RING E3 ligases form obligate homo- or heterodimers to efficiently transfer Ubiquitin onto their substrates (Deshaies and Joazeiro, 2009). In this chapter, we show that *S. pombe* Dma1 joins this subset of dimeric E3 ligases by forming a homodimer via its RING domain and that Dma1 dimerization is required for its E3 ligase activity and checkpoint function in vivo. We also find that similar to other C-terminal RING domain proteins, such as RNF4 (Liew et al., 2010), Dma1 requires the C-terminal tail to dimerize. The extra C-terminal extension likely provides stability to the dimer or is required for proper folding of the RING domain.

Although we have shown that Dma1 self-associates in vivo and preferentially forms a dimer when the RING domain is expressed in vitro, we cannot exclude the possibility that Dma1 interacts with another RING E3 to form a hetero multimer complex. However, we have not identified another RING E3 that co-purifies significantly with Dma1 in proteomics screens (data not shown). Whether Dma1 ever exists as a monomer in vivo also remains uncertain; however, Dma1's dimer status is probably not a major point of regulation since its self-association does not appear to increase significantly during a mitotic checkpoint compared to asynchronous cells (data not shown). It is more likely that Dma1 forms an obligate and constitutive dimer that is regulated by other mechanisms.

A surprising result was that a constitutively monomeric form of Dma1 has significantly reduced localization at one SPB and the cell division site. Importantly, Dma1 ubiquitination activity is not required for proper localization (Johnson and Gould, 2011), and thus this phenotype is the direct result of the inability of Dma1 to dimerize. It

is not completely clear why the monomer localizes improperly, but given that Dma1 requires its FHA domain for localization, it is possible that the presence of two FHA domains versus one increases the affinity of Dma1 for its interaction partners. Another possibility is that monomeric Dma1 lacks specific binding surface(s) that are generated upon dimerization and are required for proper Dma1 localization.

Many proteins localize asymmetrically to one SPB, including several components of the SIN and asymmetric SIN signaling is critical for proper timing of cytokinesis (Garcia-Cortes and McCollum, 2009). It is interesting that constitutively monomeric Dma1 is only observed at the SPB in which the SIN is inactive during anaphase. If monomeric Dma1 binds with less affinity to all Dma1 partners, then monomeric Dma1 might only be detectable at locations where Dma1 normally has highest affinity. This is supported by our observation that when the monomeric form is over-expressed, Dma1 localization at both SPBs and the cell division site is restored. Collectively, our data suggest that Dma1 has a stronger affinity for the inactive SPB, where it can contribute more robustly to SIN inactivation.

Although it was previously assumed that RING E3s mainly act as scaffolds to bring the E2~Ub and substrate into proximity, increasing evidence indicates that E3s actively participate in catalysis in several ways (Deshaies and Joazeiro, 2009). It is also becoming evident that oligomerization of many RING E3s enhances their catalytic roles; however, it is not completely understood why this is the case. Some studies suggest that oligomerized E3s allosterically activate their cognate E2 enzymes more efficiently to destabilize the E2~ubiquitin thioester bond and promote catalysis of ubiquitin onto the substrate (Liew et al., 2010; Plechanovova et al., 2011). Even more recently, it was

shown that the ubiquitin loaded E2 (E2~Ub) binds across homodimeric RNF4, such that one RING domain contacts the E2 enzyme while the other RING domain of the RNF4 dimer contacts a hydrophobic patch on the conjugated ubiquitin (Plechanovova et al., 2011). Both interactions are necessary to efficiently activate the thioester bond for catalysis and spatial constraints prevent a single RING domain from binding both the E2 and the conjugated Ubiquitin.

This study was the first example of an FHA-RING E3 ligase forming an obligate RING domain dimer. However, it was recently reported that RNF8 also forms a dimer (Bimbo et al., 2005). Thus, given the propensity of RING containing proteins to dimerize coupled with the structural and functional similarities that exist between the FHA-RING family members, it is plausible that our data represents a mechanistic paradigm for all FHA-RING E3 ligases.

CHAPTER V

CONCLUSIONS, PERSPECTIVES AND FUTURE DIRECTIONS

Chapter summaries

Mitotic checkpoints ensure that chromosomes are accurately distributed when cells divide. FHA-RING E3 ligases, which include human RNF8 and CHFR and fission yeast Dma1, participate in checkpoints that stall the core cycle machinery when cells encounter mitotic stress (Brooks et al., 2008). However, their mechanisms of action remain poorly understood. In this work, I have investigated the role of *S. pombe* Dma1 in a mitotic checkpoint that stalls cytokinesis when chromosomes do not segregate appropriately.

In Chapter II, I presented work elucidating the mechanism of Dma1 inhibition of cytokinesis. I found that Dma1 indirectly antagonizes the pro-cytokinesis factor Plo1 by ubiquitinating its mitotic scaffold Sid4. Sid4 is required to recruit Plo1 to SPBs during mitosis, such that Plo1 can phosphorylate critical targets to drive SIN activation and subsequently cytokinesis. In a degradation independent mechanism, Sid4 ubiquitination impedes Plo1 interaction with the SIN and thereby restrains Plo1 from triggering cytokinesis during a mitotic checkpoint (Johnson and Gould, 2011).

Like Dma1, the human homologs CHFR and RNF8 have been implicated in down-regulating Polo kinases, underscoring the functional conservation of these proteins (Kang et al., 2002; Umesono et al., 1983). CHFR is a well-documented human tumor suppressor and mitotic checkpoint protein whose exact mechanism of action in response

to microtubule destabilizing drugs is also unknown. Thus, our results may provide insight into the mechanism by which CHFR protects human cells from mitotic stresses.

In chapter III, I reported that the highly conserved protein kinase CK1 is essential for activation of the Dma1 checkpoint pathway. Our evidence indicates that CK1 relays an initial mitotic checkpoint signal to Dma1. Phosphorylation of Sid4 by CK1 recruits Dma1 via its phospho-binding FHA domain and is required for checkpoint function. Furthermore, we established that CK1 localizes in the nucleus and SPBs and accumulates at SPBs upon checkpoint activation, suggesting that CK1 transmits signals from the nucleus to SPBs.

Human CK1d/e, which are most similar to yeast CK1, localize to centrosomes and are proposed to function in mitosis (Alexandru et al., 1999); however, my results provide the first evidence that CK1 participates in a mitotic checkpoint. Moreover, this study provides the first insight into a mitotic molecular sensor for the FHA-RING E3 ligase family. Given the functional similarities between the FHA-RING E3 ligases and the apparent conserved functions of CK1 in mitosis, our data could represent a paradigm for CK1 phosphoregulation of FHA-RING E3 ligases.

In chapter IV, I presented data indicating that the RING domain of Dma1 forms a homodimer and RING domain dimerization is essential for its mitotic checkpoint function. Furthermore, I found that disruption of Dma1 dimerization impedes proper Dma1 localization and abolishes its E3 ubiquitin ligase activity in vitro (Johnson et al.). *S. pombe* Dma1 was the first FHA-RING E3 ligase reported to dimerize; however, it was recently shown that RNF8 also forms a dimer via its RING domain (Bimbo et al., 2005). Thus, given the functional and structural similarities between these proteins and the

propensity for RING domains to dimerize, it is plausible that dimerization is a common requirement for all FHA-RING E3 ligases.

Collectively, this work has defined a molecular program that stalls cytokinesis when cells encounter mitotic stress. We have identified the key players and elucidated their roles in executing this mitotic checkpoint pathway. Looking forward, I view identifying the molecular cues regulating Dma1 function as the most pressing task to expand our understanding of how the Dma1-dependent pathway is controlled. Given that *dma1* over-expression is lethal, it seems likely that its activity must be managed to prevent Dma1 from interfering with normal cell cycle progression. We have evidence that Dma1 is regulated intrinsically by post-translational modifications and extrinsically by a molecular inhibitor *dnt1* (discussed later). Characterizing how these modes of regulation impact Dma1 function, will be interesting future studies to pursue.

Mechanisms regulating Dma1 function

Negative regulation of Dma1 by Dnt1

In collaboration with Dr. Dan McCollum and Dr. Quanwen Jin, we have investigated the role of a potential Dma1 inhibitor, Dnt1. Dnt1 was identified as a Dma1-interacting protein via an MS/proteomics approach. Upon further characterization of the Dnt1-Dma1 interaction, we found that Dnt1 binds Dma1 specifically during early mitosis in order to inhibit Dma1 activity during this phase of the cell cycle (Figure 5-1A). In the absence of Dnt1, Dma1 immuno-precipitated from cells shows increased ubiquitination activity in vitro and Sid4 ubiquitination is increased compared to *wildtype* cells in vivo (Figure 5-1B). Additionally, Dma1 localization is increased at SPBs, indicating that

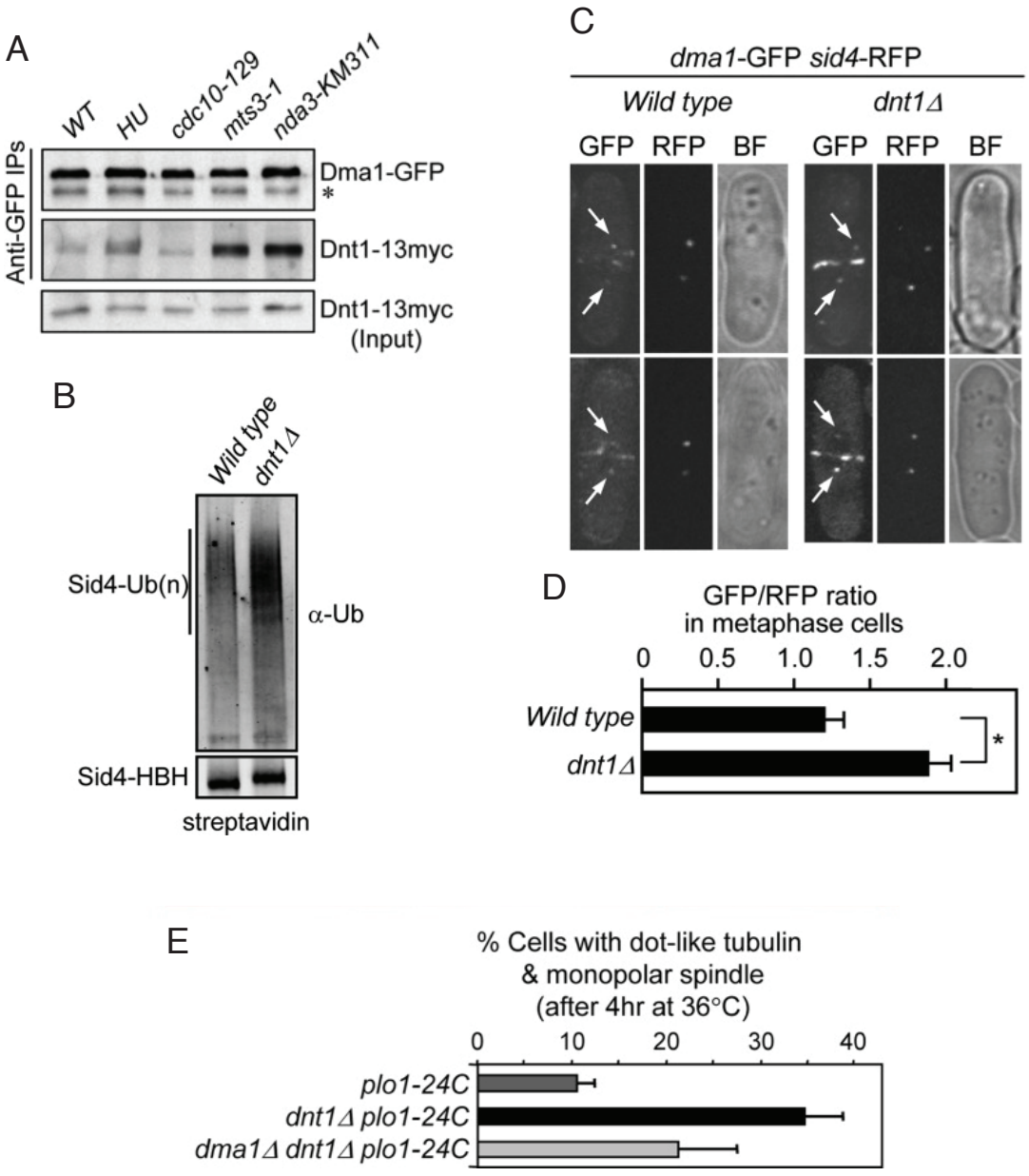

Figure 5-1

Dnt1 binds and inhibits Dma1.

A. Co-immunoprecipitation of Dma1-GFP and Dnt1-13myc. B. Sid4 ubiquitination status in *wildtype* and *dnt1*Δ cells. C. Dma1-GFP localization at SPBs in mitotic *wild-type* and *dnt1*Δ cells. D. Quantitation of Dma1-GFP at SPBs from cells used in C. E. Cells from the indicate srains were grown at 25°C and then shifted to 36°C for 4 hrs before quantitating monopolar spindles.

Dnt1 inhibits Dma1 E3 ligase activity and its SPB localization (Figure 5-1C-D). Further experiments demonstrate that inhibition of Dma1 during early mitosis is important to prevent Dma1 from antagonizing Plo1's early mitotic functions and curb Dma1's activity when a checkpoint is not activated (Figure 5-1E) (Swiatek et al., 2006).

Interestingly, a cytosolic and centrosomal protein Stil was found to bind and inhibit CHFR in a similar manner as Dnt1 (Castiel et al., 2011). Stil limits CHFR's inhibition of Plk1 in early mitosis to allow normal mitotic progression and proper centrosome assembly by affecting CHFR's stability and protein level (Castiel et al., 2011). Therefore, the activities of both Chfr and Dma1 are carefully modulated to keep them from interfering with normal mitotic progression. Although fission yeast Dnt1 and mammalian Stil do not show any amino acid sequence similarity, they do share similar functions in antagonizing their respective E3 ubiquitin ligase.

Although we know the functional relationship between Dma1 and Dnt1, it is not known how Dnt1-Dma1 interaction is regulated. Similar to Dma1-Sid4 interaction, we find that Dma1-Dnt1 interaction depends on Dnt1 phosphorylation (data not shown). Therefore, phosphorylation of Dnt1 likely provides a mechanism for the cell cycle specific interaction between the two proteins. Finding the kinase(s) responsible for Dnt1 phosphorylation will be an important goal for future studies.

Regulating Dma1's activity via auto-ubiquitination

Many E3 ubiquitin ligases auto-ubiquitinate to inhibit their own activity. Expression of a catalytically dead *dma1* mutant (*dma1(I194A))* causes Dma1 to localize to SPBs constitutively (Figure 5-2A), suggesting that Dma1 might require ubiquitination

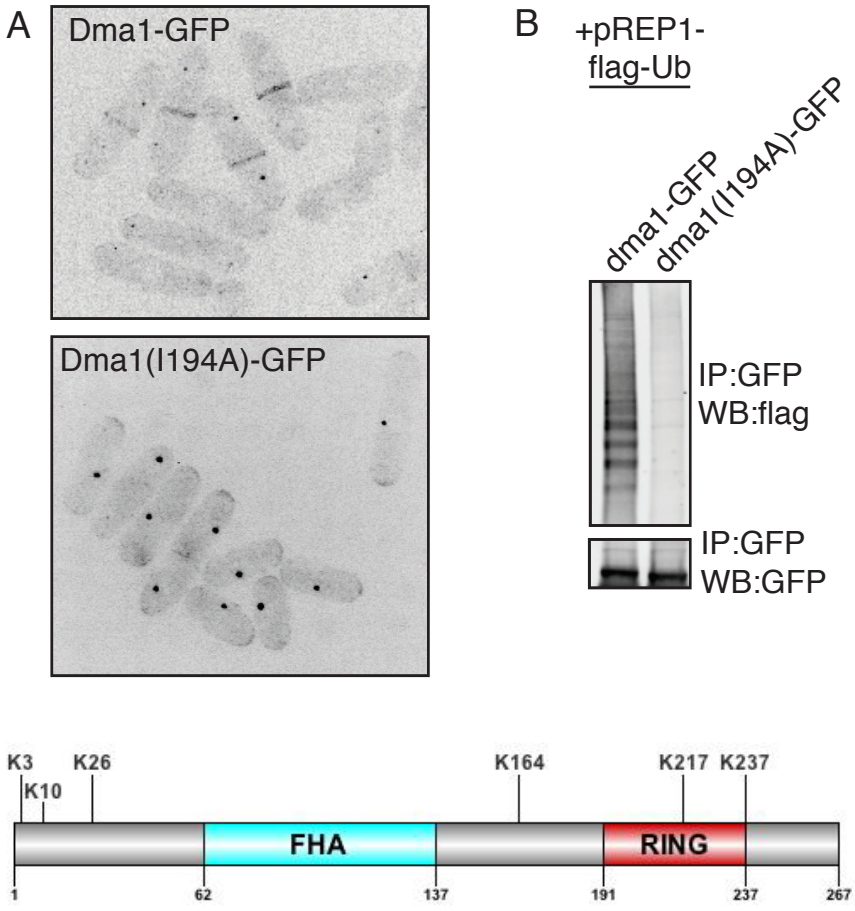

D

Site	Asynchronous #1	Asynchronous#2
K3	1	7
K10	1	7
K26	3	0
K164	2	0
K217	3	0
K237	15	5

Figure 5-2

Dma1 auto-ubiquitinates in vivo.

A. Localization of Dma1-GFP and Dma1(I194A)-GFP in cells growing asynchronously. Inverted gray-scale images are shown. B. Dma1-GFP or Dma1(I194A)-GFP were immunoprecipitated from cells over-expressing Flag-Ub and detected by immunoblot. C. Schematic of Dma1 and relative positions of potential ubiquitination sites detected by MS (D).

of its substrate (Sid4) to dissociate from SPBs. However, Dma1 does not localize to SPBs constitutively when Sid4 cannot be ubiquitinated (Figure 2-4C). An alternative possibility is that Dma1 requires auto-ubiquitination to dissociate from SPBs. In support of this model, we have found that Dma1 auto-ubiquitinates in vivo and have identified several auto-ubiquitination sites on Dma1 (Figure 5-2B-D). We hypothesize that Dma1 auto-ubiquitination provides a mechanism of Dma1 inhibition when a mitotic checkpoint is not activated.

Future studies aimed at generating and characterizing non-ubiquitinatable Dma1 mutants should clarify the role of Dma1 auto-ubiquitination. If Dma1 auto-ubiquitination inhibits its activity, we would expect these mutants to maintain a mitotic checkpoint arrest longer than *wildtype* cells. Additionally, understanding how Dma1 switches preference from ubiquitinating its substrates to itself will also be important (discussed more in the next sub-section).

Phosphoregulation of Dma1

Protein phosphorylation provides a rapid and reversible means of regulating protein function and/or localization. To understand how Dma1 responds to mitotic stress, we examined Dma1 phosphorylation sites that increase in response to mitotic stress using a mass spectrometry based approach. From this analysis, we identified three major mitotic phosphorylation sites: S251, S166 and T18 (Figure 5-3A-B). I have mapped one of these (T18) as a CK2 phosphorylation site (Figure 5-3B). Interestingly, I have found that mutating T18 to a phospho-mimetic glutamate residue abolishes Dma1 auto-ubiquitination (Figure 5-3C). Importantly, this mutant can still ubiquitinate Sid4 in vivo

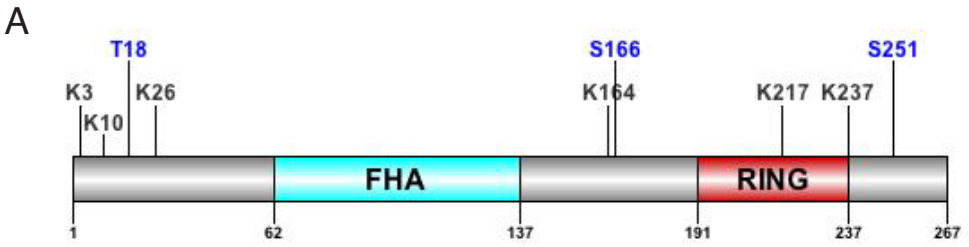

B

Site	Spectral counts	Kinase
T18	11	CK2
S166	42	CDK
S251	110	Plo1

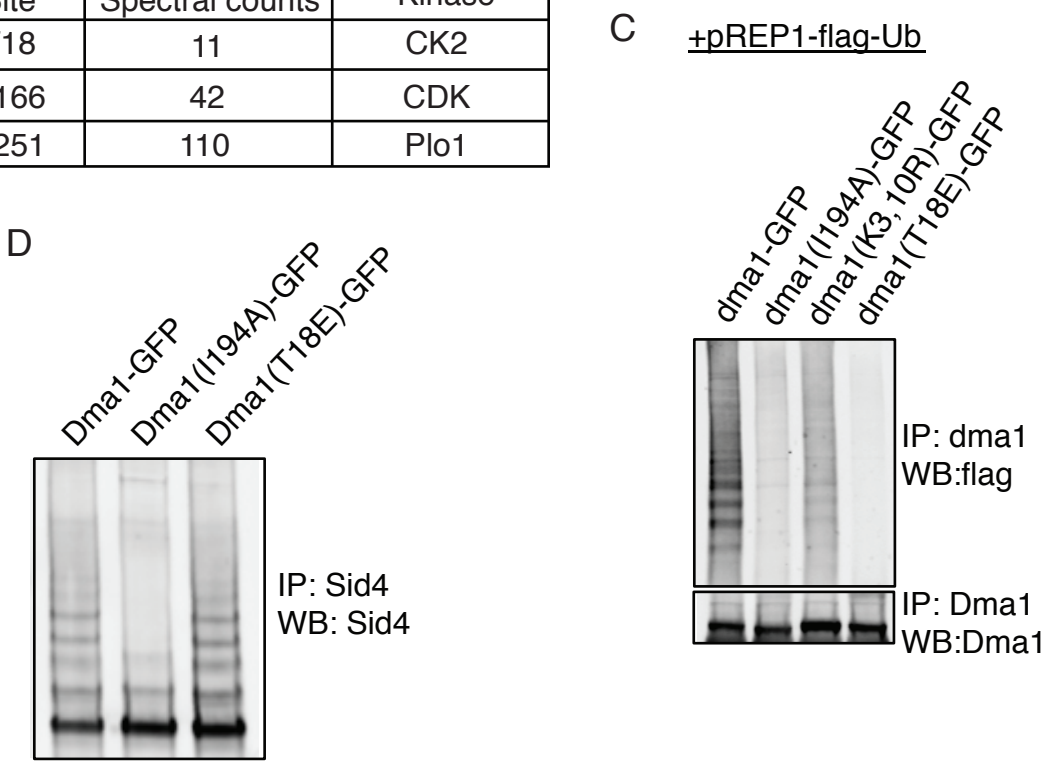

Figure 5-3

Dma1 phosphoregulation.

A. Schematic of Dma1 depicting the relative positions of ubiquitination and phosphorylation sites identified via MS (B). C. In vitro phosphorylation analysis of Dma1 by CK2. D. Dma1 was immunoprecipitated from the indicated strains and their ubiquitination status was detected by immunoblot analysis.

indicating that Dma1's catalytic activity is not affected (Figure 5-3D). Thus, Dma1 phosphorylation might regulate Dma1 auto-ubiquitination.

These preliminary results suggest that Dma1 is phospho-regulated. Future studies directed at characterizing Dma1 phospho-mutants should aid in understanding the full impact of Dma1 phosphorylation. It will also be of interest to define the relationship between Dma1 phosphorylation and auto-ubiquitination. The fact that a phospho-mimetic *dma1(T18E)* mutant abrogates Dma1 auto-ubiquitination activity suggests that phosphorylation at this site regulates the switch between substrate and auto-ubiquitination.

Conclusions

In this work, I have shown that when a mitotic checkpoint is activated, Dma1 impedes Plo1 activation of cytokinesis by ubiquitinating Plo1's mitotic scaffold Sid4. I have also identified CK1 as a novel upstream component of this pathway that is required for Dma1 to bind and ubiquitinate its substrate Sid4. Given CK1's localization pattern, it seems likely that CK1 communicates signals from the nucleus, where the checkpoint signal is generated, to SPBs, where Dma1 exerts its functions. Lastly, I revealed several mechanisms regulating Dma1 function, including RING domain dimerization, binding a protein inhibitor Dnt1, Dma1 phosphorylation and auto-ubiquitination. Collectively, these studies have defined a mitotic checkpoint program that is necessary to prevent cytokinesis when cells encounter mitotic stress.

As previously mentioned, Dma1 is functionally related to the human tumor suppressor protein CHFR (Scolnick and Halazonetis, 2000), which is also involved in a mitotic checkpoint and has been shown to antagonize the Polo kinase, Plk1 (Kang et al.,

2004; Shtivelman, 2003). However, whether CHFR antagonizes Plk1 directly or indirectly is controversial. Our data support the indirect model, since we have found that Dma1 antagonizes Plo1 by ubiquitinating its scaffold rather than Plo1 directly. While a clear Sid4 homolog has not yet been identified in metazoans, functional homologues of other SIN components are beginning to be identified. Thus, the mechanisms that we have defined for Dma1 will likely extend to CHFR and direct studies of other FHA-RING E3 ligases.

APPENDIX A

MATERIALS AND METHODS

Yeast methods

Yeast strains were grown in yeast extract media supplemented with appropriate amino acids (Moreno et al., 1991). For *in vivo* ubiquitination assays, strains were grown in 100 ml of 4x YE media, with the exception of *cdc11*-linkerHBH and *cut12*-linkerHBH which were grown in 2L 4x YE media. For *nda3*-KM311 arrests, cultures were shifted to 18°C for 6.5 hrs before harvesting. For *cdc25*-22, *cdc10-V50, cps1-191, and mts3-1* arrests, cultures were shifted to 36°C for 3.5 hrs before analysis.

For *sid4* and *dma1* gene replacements at endogenous loci, open reading frames plus at least 500 bps of 5' and 3' flanking nucleotides were subcloned into the pIRT2 plasmid containing the $LEU2^+$ marker and mutated using a site directed mutagenesis kit (Agilent Technologies). For $dma1^+$ gene replacements, a haploid *dma1Δ* strain was transformed with the mutant pIRT2 plasmids and stable integrants were selected by resistance to 5'-FOA. For $sid4^+$ gene replacements, a diploid $sid4^+/sid4\Delta$ strain was transformed with pIRT2-*sid4* mutant constructs and grown on minimal media lacking leucine, adenine and uracil. Transformants were allowed to sporulate and stable haploid integrants were selected based on resistance to 5'-FOA. Mutants were validated by colony PCR with primers outside of the 5' and 3' flanking regions.

For diploid construction, strains of opposite mating type and complementary adenine markers (*ade6-M210* and *ade6-M216*) were crossed at 25°C on sporulation

media and then plated onto minimal media lacking adenine 24 hrs later to select for diploids at 32°C.

For over-expression studies, cells harboring the pREP41 plasmid were first grown in minimal media containing thiamine and then in minimal media lacking thiamine to induce expression.

Cell synchronization methods

For hydroxyurea (HU) block and release experiments, cells were grown to log phase at 32°C before adding HU to a final concentration of 12mM. After 2 hrs, a second dose of HU (6mM final concentration) was added to the cells and after 3.5 hrs, HU was washed out and cells were released at 18°C.

For synchronization by lactose gradient, cells were grown to log phase at 32°C and sedimented by centrifugation on a 7-30% lactose gradient. Small G2 cells were extracted from the gradient, washed with fresh media and inoculated in media pre-cooled to 18°C.

In vivo ubiquitination assays of HBH tagged proteins

Proteins of interest were tagged at their endogenous C-termini with a His_6-BIO-His_6 (HBH) affinity tag with the exception of Cdc11 and Cut12, which were tagged with a linker-HBH affinity tag. Tagged proteins were purified using a modified version of the two-step tandem affinity purification under fully denatured conditions (Tagwerker et al., 2006). Cell pellets were lysed by bead disruption into Buffer 1 (8M Urea, 300 mM NaCl, 50 mM $NaPO_4$, 0.5% NP40, and 4 mM Imidazole, pH 8) and incubated with Ni-NTA

agarose beads (Qiagen) for 3-4 hrs at room temperature. After incubation, beads were washed 4x with Buffer 3 (8M Urea, 300 mM NaCl, 50 mM $NaPO_4$, 0.5% NP40 and 20 mM Imidazole, pH 6.3) and eluted in Buffer 4 (8M Urea, 200 mM NaCl, 50 mM $NaPO_4$, 0.5% NP40 and 2% SDS, 100 mM Tris and 10 mM EDTA, pH 4.3). The pH of the eluate was adjusted to 8 before adding streptavidin ultra-link resin (Pierce) and incubating overnight at room temperature. After the second incubation, streptavidin beads were washed 4x with Buffer 6 (8M Urea, 200 mM NaCl, 2% SDS and 100 mM Tris, pH 8) and 1x with Buffer 7 (8M Urea, 200 mM NaCl and 100 mM Tris, pH 8). Purified proteins were detected on a western blot using a ubiquitin anti-serum (Sigma) and fluorescently labeled streptavidin (Licor).

S. pombe protein methods

Cell pellets were lysed by bead disruption and immunoprecipitations were performed in either NP40 buffer for native lysates, or in NP40 buffer containing SDS for denatured lysates as previously described (Gould et al., 1991). For Dma1 immunoprecipitation experiments, 2 ug of either α-GFP (Roche), α-flag (Sigma) or α-V5 (Invitrogen) antibodies were used with protein G sepharose (GE healthcare). Sid4 immunoprecipitations were performed with 5ul of Sid4 anti-serum that was raised against recombinant GST-Sid4(1-300) (Cocalico). Lambda phosphatase (New England Biolabs) treatment of immunoprecipitated proteins was performed in 25 mM HEPES-NaOH pH 7.4, 150 mM NaCl, and 1 mM $MnCl_2$ for 45 minutes at 30°C. Proteins were separated separated by SDS-PAGE and detected by immunoblot using appropriate primary and fluorescently labeled secondary antibodies (Licor).

For in vitro binding experiments, MBP or MBP-Dma1 fusion proteins were purified on amylose beads (New England Biolabs) in column buffer (20mM Tris-pH 7.0, 150mM NaCl, 2mM EDTA, and 0.1% NP-40) and left on beads for in vitro binding assays with cell lysates.

In vitro ubiquitination assays

The E1-activating enzyme and E2 (Ubc13/Uev1) were purchased from Boston Biochem. Dma1 proteins were purified from *S. pombe* lysates using either a Tandem Affinity Purification method (Gould et al., 2004) or immunoprecipitation with appropriate antibodies. All components were incubated in a reaction buffer containing 50 mM Tris-HCl (pH 7.5), 2.5 mM $MgCl_2$, and 0.5 mM DTT. Reactions were incubated at room temperature for 90 min before adding SDS sample buffer to quench the reaction. To assess Dma1 activity, proteins were separated by SDS-PAGE and detected by immunobloting with appropriate antibodies.

In vitro kinase assays

Substrates were produced and purified recombinantly from bacteria. MBP proteins were purified on amylose beads (NEB) and GST fusion proteins were purified on GST bind resin (Novagen) in column buffer (20mM Tris (pH 7.0), 150mM NaCl, 2mM EDTA, and 0.1% NP-40) and eluted with either maltose (MBP fusions) or glutathione (GST fusions) per manufacturers recommendations. 1 ug of recombinant protein was used as the substrate in each reaction. Plo1 kinase reactions were performed in protein kinase buffer (10 mM Tris pH7.4, 10 mM $MgCl_2$, and 1 mM DTT) at 30°C for

30 min. Reactions were quenched by adding SDS sample buffer and proteins were separated by SDS-PAGE. Phosphorylated proteins were visualized by audioradiograph and relative protein quantities were assessed by coomassie blue staining.

For CK1 kinase assays with peptides, 1 μg of each synthetic peptide (Genescript) was incubated with $^{32}\gamma$-ATP and recombinant CK1δ (New England Biolabs) in CK1 kinase buffer (50 mM Tris pH 7.5, 10 mM $MgCl_2$, and 5 mM DTT) at 30°C for 30 min. Peptides were separated on a 15% polyacrylamide gel and visualized by autoradiography.

Microscopy methods

All fluorescence microscopy was performed using a spinning disk confocal microscope (Ultraview LCI; PerkinElmer) with a 100× NA 1.40 Plan-Apochromat oil immersion objective and either a 488-nm argon (GFP) ion or laser. Images were processed using a charge-coupled device camera (Orca-ER; Hamamatsu Photonics) and Metamorph 7.1 software (MDS Analytical Technologies). For imaging *cdc25*-22 arrested cells, slides, coverslips and immersion oil were pre-heated to 36C and cells were imaged on an objective heated to 36C. For *nda3*-KM311 strains, cells were fixed in 70% ethanol for 30 min before imaging.

DAPI and methyl blue images were obtained with a personal DeltaVision System equipped with an Olympus IX71 microscope using a 100x NA 1.40 UPlansApo oil immersion objective. Images were processed using a Cool Snap HQ^2 camera and Softworx® software.

Quantitative microscopy was performed using ImageJ software available at: http://rsbweb.nih.gov/ij/. Average GFP fluorescence intensities at SPBs were measured for at least 20 cells with background correction for each. Average RFP or mCherry fluorescence intensities were measured similarly and final values for each cell are expressed as Green:Red ratios. Measurements for the 20 cells in each group were averaged for statistical analysis.

Analytical Ultracentrifugation

Recombinant His_6-Dma1(aa187-end) fusion protein was produced in BL-21 cells by IPTG induction at 18°C overnight. Bacterial cells were lysed by sonication and proteins were affinity purified on His-bind resin (Novagen) in His bind buffer (500 mM NaCl, 40 mM Tris-HCl and 5 mM imidazole, pH 7.9). Resin was washed with 20 volumes of His bind buffer and protein was eluted with elution buffer (500 mM NaCl, 20 mM Tris-HCl, and 1 M imidazole, pH 7.9). His_6- Dma1(aa187-end) was then purified by gel filtration using an S-200 column (GE healthcare) into buffer containing 10 mM Tris-HCl (pH 7.4) and either 150 mM NaCl or 500 mM NaCl. Peak elution fractions were visualized on a Coomassie Blue (Sigma) stained gel. Fractions were combined and concentrated using a 3 MWCO Microcon column (Millipore). His_6-Dma1(aa187-end) recombinant protein (~1 mg/ml) was run on an Optima XLI (Beckman-Coulter) equipped with a four hole An60Ti rotor at 42,000 RPM at 4°C. Samples were loaded into double-sector cells (path length=1.2 cm) with charcoal-filled Epon centerpieces and quartz windows. Sedfit (v 12.0) (Schuck, 2000) was used to analyze velocity scans using every 8 scans from a total of 393 scans. Approximate size distributions were determined for a

confidence level of p=0.95, a resolution of n=300, and sedimentation coefficients between 0 and 10 S.

Yeast 2-hybrid methods

Dma1 fragments were cloned into bait and prey plasmids pGBT9 and pGAD424, respectively. Point mutations were made in pGBT9- *dma1(aa187-end)* and pGAD424- *dma1(aa187- end)* plasmids using a site directed mutagenesis kit (Agilent Technologies) and were sequence verified. Bait and Prey plasmids were simultaneously transformed into KGY1296 strain using a standard LiAc transformation procedure and transformants were selected for growth on SD media supplemented with methionine, uracil, histidine and adenine, but lacking leucine and tryptophan. 2-hybrid interactions were tested on SD media supplemented with methionine and uracil, but lacking leucine, tryptophan, histidine and adenine.

REFERENCES

Alexandru, G., W. Zachariae, A. Schleiffer, and K. Nasmyth. 1999. Sister chromatid separation and chromosome re-duplication are regulated by different mechanisms in response to spindle damage. *EMBO J*. 18:2707-2721.

Amon, A. 1999. The spindle checkpoint. *Curr Opin Genet Dev*. 9:69-75.

Bahler, J., A.B. Steever, S. Wheatley, Y. Wang, J.R. Pringle, K.L. Gould, and D. McCollum. 1998. Role of polo kinase and Mid1p in determining the site of cell division in fission yeast. *J Cell Biol*. 143:1603-1616.

Balasubramanian, M.K., D. McCollum, L. Chang, K.C. Wong, N.I. Naqvi, X. He, S. Sazer, and K.L. Gould. 1998. Isolation and characterization of new fission yeast cytokinesis mutants. *Genetics*. 149:1265-1275.

Bardin, A.J., and A. Amon. 2001. Men and sin: what's the difference? *Nat Rev Mol Cell Biol*. 2:815-826.

Behrend, L., D.M. Milne, M. Stoter, W. Deppert, L.E. Campbell, D.W. Meek, and U. Knippschild. 2000. IC261, a specific inhibitor of the protein kinases casein kinase 1-delta and -epsilon, triggers the mitotic checkpoint and induces p53-dependent postmitotic effects. *Oncogene*. 19:5303-5313.

Beltraminelli, N., M. Murone, and V. Simanis. 1999. The S. pombe zfs1 gene is required to prevent septation if mitotic progression is inhibited. *J Cell Sci*. 112 Pt 18:3103-3114.

Bimbo, A., Y. Jia, S.L. Poh, R.K. Karuturi, N. den Elzen, X. Peng, L. Zheng, M. O'Connell, E.T. Liu, M.K. Balasubramanian, and J. Liu. 2005. Systematic deletion analysis of fission yeast protein kinases. *Eukaryot Cell*. 4:799-813.

Bohnert, K.A., and K.L. Gould. 2011. On the cutting edge: post-translational modifications in cytokinesis. *Trends Cell Biol*. 21:283-292.

Bothos, J., M.K. Summers, M. Venere, D.M. Scolnick, and T.D. Halazonetis. 2003. The Chfr mitotic checkpoint protein functions with Ubc13-Mms2 to form Lys63-linked polyubiquitin chains. *Oncogene*. 22:7101-7107.

Bothos, J., R.L. Tuttle, M. Ottey, F.C. Luca, and T.D. Halazonetis. 2005. Human LATS1 is a mitotic exit network kinase. *Cancer Res*. 65:6568-6575.

Bridge, A.J., M. Morphew, R. Bartlett, and I.M. Hagan. 1998. The fission yeast SPB component Cut12 links bipolar spindle formation to mitotic control. *Genes Dev*. 12:927-942.

Brooks, L., 3rd, E.G. Heimsath, Jr., G.L. Loring, and C. Brenner. 2008. FHA-RING ubiquitin ligases in cell division cycle control. *Cell Mol Life Sci*. 65:3458-3466.

Bruno, K.S., J.L. Morrell, J.E. Hamer, and C.J. Staiger. 2001. SEPH, a Cdc7p orthologue from Aspergillus nidulans, functions upstream of actin ring formation during cytokinesis. *Mol Microbiol*. 42:3-12.

Castiel, A., M.M. Danieli, A. David, S. Moshkovitz, P.D. Aplan, I.R. Kirsch, M. Brandeis, A. Kramer, and S. Izraeli. 2011. The Stil protein regulates centrosome integrity and mitosis through suppression of Chfr. *J Cell Sci*. 124:532-539.

Cegielska, A., K.F. Gietzen, A. Rivers, and D.M. Virshup. 1998. Autoinhibition of casein kinase I epsilon (CKI epsilon) is relieved by protein phosphatases and limited proteolysis. *J Biol Chem*. 273:1357-1364.

Cegielska, A., I. Moarefi, E. Fanning, and D.M. Virshup. 1994. T-antigen kinase inhibits simian virus 40 DNA replication by phosphorylation of intact T antigen on serines 120 and 123. *J Virol*. 68:269-275.

Cerutti, L., and V. Simanis. 1999. Asymmetry of the spindle pole bodies and spg1p GAP segregation during mitosis in fission yeast. *J Cell Sci*. 112 (Pt 14):2313-2321.

Chan, E.H., M. Nousiainen, R.B. Chalamalasetty, A. Schafer, E.A. Nigg, and H.H. Sillje. 2005. The Ste20-like kinase Mst2 activates the human large tumor suppressor kinase Lats1. *Oncogene*. 24:2076-2086.

Chang, F., A. Woollard, and P. Nurse. 1996. Isolation and characterization of fission yeast mutants defective in the assembly and placement of the contractile actin ring. *J Cell Sci*. 109 (Pt 1):131-142.

Chang, L., and K.L. Gould. 2000. Sid4p is required to localize components of the septation initiation pathway to the spindle pole body in fission yeast. *Proc Natl Acad Sci U S A*. 97:5249-5254.

Chang, L., J.L. Morrell, A. Feoktistova, and K.L. Gould. 2001. Study of cyclin proteolysis in anaphase-promoting complex (APC) mutant cells reveals the requirement for APC function in the final steps of the fission yeast septation initiation network. *Mol Cell Biol*. 21:6681-6694.

Chaurushiya, M.S., C.E. Lilley, A. Aslanian, J. Meisenhelder, D.C. Scott, S. Landry, S. Ticau, C. Boutell, J.R. Yates, 3rd, B.A. Schulman, T. Hunter, and M.D. Weitzman. 2012. Viral E3 ubiquitin ligase-mediated degradation of a cellular E3: viral mimicry of a cellular phosphorylation mark targets the RNF8 FHA domain. *Mol Cell*. 46:79-90.

Chen, C.T., A. Feoktistova, J.S. Chen, Y.S. Shim, D.M. Clifford, K.L. Gould, and D. McCollum. 2008. The SIN kinase Sid2 regulates cytoplasmic retention of the S. pombe Cdc14-like phosphatase Clp1. *Curr Biol*. 18:1594-1599.

Chow, A., Y. Hao, and X. Yang. 2009. Molecular characterization of human homologs of yeast MOB1. *Int J Cancer*. 126:2079-2089.

Ciccia, A., and S.J. Elledge. 2010. The DNA damage response: making it safe to play with knives. *Mol Cell*. 40:179-204.

Clifford, D.M., B.A. Wolfe, R.H. Roberts-Galbraith, W.H. McDonald, J.R. Yates, 3rd, and K.L. Gould. 2008. The Clp1/Cdc14 phosphatase contributes to the robustness of cytokinesis by association with anillin-related Mid1. *J Cell Biol*. 181:79-88.

Cortese, M.S., V.N. Uversky, and A.K. Dunker. 2008. Intrinsic disorder in scaffold proteins: getting more from less. *Prog Biophys Mol Biol*. 98:85-106.

Cuif, M.H., F. Possmayer, H. Zander, N. Bordes, F. Jollivet, A. Couedel-Courteille, I. Janoueix-Lerosey, G. Langsley, M. Bornens, and B. Goud. 1999. Characterization of GAPCenA, a GTPase activating protein for Rab6, part of which associates with the centrosome. *EMBO J*. 18:1772-1782.

Dan, I., N.M. Watanabe, and A. Kusumi. 2001. The Ste20 group kinases as regulators of MAP kinase cascades. *Trends Cell Biol*. 11:220-230.

Deshaies, R.J., and C.A. Joazeiro. 2009. RING domain E3 ubiquitin ligases. *Annu Rev Biochem*. 78:399-434.

Durocher, D., and S.P. Jackson. 2002. The FHA domain. *FEBS Lett*. 513:58-66.

Durocher, D., I.A. Taylor, D. Sarbassova, L.F. Haire, S.L. Westcott, S.P. Jackson, S.J. Smerdon, and M.B. Yaffe. 2000. The molecular basis of FHA domain:phosphopeptide binding specificity and implications for phospho-dependent signaling mechanisms. *Mol Cell*. 6:1169-1182.

Elledge, S.J. 1996. Cell cycle checkpoints: preventing an identity crisis. *Science*. 274:1664-1672.

Fankhauser, C., and V. Simanis. 1993. The Schizosaccharomyces pombe cdc14 gene is required for septum formation and can also inhibit nuclear division. *Mol Biol Cell*. 4:531-539.

Fankhauser, C., and V. Simanis. 1994. The cdc7 protein kinase is a dosage dependent regulator of septum formation in fission yeast. *EMBO J*. 13:3011-3019.

Feoktistova, A., J. Morrell-Falvey, J.S. Chen, N.S. Singh, M.K. Balasubramanian, and K.L. Gould. 2012. The fission yeast septation initiation network (SIN) kinase, Sid2, is required for SIN asymmetry and regulates the SIN scaffold, Cdc11. *Mol Biol Cell*. 23:1636-1645.

Flory, M.R., M. Morphew, J.D. Joseph, A.R. Means, and T.N. Davis. 2002. Pcp1p, an Spc110p-related calmodulin target at the centrosome of the fission yeast Schizosaccharomyces pombe. *Cell Growth Differ*. 13:47-58.

Fong, C.S., M. Sato, and T. Toda. 2010. Fission yeast Pcp1 links polo kinase-mediated mitotic entry to gamma-tubulin-dependent spindle formation. *EMBO J*. 29:120-130.

Fraschini, R., D. Bilotta, G. Lucchini, and S. Piatti. 2004. Functional characterization of Dma1 and Dma2, the budding yeast homologues of Schizosaccharomyces pombe Dma1 and human Chfr. *Mol Biol Cell*. 15:3796-3810.

Fraschini, R., E. Formenti, G. Lucchini, and S. Piatti. 1999. Budding yeast Bub2 is localized at spindle pole bodies and activates the mitotic checkpoint via a different pathway from Mad2. *J Cell Biol*. 145:979-991.

Fukuda, T., Y. Kondo, and H. Nakagama. 2008. The anti-proliferative effects of the CHFR depend on the forkhead associated domain, but not E3 ligase activity mediated by ring finger domain. *PLoS One*. 3:e1776.

Furge, K.A., Q.C. Cheng, M. Jwa, S. Shin, K. Song, and C.F. Albright. 1999. Regions of Byr4, a regulator of septation in fission yeast, that bind Spg1 or Cdc16 and form a two-component GTPase-activating protein with Cdc16. *J Biol Chem*. 274:11339-11343.

Furge, K.A., K. Wong, J. Armstrong, M. Balasubramanian, and C.F. Albright. 1998. Byr4 and Cdc16 form a two-component GTPase-activating protein for the Spg1 GTPase that controls septation in fission yeast. *Curr Biol*. 8:947-954.

Garcia-Cortes, J.C., and D. McCollum. 2009. Proper timing of cytokinesis is regulated by Schizosaccharomyces pombe Etd1. *J Cell Biol*. 186:739-753.

Gardner, R.D., and D.J. Burke. 2000. The spindle checkpoint: two transitions, two pathways. *Trends Cell Biol*. 10:154-158.

Geymonat, M., A. Spanos, P.A. Walker, L.H. Johnston, and S.G. Sedgwick. 2003. In vitro regulation of budding yeast Bfa1/Bub2 GAP activity by Cdc5. *J Biol Chem*. 278:14591-14594.

Glotzer, M., A.W. Murray, and M.W. Kirschner. 1991. Cyclin is degraded by the ubiquitin pathway. *Nature*. 349:132-138.

Gould, K.L., S. Moreno, D.J. Owen, S. Sazer, and P. Nurse. 1991. Phosphorylation at Thr167 is required for Schizosaccharomyces pombe p34cdc2 function. *EMBO J*. 10:3297-3309.

Gould, K.L., L. Ren, A.S. Feoktistova, J.L. Jennings, and A.J. Link. 2004. Tandem affinity purification and identification of protein complex components. *Methods*. 33:239-244.

Goyal, A., M. Takaine, V. Simanis, and K. Nakano. 2011. Dividing the spoils of growth and the cell cycle: The fission yeast as a model for the study of cytokinesis. *Cytoskeleton (Hoboken)*. 68:69-88.

Grallert, A., A. Krapp, S. Bagley, V. Simanis, and I.M. Hagan. 2004. Recruitment of NIMA kinase shows that maturation of the S. pombe spindle-pole body occurs over consecutive cell cycles and reveals a role for NIMA in modulating SIN activity. *Genes Dev*. 18:1007-1021.

Gromley, A., C. Yeaman, J. Rosa, S. Redick, C.T. Chen, S. Mirabelle, M. Guha, J. Sillibourne, and S.J. Doxsey. 2005. Centriolin anchoring of exocyst and SNARE complexes at the midbody is required for secretory-vesicle-mediated abscission. *Cell*. 123:75-87.

Guertin, D.A., L. Chang, F. Irshad, K.L. Gould, and D. McCollum. 2000. The role of the sid1p kinase and cdc14p in regulating the onset of cytokinesis in fission yeast. *EMBO J*. 19:1803-1815.

Guertin, D.A., and D. McCollum. 2001. Interaction between the noncatalytic region of Sid1p kinase and Cdc14p is required for full catalytic activity and localization of Sid1p. *J Biol Chem*. 276:28185-28189.

Guertin, D.A., S. Venkatram, K.L. Gould, and D. McCollum. 2002. Dma1 prevents mitotic exit and cytokinesis by inhibiting the septation initiation network (SIN). *Dev Cell*. 3:779-790.

Hachet, O., and V. Simanis. 2008. Mid1p/anillin and the septation initiation network orchestrate contractile ring assembly for cytokinesis. *Genes Dev*. 22:3205-3216.

Hagan, I., and M. Yanagida. 1995. The product of the spindle formation gene sad1+ associates with the fission yeast spindle pole body and is essential for viability. *J Cell Biol*. 129:1033-1047.

Halder, G., and R.L. Johnson. 2011. Hippo signaling: growth control and beyond. *Development*. 138:9-22.

Hashizume, R., M. Fukuda, I. Maeda, H. Nishikawa, D. Oyake, Y. Yabuki, H. Ogata, and T. Ohta. 2001. The RING heterodimer BRCA1-BARD1 is a ubiquitin ligase inactivated by a breast cancer-derived mutation. *J Biol Chem*. 276:14537-14540.

Hergovich, A., D. Schmitz, and B.A. Hemmings. 2006. The human tumour suppressor LATS1 is activated by human MOB1 at the membrane. *Biochem Biophys Res Commun*. 345:50-58.

Hirabayashi, S., K. Nakagawa, K. Sumita, S. Hidaka, T. Kawai, M. Ikeda, A. Kawata, K. Ohno, and Y. Hata. 2008. Threonine 74 of MOB1 is a putative key phosphorylation site by MST2 to form the scaffold to activate nuclear Dbf2-related kinase 1. *Oncogene*. 27:4281-4292.

Hiraoka, Y., T. Toda, and M. Yanagida. 1984. The NDA3 gene of fission yeast encodes beta-tubulin: a cold-sensitive nda3 mutation reversibly blocks spindle formation and chromosome movement in mitosis. *Cell*. 39:349-358.

Hirota, T., T. Morisaki, Y. Nishiyama, T. Marumoto, K. Tada, T. Hara, N. Masuko, M. Inagaki, K. Hatakeyama, and H. Saya. 2000. Zyxin, a regulator of actin filament assembly, targets the mitotic apparatus by interacting with h-warts/LATS1 tumor suppressor. *J Cell Biol*. 149:1073-1086.

Hofmann, R.M., and C.M. Pickart. 1999. Noncanonical MMS2-encoded ubiquitin-conjugating enzyme functions in assembly of novel polyubiquitin chains for DNA repair. *Cell*. 96:645-653.

Hou, M.C., D.A. Guertin, and D. McCollum. 2004. Initiation of cytokinesis is controlled through multiple modes of regulation of the Sid2p-Mob1p kinase complex. *Mol Cell Biol*. 24:3262-3276.

Hou, M.C., J. Salek, and D. McCollum. 2000. Mob1p interacts with the Sid2p kinase and is required for cytokinesis in fission yeast. *Curr Biol*. 10:619-622.

Hu, F., Y. Wang, D. Liu, Y. Li, J. Qin, and S.J. Elledge. 2001. Regulation of the Bub2/Bfa1 GAP complex by Cdc5 and cell cycle checkpoints. *Cell*. 107:655-665.

Huang, Y., H. Yan, and M.K. Balasubramanian. 2008. Assembly of normal actomyosin rings in the absence of Mid1p and cortical nodes in fission yeast. *J Cell Biol*. 183:979-988.

Hwang, L.H., L.F. Lau, D.L. Smith, C.A. Mistrot, K.G. Hardwick, E.S. Hwang, A. Amon, and A.W. Murray. 1998. Budding yeast Cdc20: a target of the spindle checkpoint. *Science*. 279:1041-1044.

Ikeda, F., and I. Dikic. 2008. Atypical ubiquitin chains: new molecular signals. 'Protein Modifications: Beyond the Usual Suspects' review series. *EMBO Rep*. 9:536-542.

Jin, Q.W., M. Zhou, A. Bimbo, M.K. Balasubramanian, and D. McCollum. 2006. A role for the septation initiation network in septum assembly revealed by genetic analysis of sid2-250 suppressors. *Genetics*. 172:2101-2112.

Johnson, A.E., S.E. Collier, M.D. Ohi, and K.L. Gould. Fission yeast Dma1 requires RING domain dimerization for its ubiquitin ligase activity and mitotic checkpoint function. *J Biol Chem*. 287:25741-25748.

Johnson, A.E., and K.L. Gould. 2011. Dma1 ubiquitinates the SIN scaffold, Sid4, to impede the mitotic localization of Plo1 kinase. *EMBO J*. 30:341-354.

Johnson, A.E., D. McCollum, and K.L. Gould. 2012. Polar opposites: Fine-tuning cytokinesis through SIN asymmetry. *Cytoskeleton (Hoboken)*. 69:686-699.

Kang, D., J. Chen, J. Wong, and G. Fang. 2002. The checkpoint protein Chfr is a ligase that ubiquitinates Plk1 and inhibits Cdc2 at the G2 to M transition. *J Cell Biol*. 156:249-259.

Kang, D., J. Wong, and G. Fang. 2004. A Xenopus cell-free system for analysis of the Chfr ubiquitin ligase involved in control of mitotic entry. *Methods Mol Biol*. 280:229-243.

Katoh, S., C. Hong, Y. Tsunoda, K. Murata, R. Takai, E. Minami, T. Yamazaki, and E. Katoh. 2003. High precision NMR structure and function of the RING-H2 finger domain of EL5, a rice protein whose expression is increased upon exposure to pathogen-derived oligosaccharides. *J Biol Chem*. 278:15341-15348.

Kim, H., J. Chen, and X. Yu. 2007. Ubiquitin-binding protein RAP80 mediates BRCA1-dependent DNA damage response. *Science*. 316:1202-1205.

Kim, J.M., L. Lu, R. Shao, J. Chin, and B. Liu. 2006. Isolation of mutations that bypass the requirement of the septation initiation network for septum formation and conidiation in Aspergillus nidulans. *Genetics*. 173:685-696.

Kim, J.M., C.J. Zeng, T. Nayak, R. Shao, A.C. Huang, B.R. Oakley, and B. Liu. 2009. Timely septation requires SNAD-dependent spindle pole body localization of the septation initiation network components in the filamentous fungus Aspergillus nidulans. *Mol Biol Cell*. 20:2874-2884.

Kim, S.H., D.P. Lin, S. Matsumoto, A. Kitazono, and T. Matsumoto. 1998. Fission yeast Slp1: an effector of the Mad2-dependent spindle checkpoint. *Science*. 279:1045-1047.

Knippschild, U., A. Gocht, S. Wolff, N. Huber, J. Lohler, and M. Stoter. 2005. The casein kinase 1 family: participation in multiple cellular processes in eukaryotes. *Cell Signal*. 17:675-689.

Kolas, N.K., J.R. Chapman, S. Nakada, J. Ylanko, R. Chahwan, F.D. Sweeney, S. Panier, M. Mendez, J. Wildenhain, T.M. Thomson, L. Pelletier, S.P. Jackson, and D. Durocher. 2007. Orchestration of the DNA-damage response by the RNF8 ubiquitin ligase. *Science*. 318:1637-1640.

Komander, D., F. Reyes-Turcu, J.D. Licchesi, P. Odenwaelder, K.D. Wilkinson, and D. Barford. 2009. Molecular discrimination of structurally equivalent Lys 63-linked and linear polyubiquitin chains. *EMBO Rep*. 10:466-473.

Kops, G.J., B.A. Weaver, and D.W. Cleveland. 2005. On the road to cancer: aneuploidy and the mitotic checkpoint. *Nat Rev Cancer*. 5:773-785.

Krapp, A., E. Cano, and V. Simanis. 2003. Mitotic hyperphosphorylation of the fission yeast SIN scaffold protein cdc11p is regulated by the protein kinase cdc7p. *Curr Biol*. 13:168-172.

Krapp, A., P. Collin, E. Cano Del Rosario, and V. Simanis. 2008. Homoeostasis between the GTPase Spg1p and its GAP in the regulation of cytokinesis in S. pombe. *J Cell Sci*. 121:601-608.

Krapp, A., P. Collin, A. Cokoja, S. Dischinger, E. Cano, and V. Simanis. 2006. The Schizosaccharomyces pombe septation initiation network (SIN) is required for spore formation in meiosis. *J Cell Sci*. 119:2882-2891.

Krapp, A., E.C. Del Rosario, and V. Simanis. 2010. The role of Schizosaccharomyces pombe dma1 in spore formation during meiosis. *J Cell Sci*. 123:3284-3293.

Krapp, A., M.P. Gulli, and V. Simanis. 2004. SIN and the art of splitting the fission yeast cell. *Curr Biol*. 14:R722-730.

Krapp, A., S. Schmidt, E. Cano, and V. Simanis. 2001. S. pombe cdc11p, together with sid4p, provides an anchor for septation initiation network proteins on the spindle pole body. *Curr Biol*. 11:1559-1568.

Laney, J.D., and M. Hochstrasser. 1999. Substrate targeting in the ubiquitin system. *Cell*. 97:427-430.

Li, C., K.A. Furge, Q.C. Cheng, and C.F. Albright. 2000. Byr4 localizes to spindle-pole bodies in a cell cycle-regulated manner to control Cdc7 localization and septation in fission yeast. *J Biol Chem*. 275:14381-14387.

Li, L., M.J. Halaby, A. Hakem, R. Cardoso, S. El Ghamrasni, S. Harding, N. Chan, R. Bristow, O. Sanchez, D. Durocher, and R. Hakem. 2010a. Rnf8 deficiency impairs class switch recombination, spermatogenesis, and genomic integrity and predisposes for cancer. *J Exp Med*. 207:983-997.

Li, R. 1999. Bifurcation of the mitotic checkpoint pathway in budding yeast. *Proc Natl Acad Sci U S A*. 96:4989-4994.

Li, W.Z., Z.Y. Yu, P.F. Ma, Y. Wang, and Q.W. Jin. 2010b. A novel role of Dma1 in regulating forespore membrane assembly and sporulation in fission yeast. *Mol Biol Cell*. 21:4349-4360.

Liew, C.W., H. Sun, T. Hunter, and C.L. Day. 2010. RING domain dimerization is essential for RNF4 function. *Biochem J*. 431:23-29.

Linares, L.K., A. Hengstermann, A. Ciechanover, S. Muller, and M. Scheffner. 2003. HdmX stimulates Hdm2-mediated ubiquitination and degradation of p53. *Proc Natl Acad Sci U S A*. 100:12009-12014.

Loring, G.L., K.C. Christensen, S.A. Gerber, and C. Brenner. 2008. Yeast Chfr homologs retard cell cycle at G1 and G2/M via Ubc4 and Ubc13/Mms2-dependent ubiquitination. *Cell Cycle*. 7:96-105.

Mace, P.D., K. Linke, R. Feltham, F.R. Schumacher, C.A. Smith, D.L. Vaux, J. Silke, and C.L. Day. 2008. Structures of the cIAP2 RING domain reveal conformational changes associated with ubiquitin-conjugating enzyme (E2) recruitment. *J Biol Chem*. 283:31633-31640.

MacIver, F.H., K. Tanaka, A.M. Robertson, and I.M. Hagan. 2003. Physical and functional interactions between polo kinase and the spindle pole component Cut12 regulate mitotic commitment in S. pombe. *Genes Dev*. 17:1507-1523.

Magidson, V., F. Chang, and A. Khodjakov. 2006. Regulation of cytokinesis by spindle-pole bodies. *Nat Cell Biol*. 8:891-893.

Mah, A.S., A.E. Elia, G. Devgan, J. Ptacek, M. Schutkowski, M. Snyder, M.B. Yaffe, and R.J. Deshaies. 2005. Substrate specificity analysis of protein kinase complex Dbf2-Mob1 by peptide library and proteome array screening. *BMC Biochem*. 6:22.

Marks, J., C. Fankhauser, and V. Simanis. 1992. Genetic interactions in the control of septation in Schizosaccharomyces pombe. *J Cell Sci*. 101 (Pt 4):801-808.

Matsusaka, T., and J. Pines. 2004. Chfr acts with the p38 stress kinases to block entry to mitosis in mammalian cells. *J Cell Biol*. 166:507-516.

McCollum, D., and K.L. Gould. 2001. Timing is everything: regulation of mitotic exit and cytokinesis by the MEN and SIN. *Trends Cell Biol*. 11:89-95.

Millward, T.A., D. Hess, and B.A. Hemmings. 1999. Ndr protein kinase is regulated by phosphorylation on two conserved sequence motifs. *J Biol Chem*. 274:33847-33850.

Milne, D.M., P. Looby, and D.W. Meek. 2001. Catalytic activity of protein kinase CK1 delta (casein kinase 1delta) is essential for its normal subcellular localization. *Exp Cell Res*. 263:43-54.

Minet, M., P. Nurse, P. Thuriaux, and J.M. Mitchison. 1979. Uncontrolled septation in a cell division cycle mutant of the fission yeast Schizosaccharomyces pombe. *J Bacteriol*. 137:440-446.

Mishra, M., J. Karagiannis, M. Sevugan, P. Singh, and M.K. Balasubramanian. 2005. The 14-3-3 protein rad24p modulates function of the cdc14p family phosphatase clp1p/flp1p in fission yeast. *Curr Biol*. 15:1376-1383.

Moreno, S., A. Klar, and P. Nurse. 1991. Molecular genetic analysis of fission yeast Schizosaccharomyces pombe. *Methods Enzymol*. 194:795-823.

Morrell, J.L., G.C. Tomlin, S. Rajagopalan, S. Venkatram, A.S. Feoktistova, J.J. Tasto, S. Mehta, J.L. Jennings, A. Link, M.K. Balasubramanian, and K.L. Gould. 2004. Sid4p-Cdc11p assembles the septation initiation network and its regulators at the S. pombe SPB. *Curr Biol*. 14:579-584.

Motegi, F., M. Mishra, M.K. Balasubramanian, and I. Mabuchi. 2004. Myosin-II reorganization during mitosis is controlled temporally by its dephosphorylation and spatially by Mid1 in fission yeast. *J Cell Biol*. 165:685-695.

Mulvihill, D.P., and J.S. Hyams. 2002. Cytokinetic actomyosin ring formation and septation in fission yeast are dependent on the full recruitment of the polo-like kinase Plo1 to the spindle pole body and a functional spindle assembly checkpoint. *J Cell Sci*. 115:3575-3586.

Mulvihill, D.P., J. Petersen, H. Ohkura, D.M. Glover, and I.M. Hagan. 1999. Plo1 kinase recruitment to the spindle pole body and its role in cell division in Schizosaccharomyces pombe. *Mol Biol Cell*. 10:2771-2785.

Murone, M., and V. Simanis. 1996. The fission yeast dma1 gene is a component of the spindle assembly checkpoint, required to prevent septum formation and premature exit from mitosis if spindle function is compromised. *EMBO J*. 15:6605-6616.

Musacchio, A., and E.D. Salmon. 2007. The spindle-assembly checkpoint in space and time. *Nat Rev Mol Cell Biol*. 8:379-393.

Nurse, P. 2000. A long twentieth century of the cell cycle and beyond. *Cell*. 100:71-78.

Nurse, P., P. Thuriaux, and K. Nasmyth. 1976. Genetic control of the cell division cycle in the fission yeast Schizosaccharomyces pombe. *Mol Gen Genet*. 146:167-178.

Ohkura, H., I.M. Hagan, and D.M. Glover. 1995. The conserved Schizosaccharomyces pombe kinase plo1, required to form a bipolar spindle, the actin ring, and septum, can drive septum formation in G1 and G2 cells. *Genes Dev*. 9:1059-1073.

Ozkan, E., H. Yu, and J. Deisenhofer. 2005. Mechanistic insight into the allosteric activation of a ubiquitin-conjugating enzyme by RING-type ubiquitin ligases. *Proc Natl Acad Sci U S A*. 102:18890-18895.

Pereira, G., T.U. Tanaka, K. Nasmyth, and E. Schiebel. 2001. Modes of spindle pole body inheritance and segregation of the Bfa1p-Bub2p checkpoint protein complex. *EMBO J*. 20:6359-6370.

Perez-Hidalgo, L., A.E. Rozalen, C. Martin-Castellanos, and S. Moreno. 2008. Slk1 is a meiosis-specific Sid2-related kinase that coordinates meiotic nuclear division with growth of the forespore membrane. *J Cell Sci*. 121:1383-1392.

Pickart, C.M. 2001. Mechanisms underlying ubiquitination. *Annu Rev Biochem*. 70:503-533.

Pickart, C.M. 2004. Back to the future with ubiquitin. *Cell*. 116:181-190.

Pickart, C.M., and D. Fushman. 2004. Polyubiquitin chains: polymeric protein signals. *Curr Opin Chem Biol*. 8:610-616.

Plans, V., J. Scheper, M. Soler, N. Loukili, Y. Okano, and T.M. Thomson. 2006. The RING finger protein RNF8 recruits UBC13 for lysine 63-based self polyubiquitylation. *J Cell Biochem*. 97:572-582.

Plechanovova, A., E.G. Jaffray, S.A. McMahon, K.A. Johnson, I. Navratilova, J.H. Naismith, and R.T. Hay. 2011. Mechanism of ubiquitylation by dimeric RING ligase RNF4. *Nat Struct Mol Biol*. 18:1052-1059.

Polekhina, G., C.M. House, N. Traficante, J.P. Mackay, F. Relaix, D.A. Sassoon, M.W. Parker, and D.D. Bowtell. 2002. Siah ubiquitin ligase is structurally related to TRAF and modulates TNF-alpha signaling. *Nat Struct Biol*. 9:68-75.

Poyurovsky, M.V., C. Priest, A. Kentsis, K.L. Borden, Z.Q. Pan, N. Pavletich, and C. Prives. 2007. The Mdm2 RING domain C-terminus is required for supramolecular assembly and ubiquitin ligase activity. *EMBO J*. 26:90-101.

Roberts-Galbraith, R.H., M.D. Ohi, B.A. Ballif, J.S. Chen, I. McLeod, W.H. McDonald, S.P. Gygi, J.R. Yates, 3rd, and K.L. Gould. 2010. Dephosphorylation of F-BAR protein Cdc15 modulates its conformation and stimulates its scaffolding activity at the cell division site. *Mol Cell*. 39:86-99.

Rosenberg, J.A., G.C. Tomlin, W.H. McDonald, B.E. Snydsman, E.G. Muller, J.R. Yates, 3rd, and K.L. Gould. 2006. Ppc89 links multiple proteins, including the septation initiation network, to the core of the fission yeast spindle-pole body. *Mol Biol Cell*. 17:3793-3805.

Rotin, D., and S. Kumar. 2009. Physiological functions of the HECT family of ubiquitin ligases. *Nat Rev Mol Cell Biol*. 10:398-409.

Salimova, E., M. Sohrmann, N. Fournier, and V. Simanis. 2000. The S. pombe orthologue of the S. cerevisiae mob1 gene is essential and functions in signalling the onset of septum formation. *J Cell Sci*. 113 (Pt 10):1695-1704.

Sandrock, B., C. Bohmer, and M. Bolker. 2006. Dual function of the germinal centre kinase Don3 during mitosis and cytokinesis in Ustilago maydis. *Mol Microbiol*. 62:655-666.

Schmidt, S., M. Sohrmann, K. Hofmann, A. Woollard, and V. Simanis. 1997. The Spg1p GTPase is an essential, dosage-dependent inducer of septum formation in Schizosaccharomyces pombe. *Genes Dev*. 11:1519-1534.

Schuck, P. 2000. Size-distribution analysis of macromolecules by sedimentation velocity ultracentrifugation and lamm equation modeling. *Biophys J*. 78:1606-1619.

Scolnick, D.M., and T.D. Halazonetis. 2000. Chfr defines a mitotic stress checkpoint that delays entry into metaphase. *Nature*. 406:430-435.

Seeger, M., C. Gordon, K. Ferrell, and W. Dubiel. 1996. Characteristics of 26 S proteases from fission yeast mutants, which arrest in mitosis. *J Mol Biol*. 263:423-431.

Seshan, A., and A. Amon. 2004. Linked for life: temporal and spatial coordination of late mitotic events. *Curr Opin Cell Biol*. 16:41-48.

Shtivelman, E. 2003. Promotion of mitosis by activated protein kinase B after DNA damage involves polo-like kinase 1 and checkpoint protein CHFR. *Mol Cancer Res*. 1:959-969.

Sillibourne, J.E., D.M. Milne, M. Takahashi, Y. Ono, and D.W. Meek. 2002. Centrosomal anchoring of the protein kinase CK1delta mediated by attachment to the large, coiled-coil scaffolding protein CG-NAP/AKAP450. *J Mol Biol*. 322:785-797.

Sims, J.J., and R.E. Cohen. 2009. Linkage-specific avidity defines the lysine 63-linked polyubiquitin-binding preference of rap80. *Mol Cell*. 33:775-783.

Singh, N.S., N. Shao, J.R. McLean, M. Sevugan, L. Ren, T.G. Chew, A. Bimbo, R. Sharma, X. Tang, K.L. Gould, and M.K. Balasubramanian. 2011. SIN-inhibitory phosphatase complex promotes Cdc11p dephosphorylation and propagates SIN asymmetry in fission yeast. *Curr Biol*. 21:1968-1978.

Sohrmann, M., C. Fankhauser, C. Brodbeck, and V. Simanis. 1996. The dmf1/mid1 gene is essential for correct positioning of the division septum in fission yeast. *Genes Dev*. 10:2707-2719.

Sohrmann, M., S. Schmidt, I. Hagan, and V. Simanis. 1998. Asymmetric segregation on spindle poles of the Schizosaccharomyces pombe septum-inducing protein kinase Cdc7p. *Genes Dev*. 12:84-94.

Song, K., K.E. Mach, C.Y. Chen, T. Reynolds, and C.F. Albright. 1996. A novel suppressor of ras1 in fission yeast, byr4, is a dosage-dependent inhibitor of cytokinesis. *J Cell Biol*. 133:1307-1319.

Soutto, M., D. Peng, M. Razvi, P. Ruemmele, A. Hartmann, A. Roessner, R. Schneider-Stock, and W. El-Rifai. 2010. Epigenetic and genetic silencing of CHFR in esophageal adenocarcinomas. *Cancer*. 116:4033-4042.

Sparks, C.A., M. Morphew, and D. McCollum. 1999. Sid2p, a spindle pole body kinase that regulates the onset of cytokinesis. *J Cell Biol*. 146:777-790.

Swiatek, W., H. Kang, B.A. Garcia, J. Shabanowitz, G.S. Coombs, D.F. Hunt, and D.M. Virshup. 2006. Negative regulation of LRP6 function by casein kinase I epsilon phosphorylation. *J Biol Chem*. 281:12233-12241.

Tagwerker, C., K. Flick, M. Cui, C. Guerrero, Y. Dou, B. Auer, P. Baldi, L. Huang, and P. Kaiser. 2006. A tandem affinity tag for two-step purification under fully

denaturing conditions: application in ubiquitin profiling and protein complex identification combined with in vivocross-linking. *Mol Cell Proteomics*. 5:737-748.

Takahashi, M., A. Yamagiwa, T. Nishimura, H. Mukai, and Y. Ono. 2002. Centrosomal proteins CG-NAP and kendrin provide microtubule nucleation sites by anchoring gamma-tubulin ring complex. *Mol Biol Cell*. 13:3235-3245.

Tanaka, K., J. Petersen, F. MacIver, D.P. Mulvihill, D.M. Glover, and I.M. Hagan. 2001. The role of Plo1 kinase in mitotic commitment and septation in Schizosaccharomyces pombe. *EMBO J*. 20:1259-1270.

Toda, T., K. Umesono, A. Hirata, and M. Yanagida. 1983. Cold-sensitive nuclear division arrest mutants of the fission yeast Schizosaccharomyces pombe. *J Mol Biol*. 168:251-270.

Tomlin, G.C., J.L. Morrell, and K.L. Gould. 2002. The spindle pole body protein Cdc11p links Sid4p to the fission yeast septation initiation network. *Mol Biol Cell*. 13:1203-1214.

Toyota, M., Y. Sasaki, A. Satoh, K. Ogi, T. Kikuchi, H. Suzuki, H. Mita, N. Tanaka, F. Itoh, J.P. Issa, K.W. Jair, K.E. Schuebel, K. Imai, and T. Tokino. 2003. Epigenetic inactivation of CHFR in human tumors. *Proc Natl Acad Sci U S A*. 100:7818-7823.

Trautmann, S., B.A. Wolfe, P. Jorgensen, M. Tyers, K.L. Gould, and D. McCollum. 2001. Fission yeast Clp1p phosphatase regulates G2/M transition and coordination of cytokinesis with cell cycle progression. *Curr Biol*. 11:931-940.

Tuttle, R.L., J. Bothos, M.K. Summers, F.C. Luca, and T.D. Halazonetis. 2007. Defective in mitotic arrest 1/ring finger 8 is a checkpoint protein that antagonizes the human mitotic exit network. *Mol Cancer Res*. 5:1304-1311.

Umesono, K., T. Toda, S. Hayashi, and M. Yanagida. 1983. Cell division cycle genes nda2 and nda3 of the fission yeast Schizosaccharomyces pombe control microtubular organization and sensitivity to anti-mitotic benzimidazole compounds. *J Mol Biol*. 168:271-284.

Vavylonis, D., J.Q. Wu, S. Hao, B. O'Shaughnessy, and T.D. Pollard. 2008. Assembly mechanism of the contractile ring for cytokinesis by fission yeast. *Science*. 319:97-100.

Wang, H., L. Wang, H. Erdjument-Bromage, M. Vidal, P. Tempst, R.S. Jones, and Y. Zhang. 2004. Role of histone H2A ubiquitination in Polycomb silencing. *Nature*. 431:873-878.

Wickliffe, K., A. Williamson, L. Jin, and M. Rape. 2009. The multiple layers of ubiquitin-dependent cell cycle control. *Chem Rev*. 109:1537-1548.

Wu, J.Q., J.R. Kuhn, D.R. Kovar, and T.D. Pollard. 2003. Spatial and temporal pathway for assembly and constriction of the contractile ring in fission yeast cytokinesis. *Dev Cell*. 5:723-734.

Wu, J.Q., V. Sirotkin, D.R. Kovar, M. Lord, C.C. Beltzner, J.R. Kuhn, and T.D. Pollard. 2006. Assembly of the cytokinetic contractile ring from a broad band of nodes in fission yeast. *J Cell Biol*. 174:391-402.

Xia, H., H. Qi, Y. Li, J. Pei, J. Barton, M. Blackstad, T. Xu, and W. Tao. 2002. LATS1 tumor suppressor regulates G2/M transition and apoptosis. *Oncogene*. 21:1233-1241.

Yan, H., and M.K. Balasubramanian. 2012. A Meiotic Actin Ring (MeiAR) Essential for Proper Sporulation in Fission Yeast. *J Cell Sci*.

Yan, H., W. Ge, T.G. Chew, J.Y. Chow, D. McCollum, A.M. Neiman, and M.K. Balasubramanian. 2008. The meiosis-specific Sid2p-related protein Slk1p regulates forespore membrane assembly in fission yeast. *Mol Biol Cell*. 19:3676-3690.

Yan, J., and A.M. Jetten. 2008. RAP80 and RNF8, key players in the recruitment of repair proteins to DNA damage sites. *Cancer Lett*. 271:179-190.

Yang, X., D.M. Li, W. Chen, and T. Xu. 2001. Human homologue of Drosophila lats, LATS1, negatively regulate growth by inducing G(2)/M arrest or apoptosis. *Oncogene*. 20:6516-6523.

Yang, X., K. Yu, Y. Hao, D.M. Li, R. Stewart, K.L. Insogna, and T. Xu. 2004. LATS1 tumour suppressor affects cytokinesis by inhibiting LIMK1. *Nat Cell Biol*. 6:609-617.

Yu, X., K. Minter-Dykhouse, L. Malureanu, W.M. Zhao, D. Zhang, C.J. Merkle, I.M. Ward, H. Saya, G. Fang, J. van Deursen, and J. Chen. 2005. Chfr is required for tumor suppression and Aurora A regulation. *Nat Genet*. 37:401-406.